

Al-Farabi Kazakh national university

UDC 543.06

On manuscript rights

**IBRAGIMOVA OLGA PAVLOVNA**

**Development of simple and accurate methods for organic pollutants  
determination in the air based on solid-phase microextraction**

8D05301 – Chemistry

Thesis submitted in fulfillment of the requirements  
for the degree of  
Doctor of Philosophy (Ph.D.)

Scientific supervisors:

Ph.D., Associate Professor Nassiba  
Baimatova

Ph.D., Professor Emeritus Jacek A.  
Koziel  
Iowa State University, Ames, IA, USA

The Republic of Kazakhstan  
Almaty, 2023

## CONTENT

<b>NORMATIVE REFERENCES.....</b>	<b>5</b>
<b>LIST OF ABBREVIATIONS.....</b>	<b>6</b>
<b>INTRODUCTION.....</b>	<b>8</b>
1 LITERATURE REVIEW.....	13
1.1 The problem of air quality in the world and the importance of air quality monitoring for environmental impact assessment .....	13
1.2 Importance of quantification of organic pollutants in the air .....	14
1.3 The conventional methods for the determination of volatile organic compounds in the air.....	15
1.4 The solid-phase microextraction for determination of volatile organic compounds in the air.....	17
1.4.1 The principles and advantages of solid-phase microextraction for determination of volatile organic compounds in the air.....	17
1.4.2 Calibration approaches for determination single and time-weighted average concentrations of volatile organic compounds by solid-phase microextraction.....	19
1.4.3 Uncertainties, limitations, and problems of air analysis using solid-phase microextraction with a possible solution .....	21
1.5 Section conclusion.....	23
2 DEVELOPMENT OF METHOD FOR LOW-COST QUANTITATION OF MULTIPLE VOLATILE ORGANIC COMPOUNDS IN AIR USING SOLID-PHASE MICROEXTRACTION .....	25
2.1 Introduction .....	25
2.2 Materials and methods .....	27
2.2.1 Chemicals .....	27
2.2.2 Gas chromatography-mass spectrometry conditions .....	28
2.2.3 Selection of the optimal solid-phase microextraction fiber.....	30
2.2.4 Effects of extraction and desorption times.....	31
2.2.5 Effect of storage time .....	31
2.2.6 Estimation of the method accuracy.....	31
2.2.7 Air sampling and analysis .....	31
2.3 Results .....	33
2.3.1 Selection of the optimal solid-phase microextraction fiber.....	33
2.3.2 Effects of extraction and desorption times.....	35
2.3.3 Effect of storage time .....	37
2.3.4 Estimation of the method accuracy.....	38
2.3.5 Air sampling and analysis .....	38
2.4 Section conclusion.....	42
3 SEASONAL AND SPATIAL VARIATION OF VOLATILE ORGANIC COMPOUNDS IN AMBIENT AIR OF ALMATY CITY, KAZAKHSTAN .....	43
3.1 Introduction .....	43

3.2 Materials and Methods .....	44
3.2.1 Description of sampling sites .....	44
3.2.2 Sampling and analysis of volatile organic compounds .....	46
3.2.3 Data collection and pre-processing .....	47
3.3 Results and Discussion.....	48
3.3.1 Average seasonal variations of volatile organic compounds .....	48
3.3.2 Spatial differences of volatile organic compounds .....	52
3.3.3 BTEX source apportionment.....	54
3.4 Section conclusion.....	48
4 ASSESSING AIR QUALITY CHANGES IN LARGE CITIES DURING COVID-19 LOCKDOWNS: THE IMPACTS OF TRAFFIC-FREE URBAN CONDITIONS IN ALMATY, KAZAKHSTAN .....	58
4.1 Introduction .....	58
4.2 Methodology .....	59
4.2.1 Methodology of sampling .....	59
4.2.2 Meteorological conditions.....	59
4.3 Results and discussion.....	60
4.3.1 BTEX concentration analysis.....	60
4.3.2 Differences in meteorology .....	61
4.3.3 Spatial differences .....	62
4.3.4 Identification of BTEX emission sources .....	64
4.4 Section conclusion.....	65
5 OPTIMIZATION OF TIME-WEIGHTED AVERAGE AIR SAMPLING BY SOLID-PHASE MICROEXTRACTION FIBERS USING FINITE ELEMENT ANALYSIS SOFTWARE .....	66
5.1 Introduction .....	66
5.2 Materials and Methods .....	67
5.2.1 General parameters of modeling .....	67
5.2.2 Sampling using absorptive coatings.....	68
5.2.3 Sampling using adsorptive coatings.....	68
5.3 Results and Discussion.....	69
5.3.1 Time-weighted average sampling profiles of benzene from air using different coatings.....	69
5.3.2 Effect of diffusion coefficient and distribution constant on sampling of analytes by 85- $\mu$ m Car/PDMS coating .....	71
5.3.3 Effect of a protecting needle gauge size .....	72
5.3.4 Effect of diffusion path (Z) at constant analyte concentration in sampled air...	73
5.3.5 Effect of diffusion path (Z) at variable analyte concentration in sampled air (worst-case scenario).....	73
5.3.6 Alternative geometries for time-weighted average solid-phase microextraction sampling .....	74
5.4 Section conclusion.....	76
6 DEVELOPMENT OF THE METHOD FOR THE DETERMINATION OF TIME-	

WEIGHTED AVERAGE CONCENTRATIONS OF VOLATILE ORGANIC POLLUTANTS IN THE AIR BASED ON A MODIFIED SAMPLER WITH AN ALTERNATIVE GEOMETRY AND SOLID-PHASE MICROEXTRACTION .....	78
6.1 Experimental part .....	78
6.1.1 Reagents and materials.....	78
6.1.2 The modified sampler with an alternative geometries for time-weighted average sampling of volatile organic compounds .....	79
6.1.3 Gas chromatography-mass spectrometry conditions .....	79
6.1.4 Variability of solid-phase microextraction fibers .....	79
6.1.5 The development of system for generation of gas with known concentrations of volatile organic compounds .....	80
6.1.6 Methodology of optimization of solid-phase microextraction fiber coating ...	822
6.1.7 Comparison of GC liner and modified sampler for determination of time-weighted average concentrations .....	82
6.1.8 Effect of diffusion path length .....	833
6.1.9 Comparison of the developed method with sorbent tube-based method .....	833
6.2 Results and Discussion.....	84
6.2.1 Study of variability of solid-phase microextraction fibers .....	84
6.2.2 Study of the stability of the developed system for generation of gas with known concentrations of volatile organic compounds.....	86
6.2.3 Study of effect of solid-phase microextraction fiber coatings on analytes recoveries.....	86
6.2.4 Comparison of the accuracy of determination of time-weighted average concentrations by GC liner and modified sampler using solid-phase microextraction fiber .....	888
6.2.5 Effect of diffusion path length on the recovery obtained using a modified sampler .....	89
6.2.6 Determination of the developed method accuracy by comparison with sorbent tube-based method.....	91
6.3 Section conclusions .....	93
<b>CONCLUSION</b> .....	95
<b>REFERENCES</b> .....	97
<b>ANNEX A – Letters of copyright permission</b> .....	9710

## NORMATIVE REFERENCES

In this dissertation, references to the following standards are used:

Compendium Method TO-15. Determination of volatile organic compounds (VOCs) in air collected in specially prepared canisters and analyzed by gas chromatography-mass spectrometry (GC-MS).

Compendium Method TO-17. Determination of volatile organic compounds in ambient air using active sampling onto sorbent tubes.

GOST 16017-2-2007. Atmospheric air, the working area and enclosed spaces. Sampling of volatile organic compounds using a sorption tube with subsequent thermal desorption and gas chromatographic analysis on capillary columns.

TR CU 008/2011. Technical regulations of the customs union on the safety of toys.

MU 1649-77. Guidelines for colorimetric determination of acetophenone in air.

MUC 4.1.618-96. Guidelines for chromato-mass spectrometric determination of volatile organic substances in atmospheric air.

Method OSHA PV2003. Occupational safety and health administration. acetophenone.

Method EPA-RCA 8270D. Semivolatile organic compounds by GC-MS.

Method EPA-EAD 1625. Semivolatile organic compounds by isotope dilution GC-MS.

Method 3510C. Separatory funnel liquid-liquid extraction.

## LIST OF ABBREVIATIONS

ACN	Acetonitrile
AED	Atomic emission detector
B:T:E	Benzene, toluene, and ethylbenzene
BTEX	Benzene, toluene, ethylbenzene and xylenes
Car	Carboxen
CHPs	Combined Heat and Power Plants
COPD	Chronic obstructive pulmonary disease
DEM	Digital elevation model
DI	Direct immersion
DVB	Divinylbenzene
ECD	Electron capture detector
EPA	Environmental protection agency
ESA	European space agency
FID	Flame-ionization detector
GC-MS	Gas chromatography-mass spectrometry
GDP	Gross Domestic Product
HS	Headspace
IARC	International Agency for Research on Cancer
LODs	Limits of detection
LOQ	Limit of quantification
MOF	Metal-organic framework
MPC	Maximum permissible concentration
MTBE	Methyl tert-butyl ether
NAQMN	National Air Quality Monitoring Network
NTD	Needle-trap device
OCPs	Organochlorine pesticides
PAHs	Polycyclic aromatic hydrocarbons
PCBs	Polychlorinated biphenyls
PDMS	Polydimethylsiloxane
PM1	Ultrafine particulate matters
PM10	Coarse particulate matters
PM2.5	Fine particulate matters
PTFE	Polytetrafluoroethylene
PTV	Programmable temperature vaporization
RSDs	Relative standard deviations
S/N	Signal-to-noise
SD	Standard deviation
SIM	Selected ion monitoring
SOA	Secondary organic aerosol
SPME	Solid-phase microextraction
SRTM	Shuttle radar topography mission
SVOCs	Semivolatile organic compounds

T/B	Toluene-to-benzene
TDU	Thermal desorption unit
TSP	Total suspended particles
TVOCs	Total volatile organic compounds
TWA	Time-weighted average
USA	United states of America
VOCs	Volatile organic compounds
WHO	World health organization
X/E	<i>m-,p</i> -xylenes to ethylbenzene

## INTRODUCTION

### **Characterization of the work**

This study is aimed at the development of low-cost, accurate, “green” and simple methods for the determination of the single and time-weighted average (TWA) concentrations of volatile organic compounds (VOCs) in air based on solid-phase microextraction (SPME). Also, this study is devoted to the approbation of the developed methods for determination of VOCs in ambient air.

### **The relevance of the work**

Air pollution is a serious global problem affecting human health and the environment. According to World Health Organization (WHO), in 2019, 99% of the world breathed air, the quality of which was below WHO’s limits. Air pollution is caused by various sources, including industrial emissions, coal/biofuel combustion, transportation, and agriculture. Long-term exposure to air pollution can lead to a range of health problems including lung cancer, heart disease, and respiratory illnesses. Moreover, the direct impact of air pollution on increase of COVID-19 cases has been established. Air is one of the most complex environmental objects for the analysis. There are many drawbacks associated with the sampling, sample preparation, and transportation of air samples. Air pollutants can be divided into two main groups: inorganic, which include particulate matter, NO<sub>x</sub>, SO<sub>2</sub>, CO, ozone, heavy metals, etc., and organic pollutants, which include semi-volatile and volatile organic compounds. VOCs are a group of chemicals that can evaporate from various sources, such as solid fuel combustion, vehicle emissions, industrial activities, biogenic sources, etc. Some of VOCs can have hazard effects on human health, also VOCs can contribute to formation of secondary aerosols and ground-level ozone.

Conventional methods for the determination of organic pollutants are based on sampling on sorbent tubes or in special canisters. The use of special canisters and sorbent tubes requires preliminary cleaning from possible contaminants with high-purity gases before sampling. In addition, deactivation of the inner part of the samplers is needed to prevent analytes adsorption. For analytes desorption from sorbent tubes, expensive thermal desorption equipment or toxic solvents for chemical desorption are required. To improve separation and increase the accuracy of sample analysis, cryogenic focusing of all analytes in the inlet or column of the gas chromatography (GC) must be used. These drawbacks limit the application of standard methods in developing countries. In Kazakhstan, monitoring of organic pollutants concentrations in the air has not been carried out due to these limitations. To solve these problems, the development of cost-effective, simple, and accurate methods for the determination organic pollutants in the air are required.

The most promising method for the determination of VOCs in ambient air is SPME, which excludes the drawbacks of conventional methods. SPME combines sampling and sample preparation in a single step and meets the principles of “green” analytical chemistry. SPME is based on the sorption of VOCs by a micropolymeric coating followed by the desorption of analytes directly in the GC inlet. SPME can be



used to determine single and time-weighted average VOC concentrations. SPME is the simplest sampling method for determining of VOC concentrations in air. However, there are limitations to using SPME-based methods for air analysis, such as complex calibration, losses during storage and transportation, and the main disadvantages are low accuracy and precision. Thus, the development of methods based on SPME, which can improve the existing drawbacks for the determination of single and TWA concentrations of VOCs in the air is still an important task.

**The aim of the study:** development of simple and accurate methods based on solid-phase microextraction, which can improve the current methods, for the determination of single and time-weighted average concentrations of organic pollutants in the air.

**The tasks of the study:**

- 1) To develop a low-cost and accurate method for the determination of single concentrations of more than 20 VOCs in ambient air;
- 2) Application of the developed method for the assessment of seasonal variation and spatial distribution of VOCs and identification of their possible sources in the air of Almaty;
- 3) To assess the effect of COVID-19 restrictions measures on air quality in Almaty associated with organic pollutants;
- 4) To develop a model for SPME for the determination of TWA concentrations of VOCs using finite element analysis software;
- 5) To prove that the developed model can be used for the development of an accurate method for quantification of VOCs TWA concentrations in the field using SPME.

**Objects of the study:** methods for quantification of multiple volatile organic compounds in air using solid-phase microextraction.

**The subjects of the research:** accuracy and simplicity of methods for determination of VOCs in the air; single and TWA concentrations of VOCs in the air of Almaty.

**The methods of the research**

Complex modern physicochemical research methods were used to achieve the aim and solve tasks of the research. The following methods were used in this work: solid-phase microextraction in combination with gas chromatography-mass spectrometry (GC-MS) for the analysis of air samples; scientific method for the formulation of hypotheses and design of experiments.

**The scientific novelty of the research**

- 1) A new method for the quantitation of more than 20 VOCs single concentrations based on sampling into 20 mL vials and analysis by SPME GC-MS was developed.
- 2) Seasonal and spatial variations of organic pollutants in the ambient air of Almaty were evaluated for the first time.
- 3) For the first time, the effect of the COVID-19 lockdown measures on the concentrations of organic pollutants in Almaty air was studied.
- 4) A model for SPME extraction of VOCs by fiber coating located inside the

protecting needle was developed using finite element analysis software. The sampler with an alternative geometry was proposed to increase the accuracy of the determination of TWA concentrations of VOCs.

5) A new method for the determination of TWA concentrations of VOCs in ambient air using sampler with alternative geometry and SPME fiber was developed for the first time.

### **The validity and reliability of the results**

The obtained results were valid and reliable since all experiments were carried out with one or two independent variables, while the rest of the variables were constant. The dependent variables displayed the main parameters of the methods, such as the accuracy, recovery, analyte responses, limits of detection and quantification, and reproducibility. All measurements were conducted in two – four replicates. Gas chromatography with mass spectrometric detection was used to achieve the sensitive and selective identification and separation of VOCs.

### **Relation of the thesis with research and government programs**

This research work was conducted within the framework of projects funded by the Science Committee of the Ministry of Education and Science of the Republic of Kazakhstan: Grant No. AP05133158 “Development of analytical methods, materials and equipment for cost-efficient “green” environmental monitoring” (2018-2020 yy.) and Grant No. AP09058606 “Development of method for determination of organic pollutants time-weighted average concentrations for monitoring of ambient air of Almaty” (2021-2023 yy.).

### **The main provisions to be defended**

1) The 65- $\mu\text{m}$  polydimethylsiloxane/divinylbenzene (PDMS/DVB) SPME fiber provides a better combination of detection limits (from 0.010 to 7  $\mu\text{g}/\text{m}^3$ ) and relative standard deviations (RSDs) of slopes ( $<10\%$  for 22 analytes) compared to 85- $\mu\text{m}$  Carboxen (Car)/PDMS, 100- $\mu\text{m}$  PDMS and 50/30- $\mu\text{m}$  DVB/Car/PDMS for the determination of 25 volatile organic compounds in the air.

2) The developed method based on SPME with a 65- $\mu\text{m}$  PDMS/DVB coating provides spike recoveries in the range from 90 to 105% for 20 out of 25 studied analytes.

3) The seasonal variations of 9 out of 19 studied VOCs were significant ( $p < 0.01$ ) with maximum concentrations on winter sampling days in Almaty in 2020.

4) Decreasing diameter of the diffusion path from 0.75 to 0.34 mm allows achieving better accuracy of the determination of TWA concentrations of 9 out of 13 VOCs using Car/PDMS SPME fiber exposed in a glass liner.

### **The theoretical and practical significance of the thesis**

The theoretical significance of the work is based in the development of simple and accurate methods for the determination of multiple organic pollutants in the air. Also, the theory of the determination of time-weighted average concentrations by solid-phase microextraction was improved. The proposed sampler with alternative geometry was used for improving the accuracy of the determination of TWA concentrations by SPME.

The developed methods for the determination of single and TWA concentrations of multiple volatile organic compounds in the air can be used by the environmental laboratories to conduct monitoring. The results of the investigation of seasonal and spatial variations of organic pollutants in the air of Almaty can be used by decision makers to develop activities for air quality improvement.

### **Presentation of the practical results**

The results of the thesis were reported at the international conferences such as The International Chemical Congress of Pacific Basin Societies, “Pacifichem 2021” and the XI International Beremzhanov Congress on Chemistry and Chemical Technology, 2021.

### **Publications**

The main results of this research were published in scientific papers, including:

- 4 articles in international journals with impact factors 3.11, 10.754, 3.344, and 4.927, indexed in Web of Science and/or Scopus databases;
- 1 article in the journal recommended by the Committee for Quality Assurance in the Sphere of Education of the Ministry of Education of the Republic of Kazakhstan;
- 2 patents for invention;
- 2 abstracts at international conferences and congress, including 1 abstract at foreign international conference (United states of America (USA)).

**The author's contribution** to this research work consists in the formulation of scientific questions and hypotheses, planning and conducting experiments, statistical evaluation of the obtained data and writing reports and articles based on the final results.

**The structure of the thesis.** The thesis is presented in 110 pages and contains 25 tables, 42 figures, and 161 references. The thesis consists of introduction, six sections, conclusion, list of references, and annex.

**Acknowledgments.** I would like to express my sincerest gratitude to my supervisor Assoc. Prof. Nassiba Baimatova for the continuous support during my Ph.D. study and research career, for motivation and patience, for all knowledges and skills that I gained while working with Dr. Baimatova. Assoc. Prof. Baimatova gave me the opportunity to become a part of the scientific world, and her mentoring helped me throughout my research work.

I would like to particularly thank my supervisor Prof. Jacek Koziel for his support, encouragement and for sharing invaluable advice and ideas during my research work. Also, I would like to thank Prof. Bulat Kenessov for knowledge, support, and project management, within the framework of which part of my Ph.D. thesis was completed.

I would like to express my gratitude to Prof. Dr. Duran Karakas, Prof. Dr. Serpil Yenisoy Karakas, Dr. Hatice Karadeniz and Prof. Ferhat Karaca for organization and support during my research internship at the Engineering and Chemistry Departments of Bolu Abant Izzet Baysal University. The knowledge and skills gained during the internship helped me to conduct research related to air quality analysis.

I would like to express my special thanks to my friends and colleagues from Ecology of Biosphere Laboratory of the Center of Physical Chemical Methods of

Research and Analysis (Al-Farabi Kazakh National University) for their support and assistance during my Ph.D. research. In addition, I would like to extend gratitude to my family, especially to my husband, for the moral support throughout my Ph.D. study and thesis writing.

# 1 LITERATURE REVIEW

## 1.1 The problem of air quality in the world and the importance of air quality monitoring for environmental impact assessment

Air pollution is one of the most acute problems in modern society, the spread of which and its health effects cover the whole world and require a global solution. Air pollution leads to disturbance in ecosystems and substantial economic and social damage to society. The WHO reports that in 2019, 99% of the world breathed air, the quality of which was below the WHO's limits. The Lancet Commission estimated mortality for the same year, resulting in 6.7 million premature deaths from air pollution, including deaths from household air, ambient particulates, and ozone [1].

Air pollution has a great impact on human health and can cause many diseases, such as respiratory, and cardiovascular diseases, cancer, and chronic obstructive pulmonary disease (COPD), etc. According to the 2017 global ranking, total air pollution ranked fifth among the risk factors for overall mortality worldwide [2]. The health impact of air quality depends on the type of pollutant and the duration of exposure (long or short term) [3]. However, both types of exposure can have negative effects on population health. Moreover, recent studies have revealed a direct effect of air pollution levels on the increase in COVID-19 cases [4–8].

Besides the hazardous health effects, air pollution can lead to economic losses. The economic losses related to air pollution can be caused by the effects of pollution on human health, which results in decreased work efficiency; increased number of hospitalizations; and negative effects on other fields, such as agriculture, etc. The Lancet Commission calculated the economic losses (using the cost of statistical life) in 2015 related to pollution, which amounted to 6.2% of global Gross Domestic Product (GDP) [1, p.e539]. Outdoor and indoor air pollution accounted for 82% of the economic losses. The World Bank estimated economic losses in 2019, which were equal to 6.1% of the global GDP and were associated with household and ambient air pollution by fine particulate matters (PM<sub>2.5</sub>) [9]. It was found that middle- and low-income countries were more affected by PM<sub>2.5</sub> pollution [10].

Air pollution is a part of climate change due to the same sources of emissions that affect both issues. The sources of air pollution are complex and diverse, depending on the geographical location and quality of life. The major air pollution sources can be divided into two groups: anthropogenic and biogenic. Anthropogenic sources include fossil fuel burning for heating, electricity generation, transport, industrial activities, emissions from mining and various industries, and waste incineration. While biogenic sources include dust, sea salt, emissions from volcanoes and plants [11].

Due to the variety of pollution sources, effective and complex measures are required to improve air quality. Examples include eliminating the use of low-quality fuel in transport, optimizing the public transport system in cities, and reducing the emission limits in the industrial sector, reducing, or eliminating the use of solid fuels for electricity generation and heating by power plants and households. However, one of the main steps to improve air quality is monitoring of pollutant concentrations.

Air quality monitoring is important for environmental impact assessments. The results of the monitoring are used to comply with air quality standards, estimate pollution trends, and develop effective solutions for the improvement of air quality. Also, the data obtained during monitoring can be used for the prediction of the pollutant concentration variations and identification of ambient air content. The WHO Global air quality guidelines recommend controlling the concentrations of key pollutants, which have significant effects on human health. The WHO guidelines provide thresholds and limits for fine (PM<sub>2.5</sub>), coarse (PM<sub>10</sub>), and ultrafine (PM<sub>1</sub>) particulate matters, O<sub>3</sub>, NO<sub>2</sub>, and SO<sub>2</sub> [12]. However, volatile organic compounds, which are known for their cancerogenic effects, should be controlled during air monitoring. The ambient air quality guidelines in New Zealand, developed by the Ministry of the Environment have a wider list of pollutants including CO, NO<sub>2</sub>, O<sub>3</sub>, PM<sub>10</sub>, SO<sub>2</sub>, H<sub>2</sub>S, Pb, benzene, 1,3-butadiene, formaldehyde, acetaldehyde, benzo(a)pyrene, mercury (organic and inorganic), arsenic, arsine, and chromium IV, and III [13]. In addition, the United States Environmental Protection Agency (EPA) has implemented various programs for air quality monitoring. For instance, Air Toxics Monitoring National Program that includes such pollutants as acrolein, benzene, 1,3-butadiene, carbon tetrachloride, chloroform, tetrachloroethylene, trichloroethylene, vinyl chloride, acetaldehyde, formaldehyde, naphthalene, benzo(a)pyrene, As, Be, Cd, Mn, Pb, and Ni [14].

In Kazakhstan, the National Hydrometeorological Service of Kazakhstan “Kazhydromet” is the only organization legally responsible for air quality monitoring [15]. Kazhydromet air monitoring programs include CO, NO, NO<sub>2</sub>, SO<sub>2</sub>, and total suspended particles (TSP). Measurements of PM<sub>2.5</sub> and PM<sub>10</sub> have started recently and are carried out using a limited number of monitoring stations. In the case of VOCs, only phenol and formaldehyde are determined, and the data obtained are insufficient for air quality assessment.

## **1.2 Importance of quantification of organic pollutants in the air**

Gas sampling of organic compounds is integral to analytical chemistry, with specific applications in environmental science, air pollution, process control, reaction kinetics, and toxicology. Monitoring of volatile organic compounds in the air is a very important task because these pollutants can have high concentrations in air and cause serious health risks. VOCs are a large group of chemicals, which have high vapor pressures and can originate from biogenic and anthropogenic sources [16]. Short-term exposure to individual organic pollutants can cause headaches, eyes, throat or nose irritation [17], while long-term exposure can lead to nervous and endocrine system diseases [18], respiratory diseases [19], and COPD. In addition, Alford et al. [20] demonstrated that exposure to some VOCs can be the reason of the cardiovascular diseases. The list of most toxic VOCs include formaldehyde, benzene, ethylbenzene, styrene, phenol, benzaldehyde, naphthalene, and many other compounds, and their concentrations must be monitored.

Groups of VOCs require special attention and control due to their high toxicity

and carcinogenicity. One such group is benzene, toluene, ethylbenzene and xylenes (BTEX) [21], of which benzene has carcinogenic effect and belongs to the International Agency for Research on Cancer (IARC) group 1 [22]. Toluene has lower toxicity than benzene, ethylbenzene, and xylenes. Toluene is an irritant of the central nervous system, skin, eyes, and respiratory tract. In addition, possible occurrence of headache, drowsiness, difficulty breathing, cramps and nausea may occur [23]. Ethylbenzene directly follows benzene in terms of its harmful effects on human health. High concentrations of ethylbenzene in the air irritate the eyes and respiratory tract [24]. Xylene, as toluene, decomposes into low-toxic compounds under sunlight. Its influence on humans can cause headaches, and irritation of the eyes, skin and throat, and may disrupt comfort in the gastrointestinal tract and motor coordination [25]. Monitoring of VOCs concentrations can be used for health risk assessment by calculating of carcinogenic and non-carcinogenic risks [26].

VOCs in ambient air affect the formation of ozone, secondary organic aerosols (SOA), and PM [27–29]. Ozone is one of the major components of photochemical smog [30], and has a negative impact on agriculture [31] and human health [32]. SOA or secondary organic pollutants are formed in the atmosphere during chemical or photochemical reactions, while primary organic pollutants are emitted directly from the sources. VOCs can enter the atmosphere from various sources, such as solid and fossil fuels combustion, transport-related sources, industrial facilities, waste incineration or burning, and solvent and paint usage [29, p.9-11].

The determination of VOCs concentrations in the ambient air can be used for possible source identification based on the ratios of individual organic pollutants. The BTEX ratios can be useful for identifying sources related to coal/biomass combustion, and industrial and vehicle emissions. Toluene-to-benzene (T/B) ratio above 1 indicates the main contribution of solid fuel combustion, while ratios below 1 indicate traffic-related sources [33]. In addition, the photochemical age of air masses at sampling sites can be determined using *m,p*-xylenes-to -ethylbenzene (X/E) ratio [34]. Alkanes are indicators of air pollution from the evaporation or combustion of gasoline and are also associated with emissions from solid fuel combustion. The ratio of the concentrations of isopentane to *n*-pentane can determine whether air pollution is associated with coal burning [35]. Methyl tert-butyl ether is an indicator of air pollution from vehicle exhaust [36,37]. Propane, *n*-dodecane, *n*-undecane, naphthalene, acetone, 2-butanol, toluene, trimethylbenzenes and isopropyl alcohol are released into ambient air from passenger vehicles in which gasoline or diesel is used as fuel [38].

Quantification of organic pollutants in ambient air is an important part of an air monitoring program, however, its determination is complicated due to expensive and time-consuming conventional methods of sampling and analysis.

### **1.3 The conventional methods for the determination of volatile organic compounds in the air**

Ambient air quality standards establish limits for the average concentrations of pollutants during periods of 1 h, 8 h, 24 h, and even 1 year. Occupational exposure

standards vary from acute (typically defined as ~15 min) to chronic (typically defined on an ~8-10 h per day basis and ~40 h workweek). While the measurement of single VOCs concentrations is sometimes possible, it typically requires sophisticated instrumentation or a trade-off between specificity and sensitivity. Average concentrations can be established using the results of single measurements or time-weighted average (TWA) sampling (Figure 1). TWA sampling allows higher cost efficiency because it decreases the number of analyses and instrument sample throughput. Compared to single (e.g., instantaneous, rapid collection into a sampling vessel such as a syringe) measurements, TWA sampling can provide better accuracy due to its sensitivity to all fluctuations in analyte concentration. Periods between single measurements can be quite long, resulting in overlook of major ramps or drops in the concentration. In addition, determination of TWA concentrations using single measurements require large number of samples. On the other hand, drastic changes in VOCs concentrations can be easily omitted with TWA sampling.

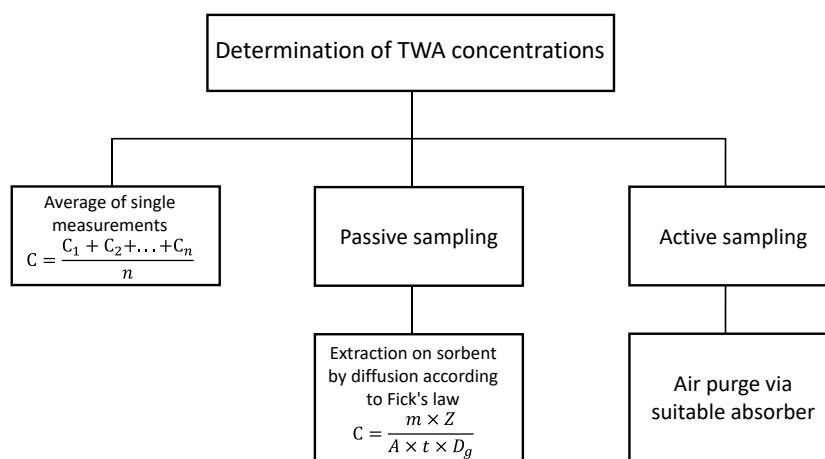


Figure 1 – Sampling approaches for determination of TWA concentrations

There are several methods for TWA quantification of VOCs in the air based on passive and active sampling (Figure 1). Active sampling is based on the purging of air via a suitable liquid or solid cumulative medium, or through samplers (canisters, calibrated bulbs) [39]. Passive sampling is an alternative to active air sampling, which does not require any additional major sampling equipment with moving parts and a power supply. Passive sampling is based on the molecular diffusion of the free gas phase of organic pollutants through the barrier between sampling and extraction media. This barrier is responsible for the extraction rate of molecules, which is limited by diffusion through it [40]. In most laboratories, passive sampling is conducted using sorbent badges, sorbent tubes or Radiello samplers [41–43]. After sampling, sorbent or cartridge is retrieved and VOCs are either (a) eluted from a tube or cartridge by a suitable solvent followed by injection of the eluate to GC or (b) undergo thermal desorption, focusing, and introduction to a GC via a transfer line.

However, the use of thermal desorption is associated with several problems.



Thermal desorber is a costly upgrade, which requires additional maintenance and expenses. Desorption of analytes can be slow and requires additional focusing before or in front of the GC column. Cryogenic focusing is required for most volatile analytes. After solvent desorption, the peaks of the most volatile analytes overlapped by a solvent peak. The detection limits after solvent elution are higher than those after thermal desorption.

Conventional methods for the determination of single and TWA concentrations of VOCs in the air are commonly based on sampling to polymer, glass, or stainless steel containers [44–46], purging via suitable sorbent followed by thermal or chemical desorption to GC [47,48] and on-site analysis using portable instruments or mobile stations [49–51]. Portable instruments do not provide sufficient accuracy but are useful for obtaining single VOC concentrations. The above-mentioned standard methods have the following disadvantages: cleanup of samplers by ultra-high purity helium, chemical desorption requiring a large volume of toxic solvents, the need of expensive additional devices for desorption and/or water trapping during thermal desorption, cryofocusing of analytes, and possible adsorption of analytes in the transfer lines of the thermal desorption unit, which can lead to cross-contamination and inaccurate results. All these disadvantages limit the use of standard methods for air monitoring in developing countries. The development of low-cost air sampling methods can solve existing problems. Cheap, robust, and accurate approaches are important for air quality assessment that requires analysis on a daily basis and at multiple sampling points. The low-cost methods are required for developing countries such as Kazakhstan that do not have the opportunity to purchase monitoring stations or use high-cost methods but need to assess air quality and its improvement.

#### **1.4 The solid-phase microextraction for determination of volatile organic compounds in the air**

1.4.1 The principles and advantages of solid-phase microextraction for determination of volatile organic compounds in the air

Solid-phase microextraction represents an advantageous alternative to conventional methods for air analysis, which partially solves the described problems [52–54]. SPME is a simple, “green”, fast, low-cost, and reusable method that combines sampling and sample preparation in one step. Such a combination allows the avoidance uncertainties and errors during sample preparation, which effects method accuracy [55]. SPME is based on the sorption of analytes by a thin (<100 μm) coating made of a pure polymer absorbent or polymer-adsorbent mixture (Figure 2). Compared with the most diffusion-based sampling methods, solid-phase microextraction does not require a separate thermal desorption unit because desorption is conducted directly in the injection port of a gas chromatograph. Several available commercial SPME fibers can detect all VOCs and semi-VOCs (SVOCs) or a narrow group of analytes depending on their polarity and volatility.

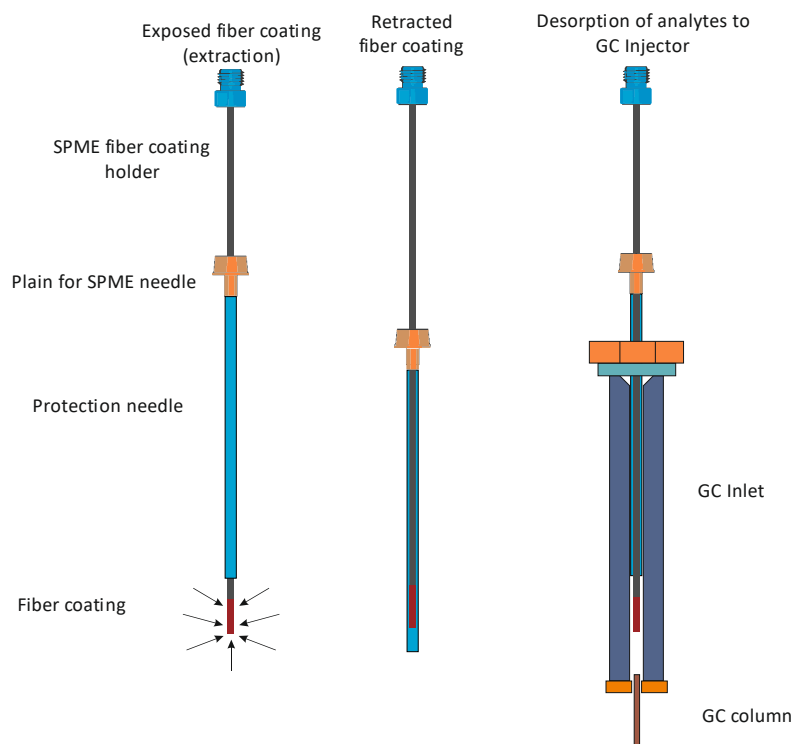


Figure 2 – Sampling and sample preparation by SPME

Three main approaches are used for the quantification of VOCs in the air by SPME:

- extraction by exposed fiber in the field;
- sampling air into a container, Teldar bags, etc., followed by exposed fiber extraction;
- extraction by retracted fiber (inside the protecting needle of the SPME device).

These methods can be used to determine single and TWA concentrations depending on the extraction time. Extraction by exposed SPME fiber is widely used for quantification of VOCs in ambient air [56,57], indoor air [58,59], and breath air [60]. However, the air flow rate had a significant impact on the mass loading rate by exposed fiber. Also, SPME fiber can be easily saturated when directly exposed to air with high concentrations of VOCs.

TWA sampling using SPME can be performed using either an exposed (<1-2 h sampling time) or retracted fiber. TWA SPME has been used for sampling outdoor and indoor air, exhaust gases from cars and technological processes [55, p.173,61,62]. When the fiber is located inside the protecting needle, the extraction rate is much slower than that of the exposed fiber and can be controlled by the depth of fiber retraction as the diffusion path length  $Z$  [54, p.1515]. The diffusion process occurs through the boundary layer between the tip of the SPME fiber and the tip of the needle housing [54, p.1514]. It avoids fiber saturation and provides continuous extraction of VOCs over long periods (>24 h). TWA concentration, which was determined by SPME

fiber, can be calculated using simplified Fick's first law (1):

$$C_{TWA} = \frac{m_f \times Z}{A \times t \times D} \quad (1)$$

where:  $C_{TWA}$  – time-weighted average concentration of an analyte, mg/m<sup>3</sup>;

$m_f$  – analyte mass extracted by fiber coating, mg;

$Z$  – diffusion path length, m;

$A$  – cross sectional area of a protective needle, m<sup>2</sup>;

$t$  – extraction (sampling) time, s;

$D$  – diffusion coefficient of an analyte, m<sup>2</sup>/s.

Compared to other TWA sampling approaches, SPME provides greater cost efficiency because analytes can be rapidly desorbed from a coating to a GC in a standard configuration without additional thermal desorber. It simplifies maintenance and provides the efficient use of an instrument (GC). The needle-trap device (NTD) is a great alternative to SPME; however, its use is associated with less reliable thermal desorption in a GC port, which can require additional modification.

Environmental conditions such as temperature, humidity, and wind speed can have substantial effects on the extraction efficiency and sampling rate during SPME. Martos et al. established that there is no significant difference in mass loading rate of analytes with partition coefficient ( $K$ ) less than 5000 between static and dynamic sampling (laminar and turbulent flows) with the same exposure time for analytes. The  $K$  values between air and the 30- $\mu$ m and 100- $\mu$ m PDMS fiber coatings were used. The authors suggested that the partition coefficient ( $K$ ) can be calculated using the literature values of the analyte heat of vaporization ( $\Delta H^v$ ) and allow the prediction of  $K$  values at different temperatures using theoretical equations without experiments. The mass uptake of the analytes by the PDMS fiber was affected by humidity higher than 90% at 290, 298, and 310 K [63]. This effect can be eliminated using a more hydrophobic fiber coating.

According to Chen et al. environmental conditions such as humidity, air flow rate and ozone concentration do not effect SPME device sampling rate using 75- $\mu$ m Car/PDMS in retracted mode. However, high concentrations of ozone the sampling environment can react with alkanes on the fiber and lead to destruction of the fiber coating. Temperature affects the compounds in different ways. An increase in temperature leads to a slight increase in the mass loading rate of alkanes with a high boiling point and a decrease in it for alkanes with a low boiling point [64]. It was established that the deactivated protecting needle of the SPME fiber and fiber coating 75- $\mu$ m Car/PDMS allows to get closer to the theoretical values of the sampling rate.

#### 1.4.2 Calibration approaches for determination single and time-weighted average concentrations of volatile organic compounds by solid-phase microextraction

Calibration is a crucial step in the quantitative determination of analytes in air samples. Precise preparation of standard gas mixtures with known analyte

concentrations is required for calibration by SPME. Standard gas-generating vials (in vial gas-generating system) that contain semipermeable membranes or sorbents are one of the methods for the preparation of gaseous standards [65–67]. Mostly, SPME calibrations are based on the equilibrium mode. Equilibrium should be reached between the air sample and the SPME fiber coating. If the equilibrium time is long, the pre-equilibrium (non-equilibrium) mode can be used [68,69]. Also, exhaustive extraction, which is not often used for SPME, can be used for calibration. The main principle of exhaustive extraction is that analytes are fully extracted by the SPME fiber coating. However, this type of extraction can only be used for samples with small volumes and large distribution constants. The cold fiber and multiple SPME are commonly used for exhaustive extraction. Cold fiber approach is based on simultaneous cooling of the fiber assembly and heating of the sample matrix [70]. The multiple extraction method is based on repeated extractions from the sample and can be calculated using multiple extractions, even if the total amount of analytes is not extracted [71]. In addition, multiple extraction can be used for determination of distribution constant between fiber and sample. However, both approaches are unsuitable for air analysis.

Traditional methods of calibration can be used for quantification of VOCs single concentrations in air samples based on external or internal standards, or standard addition methods [72]. External standard calibration is based on the analysis of a series of gaseous standard solutions with known concentrations, followed by the analysis of air samples using similar analytical parameters. Application of external standard method for air analysis required using ‘zero’ (clean) air as matrix for preparation of gas mixture. Also, loss of analytes during the storage and transportation of air samples should be controlled.

Internal standard calibration can be used to avoid the effect of analyte losses and to control changes in environmental conditions and the work of measurement devices. Internal standard calibration is based on the addition of an internal standard to calibration solutions and samples. For calibration plots, the ratio between the analytical signals of analytes and internal standard in solution with different concentrations of analytes and the constant concentration of the internal standard is used. However, finding an appropriate internal standard for complex samples is difficult task [70, p.186, 72, p.172].

Standard addition method is based on the addition of standard solutions of known concentrations to samples, containing unknown amounts of analytes. The analyte concentrations in the sample is calculated by using analytical characteristics of the calibration plot (slope and intercept). Standard addition method is used for elimination of effect of complex sample matrix and for avoiding usage of ‘zero’ air [73]. However, using the standard addition method for samples with different matrices leads to the analysis of a large number of samples, which is required for each unknown matrix [72, p.170].

As previously mentioned, the SPME fiber coating should be retracted inside the protecting needle for determination of TWA concentrations of VOCs in the air during

long sampling times. In this mode, the analytes reach the fiber coating due to their diffusion from the sample to the coating through the open part of the protection needle [72, p.176]. One of the calibration methods that based on diffusion is described by Fick's first law of diffusion (Equation 1) [70, p.187]. The calibration by liquid injection can be used to determine analyte masses extracted by the fiber coating during TWA sampling. Calibration by liquid injection should be performed if analytes are completely transferred from the SPME fiber and during the direct injection of the liquid standard. The transfer efficiency can be affected by the liner and/or column dimensions, the cross-sectional area between the inner part of the GC liner and the outer part of the column, or the presence of wool. However, the authors [74] concluded that it is possible to use a common SPME liner for calibration by liquid injection.

#### 1.4.3 Uncertainties, limitations, and problems of air analysis using solid-phase microextraction with a possible solution

SPME is widely used in environmental analysis. According to Llompart et al. [75] most of the developed methods based on SPME are toward analysis of water samples and less to analysis of solid and air samples. The lower application of SPME for air analysis can be caused by difficulties in quantification due to the effect of atmospheric parameters (temperature, humidity, and wind) on extraction efficiency [76–79], problems with reproducibility, and loss of analytes during storage and transportation of air samples [80]. The use of SPME fibers requires constant control of the effectiveness and performance of the fiber coating when analyzing a large number of samples (>100) [81]. Another limitation of wide application of SPME to air analysis is related to time- and labor-consuming calibration procedures that require standard gas-generation systems [82]. Slow or partial desorption of analytes from the fiber coating after extraction can lead to a decrease in the method accuracy [83]. The authors [64, p.2008, 83, p.5] mentioned the differences between the experimental and theoretical values during the determination of TWA concentrations of volatile organic compounds by SPME. Such differences can be caused by the desorption of analytes from the fiber coating during extraction, adsorption on the metallic surface of the SPME protecting needle, or significant drop in analyte concentrations in air. The application of SPME requires accurate sampling and sample preparation procedures. The possible limitations of SPME for the analysis of air samples and their solutions are presented in Table 1.

SPME in combination with other sampling and sample preparation (extraction) techniques is used for determination of semi-volatile organic compounds in air [84–87]. The Raeppl et al. developed a method for the determination of 30 pesticides in air using accelerated solvent extraction coupled with SPME. Sampling was carried out using glass fiber filters and XAD-2 resin traps. The developed method allows for a decrease in the method detection limit and matrix effect in comparison with conventional methods. The use of pressurized solvent extraction in combination with solid-phase extraction and SPME allow determination of approximately 150 organic compounds with different polarities and properties [85, p.8].

Table 1 – The limitations of SPME application in air analysis

Sampling method	The limitations	Possible solutions	Ref.
1	2	3	4
Sampling by exposed or retracted SPME fiber	Losses of analytes during storage or transportation	This problem can be eliminated by: <ul style="list-style-type: none"> <li>– using highly efficient sorbent of SPME fiber coating;</li> <li>– low temperature (subambient) for storage and transportation;</li> <li>– strong sealing of fiber with inert material (Teflon) or septum;</li> <li>– on-site analysis or using bed dry ice for transportation.</li> </ul>	[53,55,58,64,68,78,79,82,83,88,89]
	The competitive adsorption on SPME fiber coating	<ul style="list-style-type: none"> <li>– It can be solved by using shorter sampling time and static mode for low affinity of analytes to fiber coating.</li> <li>– Cross contamination during long storage time with reusable Teflon cap. To avoid cross contamination, it is necessary to use highly efficient sorbent or conditioning at high temperature of sealing material.</li> </ul>	
	The using standard gas generating devices that lead to time- and lab-consuming calibration	It can be solved by: <ul style="list-style-type: none"> <li>– using 20 mL vials for sampling and calibration;</li> <li>– preparation of standard gas mixture using liquid solutions.</li> </ul>	
	Adsorption of analytes on metallic surface of protecting needle during extraction by retracted fiber	This problem can be solved by: <ul style="list-style-type: none"> <li>– using deactivated protecting needle;</li> <li>– increasing of extraction temperature (partially solved);</li> <li>– using glass GC liner instead of SPME protecting needle.</li> </ul>	
	Uncertainties and complexity related to calibration	<ul style="list-style-type: none"> <li>– Fiber-to-fiber uncertainties. Solution: daily calibration of each SPME fiber or using reference standard with known concentration are needed.</li> <li>– Strict control of extraction time if calibration and analysis carried out at non-equilibrium condition.</li> <li>– Narrow linear range for dynamic mode. Solution: using static mode.</li> <li>– Sampling of non-volatile or non-stable analytes. Solution: using derivatizing agent on SPME fiber.</li> <li>– Fragile fiber coating or protecting needle. Solution: constant SPME device protection from damages.</li> </ul>	

Table 1 continued

1	2	3	4
Sampling in 20 mL vial/Tedlar bag/gas sampling bulb	Losses of analytes during storage or transportation	This problem can be eliminated by: – analyze sample as soon as possible; – using 1 L jars for storage and transportation filled with sampled air; – try to avoiding analytes transformation/decomposition in vials; using cooler for storage and transportation.	[56,57, 69,73,77]
	The competitive adsorption on SPME fiber coating	To solve this problem, authors suggested to use 2 cm SPME fiber coating due to higher sorption capacity.	
	Uncertainties and complexity related to calibration	– Strict control of extraction time if calibration and analysis carried out at non-equilibrium condition. – Reactive VOCs with low molecular weight can not be accurately quantified by Tedlar/SPME. Solution: using another device for sampling. RSDs about 25% in 20 mL that higher than using 250 mL calibrated gas sampling bulbs. Solution: strict control of analytes losses.	
Sampling by using additional devices (bubblers, filters, etc.)	Losses of analytes during storage or transportation	The sampling and sample preparation were conducted by standard method that based on the bubbler impingers. Authors placed impingers to cool box for avoiding losses of analytes during sampling.	[81]
	Uncertainties and complexity related to calibration	It is necessary to use internal standard for calibration process for improving method accuracy.	

### 1.5 Section conclusion

Monitoring of volatile organic compounds in ambient air is important for environmental impact and health risk assessment. The standard methods for quantification of VOCs are based on the sampling of special canisters or purging of air through a suitable sorbent, followed by thermal or chemical desorption. These methods require time- and labor-consuming calibrations, cleaning of samplers (canisters) using ultra-pure inert gases, toxic solvents for chemical desorption, and/or additional expensive equipment for thermal desorption. All of these drawbacks limit the application of standard methods in developing countries, such as Kazakhstan. The number of methods have been developed by researchers to overcome the above-mentioned disadvantages of conventional methods. One alternative is solid-phase microextraction, which is a solvent-free method that combines sampling and sample preparation in one step and does not require additional devices. As described in the previous sections, there are a number of SPME methods for the determination of VOCs in ambient and indoor air. However, there are still limitations for using the developed SPME method for daily monitoring or analysis in environmental laboratories.

Methods based on SPME face problems related to reproducibility and accuracy compared with standard methods. In addition, the loss of analytes from the SPME fiber coating during storage and transportation, quantification of a low number of analytes, and time-consuming experiments and calibration required to develop a method for determining TWA concentrations limit the widespread use of SPME for air analysis. In this study, the following tasks were proposed to eliminate the existing drawbacks of SPME applications for determination the single and TWA concentrations of VOCs in ambient air:

- to develop a low-cost and accurate method for the determination of single concentrations of more than 20 VOCs in ambient air;
- application of the developed method for assessment of the seasonal variation and spatial distribution of VOCs and identification of possible sources in the air of Almaty;
- to assess the effect of COVID-19 restriction measures on the air quality in Almaty;
- to develop a model for SPME extraction for determination of TWA concentrations of VOCs using a finite element analysis-based model;
- to prove that the developed model can be used for the development of an accurate method for quantification of VOCs TWA concentrations in the field using SPME.



## **2 DEVELOPMENT OF METHOD FOR LOW-COST QUANTITATION OF MULTIPLE VOLATILE ORGANIC COMPOUNDS IN AIR USING SOLID-PHASE MICROEXTRACTION**

### **Preamble**

The part of materials and results described in this section have been published in research articles “Ibragimova O.P., Baimatova N., Kenessov B. Low-cost quantitation of multiple volatile organic compounds in air using solid-phase microextraction // Separations. – 2019. – Vol.6. – p. 1-17” [57, p.1-17] and reprinted with the journal permissions (Annex A). The copyright to these materials belongs to the MDPI, and any request for further use of this information should be requested from them. The materials are licensed under the Creative Commons Attribution 4.0 International License. To view a copy of this license, visit <http://creativecommons.org/licenses/by/4.0/> or send a letter to Creative Commons, PO Box 1866, Mountain View, CA 94042, USA.

### **2.1 Introduction**

Current standard sampling approaches for quantification of VOCs in air [90] are mainly based on collecting air samples into evacuated canisters [44, p.5, 91] or trapping analytes onto sorbent tubes [47, p.5, 92] followed by the analysis on a gas chromatograph with a chosen detector, mostly being flame-ionization (FID) or mass spectrometry. Despite good reliability, these sampling techniques are quite complex, labor- and time-consuming, as well as requiring additional costly equipment. Air sampling by standard methods based, e.g., on sorbent tubes, requires additional equipment such as an air sampling pump and a thermal desorption system connected to a gas chromatograph. Before air sampling, it is necessary to thoroughly clean sorbent tubes from possible contaminants and residues from previous sampling by highly pure helium. In order to solve these problems, it is necessary to reduce the volume of organic solvents used for extraction, or completely exclude them; fully or partially automate the sampling process; integrate the sampling and measurement stages; and reduce laboratory work and time costs. Additional problems may include carryover of analytes and clogging of the cryogenic focusing system [93], which considerably limit the application of standard methods. Therefore, low-cost, simple and solvent-free methods for quantification of VOCs in the air combining sampling and sample preparation in one step are needed. Solid-phase microextraction that is based on extraction of VOCs by a micro coating, followed by desorption in a GC injection port, meets these requirements [94]. SPME is widely used for the determination of VOCs in ambient air (Table 2), indoor air and different emissions [55, p.182, 68, p.828, 88, p.50, 95–101]. Methods based on SPME do not need a pump, a thermal desorption system, and any additional equipment, which reduce the cost of analysis [102,103]. Desorption of analytes is fast resulting in narrow peaks of analytes without a cryogenic focusing.

Despite the high efficiency of the described methods for determination of VOCs in air by SPME (Table 2), thereAir Sampling and Analysis of Volatile Organic Compounds with Solid Phase Microextractio are still challenges limiting their application in routine and research environmental laboratories. Some authors report limitations due to labor-intensive calibration, i.e., requirements for construction of gas

generation system with a known concentration of analytes [62,69,78,104]. Most methods require using high-purity gases for preparation of calibration samples, which can be difficult to purchase and prepare. Baimatova et al. [56] developed a very simple, automated and accurate method for quantification of BTEX using SPME and successfully applied it for the analysis of ambient air in Almaty, Kazakhstan. Sampling was conducted with 20 mL crimp top vials, which were transported to the laboratory, located on the Combi PAL (CTC Analytics, Switzerland) autosampler tray and automatically analyzed using GC-MS. To simplify the method, the authors used standard addition calibration, which did not require any additional equipment and pure gases. The only major drawback of this method was that it allowed quantification of only four analytes [56, p.48], while more than 100 organic compounds are present in outdoor air of Almaty [105]. Lee et al. [69, p.492] developed the method for determination of 36 VOCs. However, the sampling was done into Tedlar bags, which did not allow automation. In addition, the calibration was carried out with a standard gas mixture of VOCs in pure nitrogen.

The objective of this study was to improve the method developed by Baimatova et al. [56, p.48] for quantitation of >20 VOCs in 20 mL ambient air samples using SPME and GC-MS. During this study, SPME fiber, extraction, desorption and storage times were optimized. The developed method was applied for quantification of chosen VOCs in outdoor air of Almaty, Kazakhstan.

Table 2 – Methods for quantification of organic compounds in ambient air by exposed SPME fibers

Sampling Principle	SPME Fiber, Extraction Time	Instrument	Analytes	LOD ( $\mu\text{g}/\text{m}^3$ )		Ref.
1	2	3	4	5		6
SPME from open air	75- $\mu\text{m}$ Car/PDMS, 100- $\mu\text{m}$ PDMS, 20 min	GC-AED		Car/PDMS	PDMS	[95]
			Methanethiol	0.04–0.06	4	
			Dimethyl sulfide	0.003–0.004	2	
			Isopropanethiol	0.005–0.007	2	
			Isobutanethiol	0.003–0.004	0.7	
SPME from static or moving air	75- $\mu\text{m}$ Car/PDMS, 1 min	GC-FID	Methanol	2–5		[88]
			Acetone			
			Dichloromethane			
			Methyl ethyl ketone			
			Ethyl acetate			
			Dichloroethane			
			Methyl isobutyl ketone			
			Toluene			
			Butyl acetate			
			Ethylbenzene			
			<i>p</i> -Xylene			
SPME from fan-blown air	65- $\mu\text{m}$ PDMS/DVB, 2 h	GC-MS	$\Delta^3$ -Carene	n/a		[78]
			$\alpha$ -Pinene			
			Limonene			
			Pinonaldehyde			
			Pinonic acid			
Dimethylamine + ethylamine						

Table 2 continued

1	2	3	4	5	6
Air purging via bubbler impinger with KOH solution, HS SPME	75- $\mu$ m Car/PDMS,	GC-MS	HCN	0.16	[81]
	5 min				
Sampling on XAD-2 resin, accelerated solvent extraction with ACN, dilution with water, DI SPME	100- $\mu$ m PDMS,	GC-Dual ECD	22 PCBs	$2 \times 10^{-5}$ – $4.9 \times 10^{-3}$	[87]
	40 min		19 OCPs		
Sampling of PM10 on quartz fiber filter, microwave extraction with ethanol-water mixture, dilution with water and DI SPME	50/30- $\mu$ m DVB/Car/PDMS, 5 min	GC-MS/MS	Tripropyl phosphate	20	[106]
			Tri-n-butyl phosphate	40	
			Tris(2-chloroethyl) phosphate	70	
			Tris(1-chloro-2-propyl) phosphate	42	
			Tris(1,3-dichloro-2-propyl) phosphate	138	
			Triphenyl phosphate	51	
			Tricresyl phosphate	60	
SPME from open air	100- $\mu$ m PDMS, 30-45 min	GC-MS	BTEX	1–100	[107]
			Propylbenzene		
			1,3,5-Trimethylbenzene Butyl benzene alkanes (C <sub>5</sub> , C <sub>10</sub> –C <sub>27</sub> )		
Sampling to Tedlar bags, SPME	75- $\mu$ m Car/PDMS, 15 min	GC-MS	36 VOCs	0.01–0.93	[69]
Sampling into 20-mL vials, SPME	100- $\mu$ m PDMS, 3 min	GC-MS	Benzene	5	[56]
			Toluene	2	
			Ethylbenzene	2	
			<i>o</i> -Xylene	2	
Sampling into 20-mL vials, SPME	65- $\mu$ m PDMS/DVB, 10 min	GC-MS	25 VOCs	0.01–6.9	This study

Notes: n/a—not available; ACN – acetonitrile; AED – atomic emission detector; BTEX – benzene, toluene, ethylbenzene, xylenes; Car – Carboxen; DI – direct immersion; DVB – divinylbenzene; ECD – electron capture detector; FID – flame ionization detector; GC – gas chromatography; HS – headspace; LOD – limit of detection; MS – mass spectrometry; MS/MS – tandem mass spectrometry; OCPs – organochlorine pesticides; PCBs – polychlorinated biphenyls; PDMS – polydimethylsiloxane; SPME – solid-phase microextraction; VOCs – volatile organic compounds.

## 2.2 Materials and methods

### 2.2.1 Chemicals

Analytes of interest were chosen according to the literature review of VOCs determination in ambient air in different cities [108–113] and previous studies of compounds detected in the exhausts of six arbitrarily chosen cars of different models and production years [105]. Chosen analytes belong to several classes of pollutants having various physicochemical properties (Table 3). All solutions were prepared in methanol (purity  $\geq 99.9\%$ ) that was obtained from Sigma-Aldrich (St. Louis, MO,

USA). Helium (purity > 99.995%) was obtained from “Orenburg-Tehgas” (Orenburg, Russia).

Table 3 – The list of chosen VOCs and their physical properties

Compound	Purity (%)	Origin	CAS No.	Molar mass (g/mol)	Boiling Point (°C)	
2,2,4-Trimethylpentane	≥99.5	Sigma-Aldrich (St. Louis, MO, USA)	540-84-1	114.2	99	
<i>n</i> -Heptane	≥99.0	Reachem LLO (Moscow, Russia)	142-82-5	100.2	98	
Methyl ethyl ketone	≥98.0		78-93-3	72.11	80	
Methylene chloride			75-09-2	84.93	40	
Benzene	≥99.8	EKOS-1 LLP (Moscow, Russia)	71-43-2	78.11	80	
<i>n</i> -Decane	≥99.5		124-18-5	142.3	174	
1,1,2,2-Tetrachloroethylene	≥99.5	Sigma-Aldrich (St. Louis, MO, USA)	127-18-4	165.8	121	
Toluene	≥99.8	EKOS-1 LLP (Moscow, Russia)	108-88-3	92.14	111	
1,2-Dichloroethane	≥99.0	Component-reactive LLO (Moscow, Russia)	107-06-2	98.96	83	
<i>n</i> -Undecane	≥99.0	LLO Ekroschem (St. Petersburg, Russia)	1120-21-4	156.3	196	
Ethylbenzene	≥99.0	Sigma-Aldrich (St. Louis, MO, USA)	100-41-4	106.2	136	
<i>m</i> -Xylene			108-38-3	106.2	139	
<i>p</i> -Xylene			106-42-3	106.2	138	
Propylbenzene			103-65-1	120.2	159	
<i>o</i> -Xylene			95-47-6	106.2	144	
Chlorobenzene			≥99.5	108-90-7	112.6	132
1,3,5-Trimethylbenzene			≥99.0	LLO Ekroschem (St. Petersburg, Russia)	108-67-8	120.2
1,2,4-Trimethylbenzene	≥98.0	Topan LLP (Uralsk, Kazakhstan)	95-63-6	120.2	169	
3-Picoline	≥99.0	Sigma-Aldrich (St. Louis, MO, USA)	108-99-6	93.13	144	
Benzaldehyde	≥98.0	Chemregion LLO (Nizhniy Novgorod, Russia)	100-52-7	106.1	178	
<i>n</i> -Hexadecane	≥99.0	Sigma-Aldrich (St. Louis, MO, USA)	544-76-3	226.4	287	
Naphthalene	≥99.0		91-20-3	128.2	218	
Phenol	≥99.5	Thermo Fisher Scientific (Waltham, MA, USA)	108-95-2	94.11	182	
Acenaphthene	≥99.0	Sigma-Aldrich (St. Louis, MO, USA)	83-32-9	154.2	279	
Fluorene	≥98.0		86-73-7	166.2	295	

### 2.2.2 Gas chromatography-mass spectrometry conditions

All analyses were conducted on a 7890A/5975C Triple-Axis Detector diffusion pump-based GC-MS (Agilent, Wilmington, DE, USA) equipped with a split/splitless inlet and MPS2 (Gerstel, Mülheim an der Ruhr, Germany) autosampler capable of automated SPME. The inlet was equipped with a 0.75 mm ID SPME liner (Supelco, Bellefonte, PA, USA) and operated in splitless mode. For separation, a 60 m × 0.25 mm DB-WAXetr (Agilent, Santa Clara, CA, USA) column with a film thickness of 0.50 μm was used at the constant flow of He (1.0 mL/min). Oven temperature was programmed from initial 35 °C (held for 5 min) to 150 °C (held for 5 min) at the heating rate of 10 °C/min, then to 250 °C (held for 7 min) at the heating rate of 10 °C/min.

Total GC run time of the analysis was 38.5 min. The MS detector worked in selected ion monitoring (SIM) mode. All ions were divided into six consequently detected groups for better shape of peaks and lower limits of detection (Table 4).

Table 4 – MS detection program of analytes in SIM mode

No.	Retention Time (min)	Group No.	Analyte	Quantification Ion $m/z$ (amu (dwell))	Confirmation Ions $m/z$ (amu (dwell))	Group Start Time (min)
1	5.1	1	2,2,4-Trimethylpentane	57 (100)	56, 41 (50)	0
2	5.5		<i>n</i> -Heptane	43 (50)	41 (50)	
3	9.9		Methyl ethyl ketone	43 (50)	72 (50)	
4	10.4	2	Methylene chloride	49 (100)	84 (50)	10.2
5	10.8		Benzene	78 (100)		
6	11.8		<i>n</i> -Decane	142 (100)		
7	12.6	3	1,1,2,2-Tetrachloroethylene	166 (50)	164 (50)	12.2
8	13.1		Toluene	91 (100)		
9	13.5		1,2-Dichloroethane	62 (100)	64 (50)	
10	13.8		<i>n</i> -Undecane	156 (100)		
11	14.9		Ethylbenzene			
12	15.0		<i>m</i> -Xylene	106 (100)		
13	15.1		<i>p</i> -Xylene			
14	15.7	4	Propylbenzene	105 (100)		15.5
15	15.9		<i>o</i> -Xylene	106 (50)		
16	16.5		Chlorobenzene	112 (100)	77 (50)	
17	17.0		1,3,5-Trimethylbenzene	105 (100)		
18	17.7		1,2,4-Trimethylbenzene			
19	18.1		3-Picoline	93 (100)	66 (50)	
20	23.4	5	Benzaldehyde	77 (100)		22.0
21	24.8		<i>n</i> -Hexadecane	57 (100)	43 (100)	
22	27.9		Naphthalene	128 (100)		
23	31.0	6	Phenol	94 (100)		30.0
24	33.7		Acenaphthene	153 (100)		
25	36.8		Fluorene	166 (100)		

An example of a chromatogram is shown in Figure 3. Peaks were identified using retention times of each analyte, which were preliminarily determined by analyzing standard solutions of pure analytes and confirmed in full scan ( $m/z$  10–250 amu) mode of the MS detector. Optimal dwell time for each ion was 50–100 ms. The temperatures of MS interface, ion source and quadrupole were 250, 230 and 150 °C, respectively.

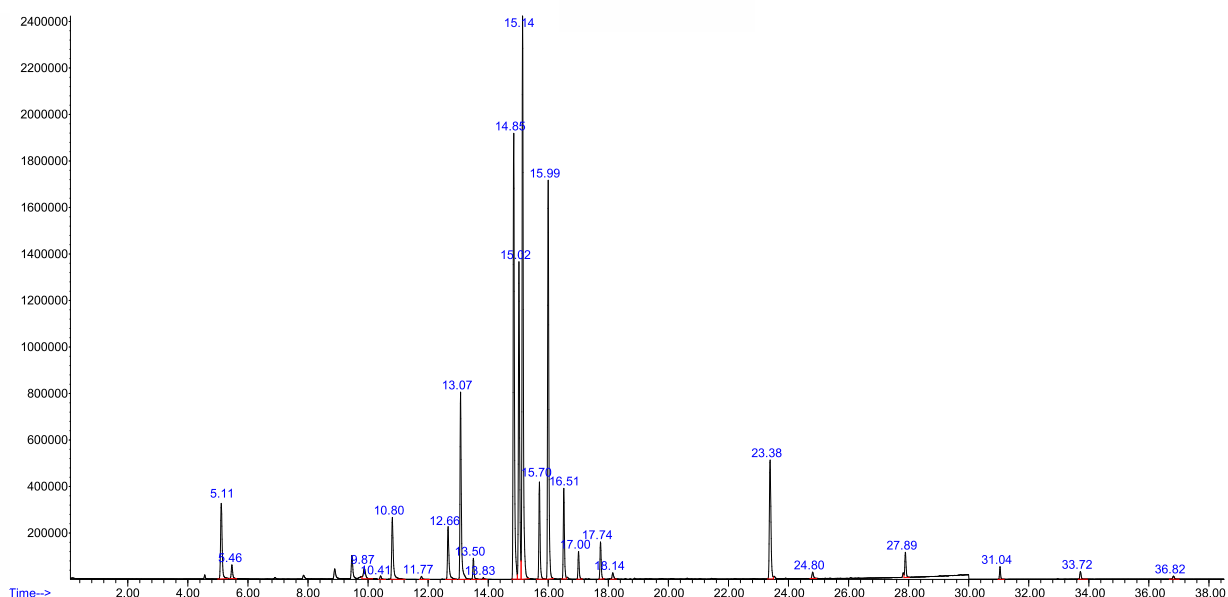


Figure 3 – Chromatogram obtained using the developed method based on SPME-GC-MS of air sample with  $C_{add} = 100 \mu\text{g}/\text{m}^3$

### 2.2.3 Selection of the optimal solid-phase microextraction fiber

Standard addition calibration plots were obtained for all 25 analytes using the four most common commercially available SPME fibers: 85  $\mu\text{m}$  Car/PDMS, 100  $\mu\text{m}$  PDMS, 65  $\mu\text{m}$  PDMS/DVB and 50/30  $\mu\text{m}$  DVB/Car/PDMS (all—from Supelco, Bellefonte, PA, USA). The calibration process was the same as described by Baimatova et al. [56, p.48]. Calibration samples were prepared by adding 1.00  $\mu\text{L}$  of a standard solution of analytes (0.50, 1.00, 2.00 and 4.00  $\text{ng}/\mu\text{L}$  for benzene, toluene and alkanes; and 0.050, 0.100, 0.200 and 0.400  $\text{ng}/\mu\text{L}$  for other analytes) into the 20 mL crimp-top headspace vial (HTA, Brescia, Italy) filled with laboratory air. Ranges of concentrations of VOCs added to calibration samples were chosen in order to cover their real concentrations in ambient air (according to the preliminary screening results). Added concentrations of benzene, toluene, and alkanes in the calibration samples were 25, 50, 100 and 200  $\mu\text{g}/\text{m}^3$ . Added concentrations of ethylbenzene, *m*-, *p*-, *o*-xylenes, polycyclic aromatic hydrocarbons and other analytes were 2.5, 5, 10 and 20  $\mu\text{g}/\text{m}^3$ . Extraction was conducted at room temperature (22 °C) for 10 min; desorption time was 1 min.

From the calibration plots, relative standard deviations (RSDs) of slopes and limits of detection (LODs) were determined. RSDs of slopes were determined using the LINEST () function of Microsoft Excel software (Microsoft® Excel for Office 365, Version 1909, Redmond, WA, USA). LODs were calculated using:

$$\text{LOD} = \frac{\left(\frac{b}{a} + C_{add}\right) \times 3}{S/N} \quad (2)$$

where:  $b$  – the intercept of a calibration plot;  
 $a$  – the slope of a calibration plot;  
 $C_{add}$  – the standard addition concentration ( $\mu\text{g}/\text{m}^3$ );  
 $S/N$  – the signal-to-noise ratio.

#### 2.2.4 Effects of extraction and desorption times

The experiment was conducted on air samples with standard additions of all analytes at  $100 \mu\text{g}/\text{m}^3$ . The following extraction times were studied: 1, 3, 5, 7, 10, 20 and 30 min followed by a 5 min desorption. Desorption times 1, 3, 5, 7 and 10 min were studied after 10 min extraction of analytes by  $65 \mu\text{m}$  PDMS/DVB fiber.

#### 2.2.5 Effect of storage time

Effects of storage time on the responses of analytes were studied in crimped 20 mL vials with concentrations of standard additions of analytes at  $100 \mu\text{g}/\text{m}^3$ . Samples were stored at room temperature ( $22 \text{ }^\circ\text{C}$ ) on the autosampler tray during 0, 2, 4, 8, 16, 24, 36 and 48 h, and extracted by  $65 \mu\text{m}$  PDMS/DVB fiber for 10 min followed by a 1 min desorption. Two replicate samples were analyzed after each storage time. Significance of differences ( $p$ -value) between the initial response of analytes and its response after a certain storage time was estimated using a two-sample two-tailed Student's  $t$ -test with a preset relative standard deviation (10%).

#### 2.2.6 Estimation of the method accuracy

Accuracy of the method was estimated using spike recoveries from laboratory air samples. Concentrations of analytes in laboratory air were determined using a standard addition calibration by dividing intercepts by slopes. Three replicate laboratory air samples, which were collected at the same time as samples used for preparing calibration standards, were spiked at  $C = 100 \mu\text{g}/\text{m}^3$  for benzene, toluene and alkanes, and at  $C = 10.0 \mu\text{g}/\text{m}^3$  for other analytes. After analysis, spike recoveries ( $R$ , %) were determined using

$$R = \frac{C_{meas} - C_{air}}{C_{sp}} \times 100\%, \quad (3)$$

where,  $C_{meas}$  – the determined concentration of an analyte in a spiked sample ( $\mu\text{g}/\text{m}^3$ );

$C_{air}$  – the concentration of an analyte in the laboratory air ( $\mu\text{g}/\text{m}^3$ );

$C_{sp}$  – the concentration of the standard addition of an analyte ( $\mu\text{g}/\text{m}^3$ ).

#### 2.2.7 Air sampling and analysis

The developed method was applied for monitoring of VOCs in ambient air in Almaty on 30 March, 2 April and 4 April 2019. The sampling process and coordinates of sampling locations (Table 5) were identical to those used by Baimatova et al. in 2015 [56, p.49].

Table 5 – Description of VOCs sampling sites

Code	Crossroad	Coordinates	Elevation (m)	Distance to CHP-2	Distance to CHP-3	Objects close to sampling sites
S1	Radostovets str. – al-Farabi ave.	N43°12.007' E76°53.774'	978	13	26	Residential area with high buildings, Mega Center Alma-Ata mall, Kazakh-Russian Gymnasium №38, Almaty Management University
S2	Mendikulov str. – al-Farabi ave.	N43°13.654' E76°57.252'	944	15	22	Residential and office areas with high buildings, Al-Farabi highway
S3	Nauryzbay Batyr str. – Raiymbek ave.	N43°16.099' E76°56.062'	764	11	18	Residential and office are with low buildings, Atrium mall, parking, Kazakh Academy of Labor and Social Relations, Kazakh-Russian Medical University, crossroad with high traffic load
S4	Papanin str. – Suyunbay ave.	N43°19.095' E76°57.781'	700	14	12	Private low buildings, household warehouse, small parking
S5	Raiymbek ave. – Akhrimenko str.	N43°14.950' E76°50.844'	770	6	23	Private low buildings, crossroad with high traffic load, bakery plant
S6	Shevchenko str. – Gagarin ave.	N43°14.612' E76°53.586'	803	9	22	Mahatma Gandhi Park, office, and residential areas with middle-rise buildings

Prior to sampling, all 20 mL vials and septa were washed using distilled water and conditioned at 160 °C for 4 h. Ambient air samples were collected into 20 mL crimp vials (i.e., by opening the vial to air and shaking for ~60 sec) and then sealed with aluminum caps and polytetrafluoroethylene (PTFE)-silicone septa (Agilent, Santa Clara, CA, USA). Vials were transported to the laboratory in 1 L clean glass jars to prevent possible losses of analytes during the transportation. Vials with air samples were placed on the autosampler tray. Air samples were extracted from the vial using 65 µm PDMS/DVB fiber coating at optimized method parameters. Calibration plots were obtained before each sampling day. Weather conditions, such as temperature, humidity, wind velocity and pressure, were taken from the public database Gismeteo (Table 6).



Table 6 – Weather conditions on sampling days

Sampling Date (weather)	Temperature (°C)		Wind Velocity (m/s)		Pressure (mmHg)		Humidity (%)	
	8:00 AM	8:00 PM	8:00 AM	8:00 PM	8:00 AM	8:00 PM	8:00 AM	8:00 PM
03/30/19 (rainy)	9	11	0.7	0.3	692	694	80	67
04/02/19 (cloudy)	10	6	1	1	693	696	75	95
04/04/19 (cloudy)	16	14	1	1	692	693	69	77

## 2.3 Results

### 2.3.1 Selection of the optimal solid-phase microextraction fiber

Analytes of interest were chosen according to the literature review of VOCs determination in ambient air in different cities [108,110–114] and previous studies of compounds detected in the exhausts of six arbitrarily chosen cars of different models and production years [105, p.56-57]. Chosen analytes belong to several classes of pollutants having various physicochemical properties.

Selection of the optimal SPME fiber for quantification of multiple analytes having different physicochemical properties is a difficult process. In most cases, the fibers are chosen based on an experimental or theoretical basis. Experimental fiber selection is straightforward only when one fiber provides greater responses for all analytes. In other cases, a theoretical approach can be involved based on known selectivity of the coatings to compounds having different molecular weights and polarities [72, p.105]. In our study, the selection of the optimal fiber was conducted based on the two most important indicators: limit of detection and relative standard deviation of a calibration slope. Lower LODs will allow greater applicability of the method, while lower RSDs would provide better accuracy and precision. We estimated how many analytes can be determined at different LODs and RSDs. After determining LOD and RSD for each analyte using the four most common commercial fibers (Car/PDMS, PDMS, DVB/Car/PDMS and PDMS/DVB), it was checked how many analytes have LODs below 1, 2, 5 and 10  $\mu\text{g}/\text{m}^3$ , and RSDs below 1%, 2%, 5% and 10% using each fiber.

LODs  $\leq 1 \mu\text{g}/\text{m}^3$  for the greatest number of analytes (20 of 25) were achieved using the DVB/Car/PDMS fiber (Table 7). Car/PDMS and PDMS/DVB fibers provided such LODs only for 17 analytes. LODs  $\leq 2 \mu\text{g}/\text{m}^3$  were achieved for 23 analytes using DVB/Car/PDMS and PDMS/DVB fibers. Such LOD using these fibers was not achieved only for *n*-hexane and *n*-hexadecane. LODs  $\leq 5 \mu\text{g}/\text{m}^3$  were achieved for 24 analytes using PDMS/DVB fiber. LODs  $\leq 10 \mu\text{g}/\text{m}^3$  were achieved for all 25 analytes using PDMS, DVB/Car/PDMS and PDMS/DVB fibers. Overall, DVB/Car/PDMS and PDMS/DVB fibers provide greatest numbers of analytes at most target LODs. At the same time, PDMS/DVB provides lower LODs for three polycyclic aromatic hydrocarbons (PAHs), which are considered more toxic compared to other analytes.

Table 7 – Limits of detection obtained using different SPME fibers

Analyte	Limit of Detection ( $\mu\text{g}/\text{m}^3$ )			
	Car/PDMS	PDMS	DVB/Car/PDMS	PDMS/DVB
2,2,4-Trimethylpentane	3	8	0.7	1.8
<i>n</i> -Heptane	50	9	8	7
Methyl ethyl ketone	15	7	0.8	1.9
Methylene chloride	1.8	9	1.1	0.6
Benzene	0.6	6	0.5	1.2
<i>n</i> -Decane	3	3	1.2	1.5
1,1,2,2-Tetrachloroethylene	0.04	0.2	0.04	0.04
Toluene	0.5	4	1.6	1.2
1,2-Dichloroethane	0.2	1.2	0.8	1.7
<i>n</i> -Undecane	2	1.0	0.8	1.0
Ethylbenzene	0.010	0.10	0.2	0.03
<i>m</i> -Xylene	0.2	0.2	0.6	0.2
<i>p</i> -Xylene	0.10	0.2	0.2	0.2
Propylbenzene	0.3	0.3	0.2	0.10
<i>o</i> -Xylene	0.04	0.10	0.10	0.04
Chlorobenzene	0.04	0.10	0.05	0.04
1,3,5-Trimethylbenzene	0.3	0.10	0.10	0.10
1,2,4-Trimethylbenzene	0.2	0.04	0.04	0.10
3-Picoline	0.5	0.2	0.10	0.010
Benzaldehyde	0.10	0.10	0.4	0.10
<i>n</i> -Hexadecane	-	5	10	5
Naphthalene	0.2	0.10	0.10	0.04
Phenol	0.8	0.10	0.10	0.10
Acenaphthene	0.3	0.10	0.2	0.10
Fluorene	5	0.10	0.6	0.10
Number of analytes with a limit of detection $\leq$				
1 $\mu\text{g}/\text{m}^3$	17	16	20	17
2 $\mu\text{g}/\text{m}^3$	19	17	23	23
5 $\mu\text{g}/\text{m}^3$	22	20	23	24
10 $\mu\text{g}/\text{m}^3$	22	25	25	25

When comparing RSDs of calibration slopes (Table 8), PDMS/DVB fiber also provides better values. RSDs are below 5% for 17 analytes and below 10% – for 22 analytes, which is greater than for DVB/Car/PDMS fiber – 11 and 20 analytes, respectively. When using PDMS/DVB fiber, RSDs of slopes above 10% were obtained only for methyl ethyl ketone (25%), 1,2-dichloroethane (20%) and *p*-xylene (15%). When using DVB/Car/PDMS fiber, RSDs of slopes for benzaldehyde and *n*-hexadecane were 79% and 32%, respectively. Thus, based on these results, PDMS/DVB fiber was chosen as most appropriate for simultaneous quantification of 25 VOCs.

Table 8 – Relative standard deviations of calibration slopes obtained using different SPME fibers

Analyte	Relative Standard Deviation of a Slope (%)			
	Car/PDMS	PDMS	DVB/Car/PDMS	PDMS/DVB
2,2,4-Trimethylpentane	0.50	2.7	1.7	2.7
<i>n</i> -Heptane	44	11	4.5	5.2
Methyl ethyl ketone	42	14	7.8	25
Methylene chloride	95	200	5.3	4.2
Benzene	4.4	9.4	3.2	1.1
<i>n</i> -Decane	3.5	5.6	0.50	5.9
1,1,2,2-Tetrachloroethylene	2.6	1.2	0.40	3.1
Toluene	18	3.4	5.8	6.4
1,2-Dichloroethane	2.1	9.0	10	20
<i>n</i> -Undecane	5.9	5.7	1.8	4.7
Ethylbenzene	0.50	2.7	4.8	4.4
<i>m</i> -Xylene	3.8	1.7	9.6	4.6
<i>p</i> -Xylene	1.2	6.8	7.5	15
Propylbenzene	4.0	2.4	9.6	2.2
<i>o</i> -Xylene	0.60	1.3	7.5	3.4
Chlorobenzene	3.8	1.3	1.3	1.3
1,3,5-Trimethylbenzene	0.30	0.80	2.2	3.2
1,2,4-Trimethylbenzene	7.6	3.5	6.1	3.8
3-Picoline	5.1	6.5	15	6.2
Benzaldehyde	8.0	3.2	79	3.7
<i>n</i> -Hexadecane	-	4.5	32	8.3
Naphthalene	5.7	1.8	20	2.2
Phenol	15	1.4	24	2.5
Acenaphthene	4.2	5.3	4.3	2.5
Fluorene	5.5	1.5	4.0	3.5
Number of analytes with a relative standard deviation of a slope $\leq$				
1%	4	1	2	0
2%	5	8	5	2
5%	13	15	11	17
10%	19	22	20	22

### 2.3.2 Effects of extraction and desorption times

Extraction and desorption times are important parameters of VOC quantification by SPME, which have an impact on intensity of analyte responses. Speed of equilibration during the extraction stage depends on a vessel volume, the diffusion coefficient of an analyte and its distribution constant between the coating and the air [115]. The equilibrium between the fiber and air for almost all analytes was reached after 5–10 min of extraction (Figure 4). Extraction time did not affect the responses of methylene chloride, methyl ethyl ketone and 1,2-dichloroethane—their responses varied by 1–13%. The responses for benzene were stabilized after 3 min of extraction. Based on the obtained results, an extraction time of 10 min was chosen as optimal.

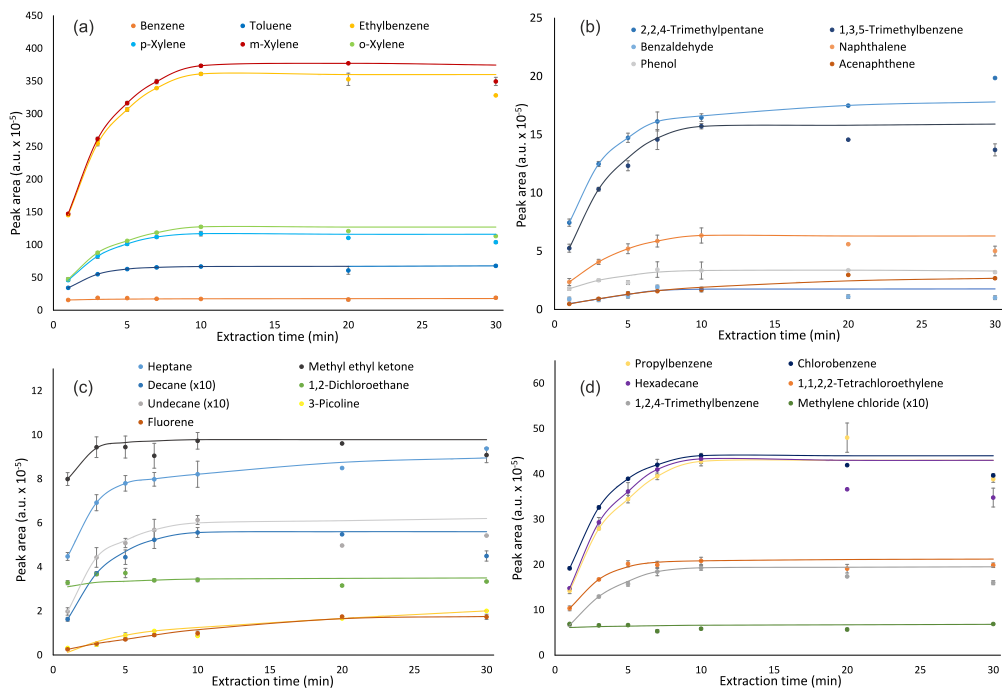


Figure 4 – Effects of extraction time on responses of analytes

The increase in desorption time above 1 min had no significant effects on responses of all studied VOCs (Figure 5). After this time, the responses varied by 0.43–15%. Therefore, the desorption time of 1 min was chosen as the optimal.

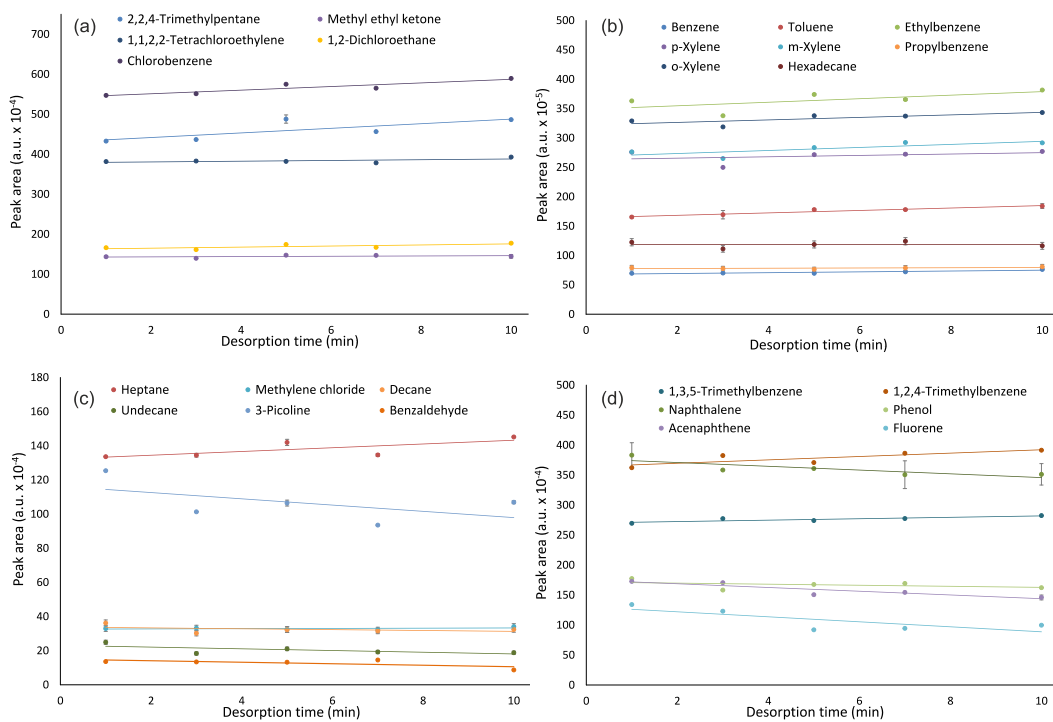


Figure 5 – Effect of desorption time on responses of analytes

### 2.3.3 Effect of storage time

During transportation and storage of air samples, concentrations of analytes can decrease due to their decomposition, losses via leaks and adsorption to internal walls of a vial and septum. The approach proposed by Baimatova et al. [56, p.49] was used to minimize the losses of analytes. The goal of this experiment was to estimate losses of analytes during their storage on the autosampler tray.

Figure 6 shows the effect of storage time on responses of analytes. Two-sample two-tailed t-tests indicated that the changes in responses of *n*-undecane, acenaphthene and fluorene in relation to initial values were significant ( $p < 0.05$  at RSD = 10%) after 24 h of storage (Table 9), while responses of other 22 analytes were stable. After 48 h of storage, changes in responses of *n*-undecane, *n*-hexadecane, acenaphthene and fluorene were significant. Greater losses of more hydrophobic analytes could be explained by their adsorption to a hydrophobic surface of a PTFE-lined septum being in direct contact with air. Despite these septa being considered highly inert, adsorption of very hydrophobic compounds by PTFE was earlier reported in the literature [116]. For achieving the greatest accuracy for these analytes, samples should be analyzed as quickly as possible, e.g., during the first 8 h after sampling.

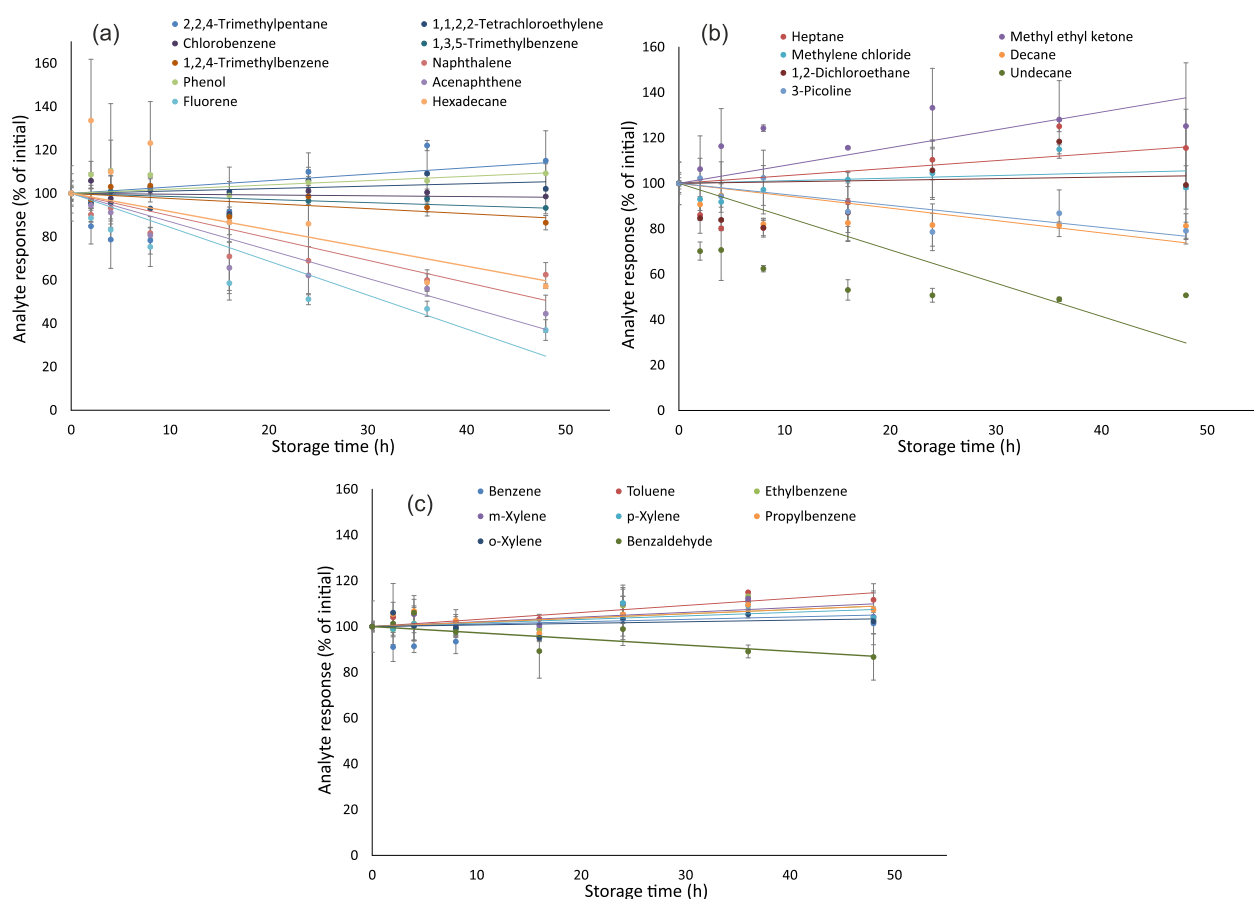


Figure 6 – Effect of storage time on responses of analytes

Table 9 – Probabilities of difference between initial responses of analytes and their responses after different storage times

Analyte	Storage time, h				
	0–8	0–16	0–24	0–36	0–48
	P values				
2,2,4-Trimethylpentane	0.14	0.47	0.44	0.19	0.30
<i>n</i> -Heptane	0.16	0.49	0.43	0.16	0.29
Methyl ethyl ketone	0.16	0.28	0.11	0.13	0.16
Methylene chloride	0.80	0.89	0.71	0.30	0.87
Benzene	0.57	0.94	0.68	0.40	0.90
<i>n</i> -Decane	0.19	0.20	0.18	0.18	0.18
1,1,2,2-Tetrachloroethylene	0.55	0.95	0.62	0.47	0.85
Toluene	1.00	0.78	0.47	0.30	0.38
1,2-Dichloroethane	0.16	0.30	0.63	0.23	0.95
<i>n</i> -Undecane	0.05	0.03	0.02	0.02	0.01
Ethylbenzene	0.95	0.91	0.47	0.34	0.77
<i>m</i> -Xylene	0.87	0.96	0.44	0.37	0.72
<i>p</i> -Xylene	0.93	0.74	0.43	0.48	0.73
Propylbenzene	0.82	0.79	0.66	0.46	0.55
<i>o</i> -Xylene	0.96	0.66	0.77	0.65	0.84
Chlorobenzene	0.90	0.42	0.92	0.97	0.90
1,3,5-Trimethylbenzene	0.80	0.39	0.76	0.83	0.56
1,2,4-Trimethylbenzene	0.76	0.37	0.90	0.57	0.29
3-Picoline	0.83	0.31	0.14	0.30	0.15
Benzaldehyde	0.83	0.37	0.92	0.37	0.29
<i>n</i> -Hexadecane	0.17	0.29	0.27	0.04	0.03
Naphthalene	0.18	0.08	0.07	0.04	0.05
Phenol	0.50	0.93	0.67	0.63	0.39
Acenaphthene	0.17	0.06	0.05	0.03	0.02
Fluorene	0.11	0.04	0.03	0.02	0.01
Number of analytes, responses of which were significantly different from initial values at $p < 0.05$ and RSD = 10%	1	2	3	5	5

#### 2.3.4 Estimation of the method accuracy

Spike recoveries of all analytes except methyl ethyl ketone, methylene chloride, 3-picoline and *n*-hexadecane were 90–105% (Table 10), which is consistent with the results of previous experiments. Lower recoveries of methyl ethyl ketone, methylene chloride, 3-picoline and *n*-hexadecane could be explained by high RSDs in their determined concentrations, which were 7.4%, 17%, 43% and 11%, respectively. RSDs of other analytes were 1.8–6.5%.

#### 2.3.5 Air sampling and analysis

During the monitoring of the atmospheric air in Almaty using the optimized method, all analytes were detected except methyl ethyl ketone and 1,2-dichloroethane.

Mean concentrations of analytes ranged from 0.2 to 83, from 0.1 to 70 and from 0.1 to 74  $\mu\text{g}/\text{m}^3$  on 30 March, 2 April and 4 April, respectively.

Table 10 – Spike recoveries of analytes

Analyte	$C_{air}$ ( $\mu\text{g}/\text{m}^3$ )	$C_{sp}$ ( $\mu\text{g}/\text{m}^3$ )	$C_{meas}$ ( $\mu\text{g}/\text{m}^3$ )	Recovery (%)
2,2,4-Trimethylpentane	22.3	100	124	102
<i>n</i> -Heptane	55.0	100	158	103
Methyl ethyl ketone	88.4	10	93.6	51
Methylene chloride	20.7	10	29.6	89
Benzene	80.2	100	183	103
<i>n</i> -Decane	17.7	100	117	100
1,1,2,2-Tetrachloroethylene	0.58	10	10.6	100
Toluene	25.7	100	128	102
1,2-Dichloroethane	n/d	10	9.3	93
<i>n</i> -Undecane	50.2	100	146	96
Ethylbenzene	1.36	10	11.4	101
<i>m</i> -Xylene	1.74	10	11.9	102
<i>p</i> -Xylene	1.92	10	12.0	100
Propylbenzene	1.17	10	11.2	100
<i>o</i> -Xylene	1.57	10	11.7	101
Chlorobenzene	0.60	10	10.6	100
1,3,5-Trimethylbenzene	1.82	10	11.6	97
1,2,4-Trimethylbenzene	4.33	10	14.2	98
3-Picoline	8.63	10	17.2	86
Benzaldehyde	0.83	10	10.4	96
<i>n</i> -Hexadecane	132	100	213	81
Naphthalene	3.80	10	13.6	98
Phenol	3.52	10	13.5	100
Acenaphthene	1.61	10	12.1	105
Fluorene	4.64	10	14.7	101

The highest concentrations (0.7–89  $\mu\text{g}/\text{m}^3$ ) for 16 of the 23 analytes were detected on the 3rd day of sampling (Table 11). It can be caused by higher temperatures (14–16 °C) than on previous sampling days (6–11 °C). The highest concentrations for the rest of the VOCs, such as benzene, propylbenzene, benzaldehyde and hexadecane, were detected on March 30, which made up 56, 0.3, 1.8 and 123  $\mu\text{g}/\text{m}^3$ , respectively. The 2nd sampling day showed the highest concentrations of naphthalene, phenol and fluorene—2.4, 3.9 and 0.8  $\mu\text{g}/\text{m}^3$ , respectively. The lowest concentrations of the greatest number of analytes (16) were detected in sampling point S2 (Table 12) located in the upper part of the city close to mountains. The highest concentrations of the greatest number of analytes (12) were detected in sampling point S3 located in the central part of the city. The relative standard deviations of three replicate analyses of the air samples did not exceed 15.6%.

Table 11 – Measured VOC concentrations in air

Sampling date >>	Concentration ± Standard Deviation (µg/m <sup>3</sup> )									Outliers	
	Saturday, 30 March			Tuesday, 2 April			Thursday, 4 April				
Analyte	8 AM	8 PM	Mean	8 AM	8 PM	Mean	8 AM	8 PM	Mean	Number	%
2,2,4-Trimethylpentane	18 ± 2	20 ± 2	19 ± 2	19 ± 3	15 ± 2	17 ± 2	34 ± 6	22 ± 2	28 ± 4	6	5.7
<i>n</i> -Heptane	46 ± 5	53 ± 5	50 ± 5	46 ± 3	38 ± 5	42 ± 4	89 ± 9	60 ± 6	74 ± 8	5	4.6
Methyl ethyl ketone	n/d	n/d	n/d	n/d	n/d	n/d	n/d	n/d	n/d	n/a	n/a
Methylene chloride	25 ± 7	25 ± 5	25 ± 6	10 ± 1	8 ± 2	9 ± 2	45 ± 7	53 ± 13	49 ± 10	14	13
Benzene	40 ± 5	56 ± 4	48 ± 4	37 ± 3	46 ± 9	41 ± 6	48 ± 4	56 ± 7	52 ± 6	6	5.6
<i>n</i> -Decane	11 ± 3	13 ± 2	12 ± 2	4.8 ± 1.2	8.4 ± 1.0	6.6 ± 1.1	30 ± 6	28 ± 4	29 ± 5	6	5.6
1,1,2,2-Tetrachloroethylene	0.14 ± 0.05	0.18 ± 0.03	0.16 ± 0.04	0.08 ± 0.01	0.12 ± 0.07	0.10 ± 0.04	1.3 ± 0.6	1.2 ± 0.2	1.2 ± 0.4	9	8.3
Toluene	34 ± 3	50 ± 3	42 ± 3	28 ± 1	21 ± 6	25 ± 3	81 ± 15	60 ± 6	70 ± 11	6	5.6
1,2-Dichloroethane	n/d	n/d	n/d	n/d	n/d	n/d	n/d	n/d	n/d	n/a	n/a
<i>n</i> -Undecane	22 ± 6	27 ± 3	25 ± 4	13 ± 2	14 ± 2	13 ± 2	36 ± 7	22 ± 4	29 ± 5	13	12
Ethylbenzene	0.49 ± 0.13	0.68 ± 0.05	0.58 ± 0.09	0.43 ± 0.02	0.35 ± 0.03	0.39 ± 0.03	0.94 ± 0.14	0.84 ± 0.08	0.89 ± 0.11	n/d	n/d
<i>m</i> -Xylene	0.55 ± 0.14	0.90 ± 0.05	0.73 ± 0.09	0.67 ± 0.03	0.47 ± 0.04	0.57 ± 0.04	1.3 ± 0.2	0.99 ± 0.09	1.1 ± 0.2	n/d	n/d
<i>p</i> -Xylene	0.81 ± 0.16	1.26 ± 0.09	1.04 ± 0.13	0.95 ± 0.04	0.72 ± 0.07	0.83 ± 0.05	1.9 ± 0.2	1.82 ± 0.12	1.9 ± 0.2	1	1.0
Propylbenzene	0.28 ± 0.12	0.11 ± 0.02	0.20 ± 0.07	0.18 ± 0.01	0.06 ± 0.02	0.12 ± 0.02	0.22 ± 0.13	0.07 ± 0.02	0.14 ± 0.08	11	10
<i>o</i> -Xylene	0.55 ± 0.14	0.59 ± 0.04	0.57 ± 0.09	0.45 ± 0.13	0.30 ± 0.02	0.37 ± 0.08	0.70 ± 0.16	0.61 ± 0.04	0.65 ± 0.10	2	1.9
Chlorobenzene	1.1 ± 0.4	1.49 ± 0.09	1.3 ± 0.2	1.1 ± 0.3	0.76 ± 0.06	0.9 ± 0.2	1.5 ± 0.2	1.25 ± 0.07	1.38 ± 0.18	2	1.9
1,3,5-Trimethylbenzene	2.0 ± 0.6	1.22 ± 0.08	1.6 ± 0.4	2.1 ± 0.2	0.79 ± 0.05	1.45 ± 0.13	3.1 ± 1.0	1.09 ± 0.05	2.1 ± 0.5	3	2.8
1,2,4-Trimethylbenzene	1.3 ± 0.5	2.97 ± 0.14	2.2 ± 0.3	1.3 ± 0.4	1.57 ± 0.11	1.4 ± 0.3	2.0 ± 0.8	3.2 ± 0.7	2.6 ± 0.7	5	4.6
3-Picoline	8.1 ± 2.6	0.9 ± 0.2	4.5 ± 1.4	7.0 ± 1.9	0.39 ± 0.08	3.7 ± 1.0	12.5 ± 5.3	1.4 ± 1.1	7.0 ± 3.2	9	8.3
Benzaldehyde	1.3 ± 0.7	1.8 ± 0.3	1.5 ± 0.5	0.7 ± 0.4	1.4 ± 0.2	1.1 ± 0.3	0.6 ± 0.4	1.4 ± 0.5	1.0 ± 0.4	8	7.4
<i>n</i> -Hexadecane	123 ± 16	44 ± 6	84 ± 11	90 ± 10	50 ± 9	71 ± 10	85 ± 14	47 ± 4	66 ± 9	19	18
Naphthalene	1.8 ± 0.6	1.8 ± 0.2	1.8 ± 0.4	1.3 ± 0.4	2.4 ± 0.6	1.9 ± 0.5	1.5 ± 0.3	2.3 ± 0.4	1.9 ± 0.3	4	3.7
Phenol	2.1 ± 0.6	2.9 ± 0.5	2.5 ± 0.5	2.4 ± 0.6	3.9 ± 0.9	3.1 ± 0.8	3.3 ± 1.1	3.3 ± 1.2	3.3 ± 1.2	10	9.3
Acenaphthene	2.24 ± 0.13	0.13 ± 0.04	1.19 ± 0.09	2.6 ± 0.8	0.3 ± 0.03	1.4 ± 0.4	2.6 ± 0.8	0.29 ± 0.10	1.5 ± 0.5	12	12
Fluorene	0.4 ± 0.2	0.59 ± 0.01	0.48 ± 0.11	0.8 ± 0.2	0.57 ± 0.12	0.7 ± 0.2	0.6 ± 0.3	0.5 ± 0.3	0.5 ± 0.3	7	7.2

Note: n/d—not detected; n/a – not available.



Table 12 – Sampling locations where lowest and highest concentrations of analytes were determined at different sampling times

Sampling date >>	Locations where lowest/highest concentrations were determined					
	Saturday, March 30		Tuesday, April 2		Thursday, April 4	
Analyte	8 AM	8 PM	8 AM	8 PM	8 AM	8 PM
2,2,4-Trimethylpentane	S2/S3	S4/S3	S1/S3	S2/S5	S2/S4	S2/S5
<i>n</i> -Heptane	S2/S3	S5/S3	S1/S3	S1/S5	S1/S4	S4/S5
Methyl ethyl ketone	n/d	n/d	n/d	n/d	n/d	n/d
Methylene chloride	S4/S3	S1/S5	S3/S2	S1/S2	S2/S4	S6/S2
Benzene	S1/S3	S1/S3	S1/S3	S3/S4	S1/S3	S2/S6
<i>n</i> -Decane	S5/S1	S5/S6	S2/S6	S5/S2	S2/S4	S4/S3
1,1,2,2-Tetrachloroethylene	S4/S1	S6/S2	S1/S2	S1/S3	S1/S3	S1/S6
Toluene	S1/S3	S1/S5	S1/S3	S6/S4	S2/S4	S4/S5
1,2-Dichloroethane	n/d	n/d	n/d	n/d	n/d	n/d
<i>n</i> -Undecane	S5/S4	S3/S2	S2/S6	S4/S2	S2/S4	S6/S5
Ethylbenzene	S2/S5	S2/S5	S2/S3	S6/S5	S1/S4	S4/S3
<i>m</i> -Xylene	S2/S4	S1/S5	S1/S3	S6/S5	S2/S4	S4/S5
<i>p</i> -Xylene	S1/S3	S1/S5	S1/S3	S6/S5	S1/S4	S1/S3
Propylbenzene	S1/S3	S2/S5	S1/S3	S1/S5	S6/S4	S4/S1
<i>o</i> -Xylene	S1/S3	S1/S5	S1/S3	S1/S5	S1/S3	S4/S5
Chlorobenzene	S1/S3	S2/S5	S1/S3	S6/S5	S2/S4	S1/S3
1,3,5-Trimethylbenzene	S1/S3	S2/S5	S1/S3	S1/S5	S1/S4	S1/S6
1,2,4-Trimethylbenzene	S2/S5	S2/S5	S2/S5	S1/S5	S2/S5	S1/S3
3-Picoline	S1/S3	S2/S1	S1/S3	S5/S6	S1/S4	S1/S3
Benzaldehyde	S3/S2	S1/S4	S2/S5	S5/S6	S3/S5	S4/S3
<i>n</i> -Hexadecane	S5/S2	S2/S3	S5/S2	S4/S6	S5/S3	S3/S2
Naphthalene	S4/S2	S3/S4	S6/S3	S1/S4	S6/S5	S1/S3
Phenol	S6/S3	S1/S4	S1/S3	S3/S4	S1/S3	S1/S2
Acenaphthene	S5/S4	S3/S4	S5/S2	S3/S4	S5/S3	S1/S3
Fluorene	S5/S2	S3/S2	S3/S5	S2/S4	S3/S5	S1/S2

Note: n/d – not detected

From 108 measurements, the greatest numbers of outliers (one out of three replicate measurements according to Grubbs' test) were identified for *n*-hexadecane (19), methylene chloride (14), *n*-undecane (13) and acenaphthene (12). No outliers were identified for ethylbenzene and *m*-xylene.

Toluene-to-benzene concentration ratios during the sampling period varied from 0.46 to 1.69. During the first two days of sampling, T/B ratios were below 1 indicating that the main source of BTEX was not transport. During these two days, the temperatures were 3–7 °C lower than during the third day of sampling, and the central and domestic heating systems were more active. During the third day of sampling, T/B ratios were 1.69 and 1.06, and the main BTEX emissions originated from transport. The same trend was reported for the similar period in 2015 [56, p.50]. However, T/B were lower than 1 mostly in days with negative temperatures. In 2019, such ratios were observed at temperatures between 6 and 11 °C, which could mean that the fraction of BTEX emissions from transport-related sources decreased since 2015.

## 2.4 Section conclusion

A low-cost method for quantitation of multiple VOCs in ambient air using SPME-GC-MS was developed. It was proven that 65  $\mu\text{m}$  PDMS/DVB fiber provides a better combination of detection limits, accuracy and precision compared to 85  $\mu\text{m}$  Car/PDMS, 100  $\mu\text{m}$  PDMS and 50/30  $\mu\text{m}$  DVB/Car/PDMS. The increase in extraction time above 10 min did not have a significant impact on the responses of analytes. Optimal desorption time is 1 min. For quantification of all analytes, except *n*-undecane, vials with samples should not stand on the autosampler tray for more than 8 h. Quantification of 22 of the most stable analytes can be conducted during 24 h after sampling. Spike recoveries of 21 of the 25 chosen analytes were 90–105%. Recoveries of other analytes were 51–89% at RSDs of 7.4–43%.

The developed method was successfully applied for quantification of chosen analytes in atmospheric air of Almaty in Spring, 2019. On average, the completely automated analysis of one sample took 50–60 min, which was enough to analyze 24 (18 air + 6 calibration) air samples per day. All analytes were detected, except methyl ethyl ketone and 1,2-dichloroethane. RSDs of the responses of 23 VOCs varied from 0.1% to 15.6%. The use of three replicate samples allowed identifying outliers. For 18 detected analytes, the fraction of outliers was <18%. Results for the other five detected analytes contained 10–20% outliers. Mean concentrations of 23 VOCs during all sampling times ranged from 0.1 to 83  $\mu\text{g}/\text{m}^3$ . Toluene-to-benzene concentrations ratios were below 1.0 in colder days of sampling, indicating that most BTEX in these days originated from non-transport-related sources. The obtained results prove that the method is very simple, automated, low-cost and provides sufficiently low detection limits, which allow recommending it for monitoring of a wide range of VOCs in atmospheric air of Almaty and other similar cities. The measured concentrations cannot be used to generalize the air pollution problem in Almaty because additional research is needed for this purpose. These data along with the developed method can be useful for improving the air pollution monitoring program in Almaty.

### **3 SEASONAL AND SPATIAL VARIATION OF VOLATILE ORGANIC COMPOUNDS IN AMBIENT AIR OF ALMATY CITY, KAZAKHSTAN**

#### **Preamble**

The part of materials and results described in this section have been published in research articles “Olga P. Ibragimova, Anara Omarova, Bauyrzhan Bukenov, Aray Zhakupbekova, Nassiba Baimatova. Seasonal and Spatial Variation of Volatile Organic Compounds in Ambient Air of Almaty City, Kazakhstan // Atmosphere. – 2021. – Vol.12. – 1592” [117] and reprinted with the journal permissions (Annex A). The copyright to these materials belongs to the MDPI, and any request for further use of this information should be requested from them. The materials are licensed under the Creative Commons Attribution 4.0 International License. To view a copy of this license, visit <http://creativecommons.org/licenses/by/4.0/> or send a letter to Creative Commons, PO Box 1866, Mountain View, CA 94042, USA.

#### **3.1 Introduction**

The developed method in Section 2 was successfully applied for monitoring of VOCs in ambient air of Almaty, Kazakhstan during 2020 and in ambient air in Taldykorgan during 2018 [118]. Almaty, the former capital and the largest (2 million people) [119] city of Kazakhstan, is located in the center of the Eurasian continental area at the foot of the Trans-Ili Alatau Mountains, with a continental climate covering 700 km<sup>2</sup>. The urban part of Almaty is situated from 600 m (in the north) to 1400 m (in the south) above sea level, while the elevation of the mountainous areas reaches up to 4000 m. The geographical location of the city and air movements from the mountains can cause temperature inversion, which may affect the pollution dispersion. Electricity and heat in Almaty are provided by three Combined Heat and Power Plants (CHP-1, CHP-2, CHP-3). The CHP-2 and CHP-3 are located within and 3 km away from the city, respectively. The CHP-1 uses natural gas as a fuel, while CHP-2 and CHP-3 burn approximately 3.7 million tons of low-grade coal with a high ash content (~40%) annually [120]. Advanced emissions-control technologies (desulfurization, denitrification) are not used at coal power plants, and the removal of pollutants is not reported. The number of registered passenger cars of Almaty is about 467 thousand, with additional vehicles from suburban areas of the city [121].

Almaty is one of the most polluted cities in Kazakhstan with unacceptable carcinogenic risk, high acute and chronic effects, and a high hazard index for the respiratory system's chronic exposure [122]. It was observed that outdoor workers in Almaty are at high risk of respiratory diseases in the cold season [123].

The number of studies based on the assessment of air quality in Almaty is very limited. Previous studies were aimed at the effect of inorganic air pollutants on human health [122–125], evaluation of air pollution data and environmental situation [126], spatiotemporal variations and contributing factors of inorganic air pollutants [127], characteristics [128], and traffic component of air pollution in Almaty [105, p.49], quantification of VOCs, including BTEX in Almaty under the application of developed

simple and cost-effective methods [56, p.46, 57, p.1], and accessing of air quality during COVID-19 lockdown [129].

Data on the VOCs concentrations are not available for all cities in Kazakhstan, except Almaty, where only several short-term studies were carried out [56, p. 49, 57, p.8, 105, p.53, 129 p.2,130]. According to the previous study [56, p.50], average concentrations of BTEX in ambient air of Almaty on 31 March – 4 April 2015 were 53, 57, 11, and 14  $\mu\text{g}/\text{m}^3$ , respectively. The maximum benzene concentration was 237  $\mu\text{g}/\text{m}^3$ , comparable with highly polluted cities, such as New Delhi, Cairo, and Rome [56, p.50]. On 30 March - 4 April 2019, the mean concentrations of benzene homologues, alkanes, polycyclic aromatic compounds, and chlorinated VOCs were in the range of 0.1-81  $\mu\text{g}/\text{m}^3$ , 5-123  $\mu\text{g}/\text{m}^3$ , 1.3-2.6  $\mu\text{g}/\text{m}^3$ , and 0.1-53  $\mu\text{g}/\text{m}^3$ , respectively [57, p.14].

Air pollution in Almaty has a complex nature [129, p.6]. It may be caused by various factors, including the geographical location of the city, meteorological conditions, several manufacturing enterprises, a vast number of vehicles, and coal combustion at power plants. The appropriate identification of the sources of emissions in Almaty remains a challenge due to the lack of capacity, outdated methodologies, scarcity of data, and nontransparent energy statistics. In addition, previous short-term studies are insufficient for a detailed description of VOCs concentrations and their sources in the air of Almaty. The assessment of spatial and seasonal variations of VOCs and their possible sources are needed for developing effective measures for air quality improvement by reducing harmful emissions.

Therefore, the goals of this Section were to evaluate (1) seasonal variation of VOCs in the air in 2020, (2) spatial distribution of total VOCs by season, and (3) to identify the emission sources of BTEX.

## **3.2 Materials and Methods**

### **3.2.1 Description of sampling sites**

Air sampling of VOCs was conducted at six sites S1-S6 (Table 4 in Section 2.2.7). Each sampling site was more than 15 m away from the road. VOCs sampling locations were selected to represent five districts (Almaly, Auezov, Bostandyk, Medeu, and Turksib) of Almaty (Figure 7).

Average temperatures in sampling periods in winter, spring, summer, and autumn in Almaty in 2020 were -5.7, 15.8, 24.3, and 9.3 °C, respectively. The heating season in Almaty lasted from 15 October 2019 to 21 April 2020 and resumed on 28 September 2020.

Concentrations of  $\text{NO}_2$ ,  $\text{SO}_2$ , and CO were obtained from The National Air Quality Monitoring Network (NAQMN) operated by the National Hydrometeorological Service of Kazakhstan “Kazhydromet” and were used for correlation analysis. Air is analyzed using OP-824TTs and OP-280 aspirators, K-100 gas analyzer, and AFA-VP-20-1 filters (JSC OPTEK, Saint Petersburg, Russia). Data are published each month and year by “Kazhydromet” in the information bulletins [131].

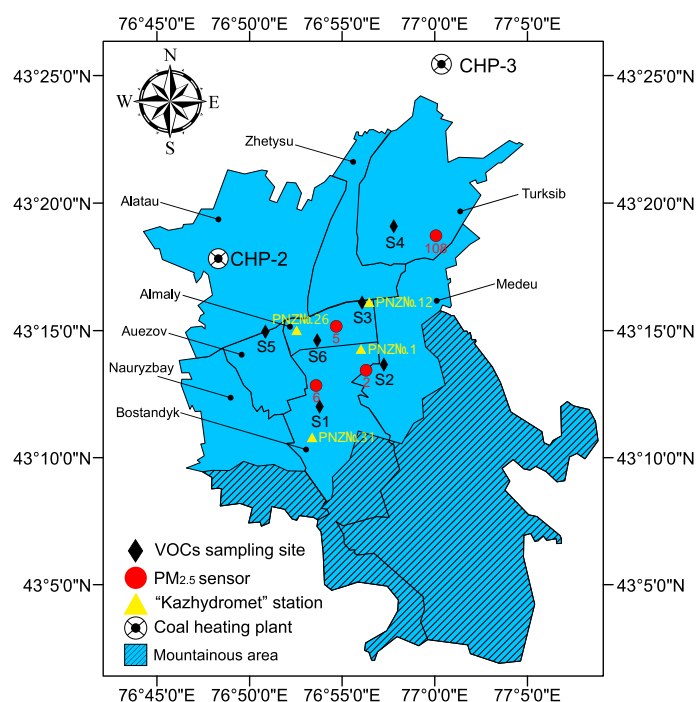


Figure 7 – Map showing the location of the sampling sites in Almaty, Kazakhstan

The data of  $PM_{2.5}$  were obtained from the public network “Airkaz” [132], which uses  $PM_{2.5}$  sensors (The Plantower Pms5003, Beijing, China) for air quality monitoring based on  $PM_{2.5}$  concentrations. Four (4) stations (Figure 7, Table 13) of the network, close to VOCs sampling sites, were selected for this study. Due to technical problems of sensors, 23.3% of the data on  $PM_{2.5}$  concentrations were omitted.

Table 13 – Coordinates of Kazhydromet and  $PM_{2.5}$  sampling sites

“Kazhydromet” stations			
No.	Coordinates	Crossroad	Closest VOCs sampling sites
PNZ 31	N43°10' 48.5574" E76°53' 22.5348"	Al-Farabi av.	S1
PNZ 1	N43°14' 16.6128" E76°56' 0.3048"	Amangeldy str. – Satpaeva str.	S2
PNZ 12	N43°16' 9.9618" E76°56' 3.4044"	Raiymbek av. - Nauryzbay batyr str.	S3
PNZ 26	N43° 15' 1.047" E76°52' 31.8858"	Tole bi str. – Brusilovsky str.	S5, S6
PM <sub>2.5</sub> stations			
6	N 43°12'50.2" E76°53'35.2"	Rozybakieva str. – Baikadamova str.	S1
2	N 43°13'26.0" E76°56'17.2"	Al-Farabi av. – Markova str.	S2
108	N 43°18'43.5" E77°00'03.8"	Zhana Kairat microdistrict	S4
5	N 43°15'09.8" E76°54'40.6"	Tole bi str. – Baizakova str.	S6

Spatial distribution of total VOCs across Almaty in different sampling periods in 2020 were obtained using Geographic Information System software – ArcGIS (ArcMap 10.8.1) and cokriging Geostatistical Analyst tool. A simple cokriging method with normal score transformation and exponential model of semivariogram was used to build the map for the primary dataset. As a secondary dataset, the digital elevation

model (DEM) of Almaty was used. The DEM was obtained from United States Geological Survey and Shuttle Radar Topography Mission data.

### 3.2.2 Sampling and analysis of volatile organic compounds

Air samples were collected at the height of 1.5 m above the ground. Samples were collected at 9 A.M. and 9 P.M. on 15, 17, and 19 January (winter); 3, 5, and 7 April (spring: heating period); 28, 30 April, and 3 May (spring: non-heating period); 22, 24, and 26 July (summer); 21, 23 and 25 October (autumn) (Table 14).

Table 14 – Description of VOCs sampling periods

Sampling period	Sampling season	Description of sampling	The average value of the meteorological parameter				
			T, °C	Humidity, %	Wind speed, m/s	Precipitation, mm	Pressure, mm Hg
15, 17, and 19 January	Winter	Peak of the heating season	-5.7	78.3	0.3	0	774.7
3, 5, and 7 April	Spring: heating period	Two weeks before the end of the heating season, lockdown	14.0	56.5	0.3	0.2	763.4
28, 30 April, and 3 May	Spring: non-heating period	One week after the end of the heating season, post-lockdown	17.6	68.8	0.3	1.8	759.9
22, 24, and 26 July	Summer	non-heating season, lockdown	24.3	50.3	1.5	0.4	755.7
21, 23 and 25 October	Autumn	Three weeks after the start of the heating season	9.3	56.5	0.2	0.7	768.2

The obtained data do not represent the whole season due to limited sampling days. Air sampling and analysis were carried out by the methods described by Baimatova et al. [56, p.49] and in the Section 2.2. Air samples were collected in triplicates into 20-mL crimp-top vials. Solid-phase microextraction of VOCs from 20-mL vials was conducted using exposed 65- $\mu\text{m}$  DVB/PDMS at 22 °C (room temperature) for 10 min followed by analysis on 7890A/5975C Triple-Axis Detector diffusion pump-based gas chromatography with mass-spectrometric detection. A detailed description of the parameters of GC-MS analysis is provided in Section 2.1.2. Calibration curves ( $R^2=0.97-0.99$ ) were obtained before each sampling day. The concentrations units ( $\mu\text{g m}^{-3}$ ) of VOCs were not adjusted to temperature and pressure changes between sampling sites and analysis, contributing uncertainties to concentration measurement. Thirty-six samples were taken on each sampling day; the total number of the analyzed samples was 540 (180 measurements in triplicates).

### 3.2.3 Data collection and pre-processing

Meteorological parameters (temperature, wind speed, pressure, and air humidity) were taken from [133] (Table 15).

Table 15 – Air sampling periods and meteorological parameters

Date	Time	Temperature, °C	Humidity,%	Wind speed, m/s	Precipitation, mm	Pressure, mm Hg
01/15/2020	9:00 AM	-6.7	91	0	0	774.3
	9:00 PM	-1.9	72	0	0	775.6
01/17/2020	9:00 AM	-9.7	88	1	0	782.2
	9:00 PM	-6.2	87	0	0	780.0
01/19/2020	9:00 AM	-9.1	80	0	0	769.1
	9:00 PM	-0.5	52	1	0	767.2
04/03/2020	9:00 AM	9.3	90	0	1	766.8
	9:00 PM	11.0	81	1	0	766.4
04/05/2020	9:00 AM	15.4	30	0	0	762.5
	9:00 PM	17.0	36	1	0	762.1
04/07/2020	9:00 AM	13.7	55	0	0	760.5
	9:00 PM	17.4	47	0	0	761.8
04/28/2020	9:00 AM	22.4	49	0	0	752.7
	9:00 PM	24.6	43	0	0	754.9
04/30/2020	9:00 AM	13.2	94	1	3	765.7
	9:00 PM	14.0	79	0	2	767.3
05/03/2020	9:00 AM	18.0	57	0	0	756.6
	9:00 PM	13.1	91	1	6	762.4
07/22/2020	9:00 AM	25.2	36	1	0	752.3
	9:00 PM	22.6	44	1	0.3	756.7
07/24/2020	9:00 AM	29.0	39	0	0	751.0
	9:00 PM	19.2	78	5	2	761.4
07/26/2020	9:00 AM	26.8	40	1	0	755.8
	9:00 PM	22.9	65	1	0.3	757.0
10/21/2020	9:00 AM	17.7	21	0	0	761.3
	9:00 PM	14.5	30	0	0	763.9
10/23/2020	9:00 AM	6.2	79	0	0	766.2
	9:00 PM	5.1	90	1	4	771.7
10/25/2020	9:00 AM	4.3	69	0	0	773.4
	9:00 PM	7.9	50	0	0	772.6

Descriptive statistics of the VOC concentrations during study periods are presented in Table 16. Data of VOCs concentrations lower than LODs (23.8% from the total number of measurements) and outliers (4.9% of the total number of samples) were omitted.

The mean concentrations of benzene, toluene, methylene chloride, and *n*-heptane in all sampling days and sampling sites ranged from 23 to 64  $\mu\text{g}/\text{m}^3$ . The maximum benzene concentration exceeded the WHO limit (5  $\mu\text{g}/\text{m}^3$ ) by 68 times during the sampling period. While the mean concentrations of ethylbenzene, *m*-, *p*-xylenes, *o*-xylene, 1,2,4-trimethylbenzene, phenol, benzaldehyde, 3-picoline, naphthalene, 1,3,5-trimethylbenzene, and *n*-decane were 1.2-8.5  $\mu\text{g}/\text{m}^3$  and for propylbenzene, and fluorene – 0.53-0.96  $\mu\text{g}/\text{m}^3$ .

Table 16 – Descriptive statistics of the VOC concentrations during the study period

No	Analytes	N*	Concentration, $\mu\text{g}/\text{m}^3$			
			Mean	SD	Minimum	Maximum
1	Benzene	179	64	67	2.3	341
2	Toluene	180	39	43	1.4	223
3	Ethylbenzene	180	1.8	1.4	0.13	9.5
4	<i>m</i> -Xylene	177	3.8	3.9	0.2	41
5	<i>p</i> -Xylene					
6	<i>o</i> -Xylene	180	2.7	2.5	0.15	20
7	1,2,4-Trimethylbenzene	180	2.3	3.3	0.12	36
8	1,3,5-Trimethylbenzene	177	1.2	1.5	0.10	13
9	Propylbenzene	117	0.53	2.5	0.10	27
10	Phenol	180	3.1	3.9	0.19	31
11	Chlorobenzene	156	0.21	0.68	0.040	8.2
12	Benzaldehyde	180	3.4	2.7	0.11	13
13	3-Picoline	131	2.5	3.7	0.10	23
14	Naphthalene	180	2.5	3.3	0.39	26
15	Fluorene	101	0.96	1.39	0.14	11
16	1,2-Dichloroethane	84	4.0	4.8	1.7	42
17	Methylene chloride	137	23	29	0.66	168
18	<i>n</i> -Decane	142	8.5	5.7	1.5	28
19	<i>n</i> -Heptane	99	64	48	8.7	235

\*Note: N – number of measurements; SD – standard deviation

The data of PM<sub>2.5</sub> and inorganic pollutants with concentrations lower than LODs (6.2% of the measurements) were omitted. The mean concentrations of NO<sub>2</sub>, PM<sub>2.5</sub>, SO<sub>2</sub>, and CO during the studied period were 81  $\mu\text{g}/\text{m}^3$ , 44  $\mu\text{g}/\text{m}^3$ , 8.4  $\mu\text{g}/\text{m}^3$  and 1.2  $\text{mg}/\text{m}^3$ , respectively (Table 17). Maximum concentrations of NO<sub>2</sub> (436  $\mu\text{g}/\text{m}^3$ ) and PM<sub>2.5</sub> (260  $\mu\text{g}/\text{m}^3$ ) exceeded WHO limits by 17 times (Table 17).

Table 17 – Descriptive statistics of the concentrations of NO<sub>2</sub>, SO<sub>2</sub>, CO, and PM<sub>2.5</sub>

Analyte	N*	Concentration, $\mu\text{g}/\text{m}^3$				WHO (24-hour limit)
		Mean	SD	Minimum	Maximum	
NO <sub>2</sub>	81	81	68	0.10	436	25
PM <sub>2.5</sub>	92	44	49	2.00	260	15
SO <sub>2</sub>	67	8.4	8.5	0.10	36	40
CO, $\text{mg}/\text{m}^3$	69	1.2	1.2	0.06	5.0	-

\*Note: N – number of measurements; SD – standard deviation

### 3.3 Results and Discussion

#### 3.3.1 Average seasonal variations of volatile organic compounds

Significant seasonal variations (one-way ANOVA, Tukey test,  $p < 0.01$ ) were observed for 9 out of 19 VOCs (Figure 8). However, those 9 VOCs (benzene, propylbenzene, benzaldehyde, 3-picoline, naphthalene, fluorene, methylene chloride,



n-decane, and n-heptane) resulted in a non-significant or low correlation with humidity and precipitation (Table 18). The pollutants correlated negatively with temperature and positively with pressure except for benzaldehyde, which exhibited a reverse trend. The increasing benzaldehyde level by 5 times in sampling days in summer compared to winter can be caused by higher photochemical activity in that season, leading to secondary carbonyl compounds. Similar seasonal variations were obtained by Liu et al. [134], who proposed that the primary source of benzaldehyde is vehicle emissions.

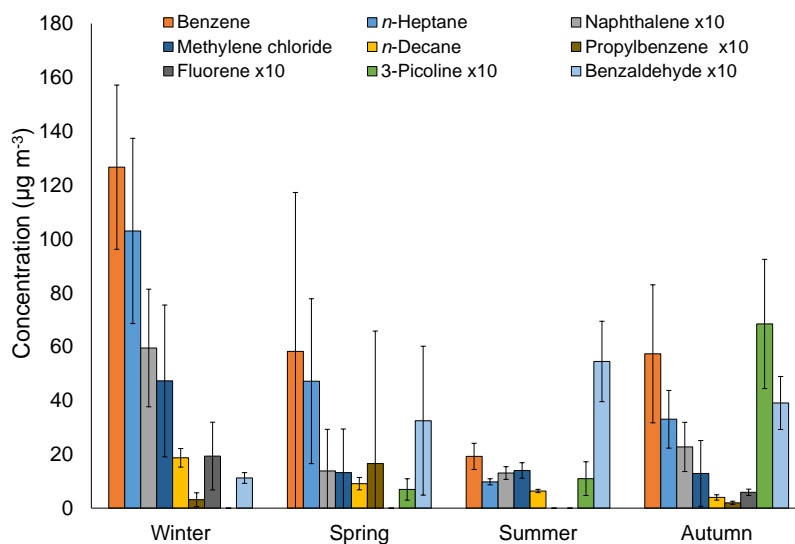


Figure 8 – Seasonal concentrations (mean of the sampling days in each season  $\pm$  SD) of the VOCs

The concentrations of n-heptane, naphthalene, and benzene decreased gradually by 78-90% from winter to summer sampling days and then increased by 2-3 times in sampling days in autumn (Figure 8). Fluorene concentrations were detected in winter and autumn sampling periods, while in spring and summer, concentrations were below LODs. Moreover, in the winter sampling periods, the maximum concentrations of n-decane ( $19 \mu\text{g}/\text{m}^3$ ) and methylene chloride ( $47 \mu\text{g}/\text{m}^3$ ) were observed.

The high levels of the above-mentioned VOCs in sampling periods in winter can be attributed to meteorological conditions of Almaty and specific geographic location [127, p. 1341]. During winter sampling, the mean temperature and pressure were  $-5.7^\circ\text{C}$  and 775 mm Hg, while during sampling in spring, summer, and autumn, it varied from 9.3 to  $24.3^\circ\text{C}$  and from 762 to 768 mm Hg (Table 14). The highest average wind speed was observed during the sampling period in summer (1.5 m/s); in other seasons' sampling periods, average wind speed ranged from 0.2 to 0.3 m/s. Liang et al. [135] proposed that high TVOCs concentrations in the heating season (winter) can be attributed to the decreasing VOCs photodegradation. In addition, high concentrations of VOCs in winter may be associated with poorer dispersion conditions caused by high pressure [136], low planetary boundary layer heights, or the presence of low-level inversion layers.

Table 18 – Pearson correlation between the concentration of pollutants and meteorological parameters

No.	Compounds	Correlation coefficients																		
		1	2	3	4	5	6	7	8	9	10	11	12	13	14	15	16	17	18	19
1	Benzene	1.0***	0.5***	0.0	0.08	0.15	0.43***	0.16	0.08	0.46***	0.05	-0.44***	0.28	0.65***	0.43**	0.43*	0.64***	0.61***	0.69***	
2	Toluene	0.5***	1.0***	0.54***	0.49***	0.61***	0.64***	0.51***	0.43**	-0.02	0.44***	0.12	0.5***	0.25	-0.26	0.51***	0.07	-0.01	0.05	
3	Ethylbenzene	0.0	0.54***	1.0***	0.89***	0.95***	0.7***	0.68***	0.4**	0.11	0.34*	0.67***	0.58***	0.27	-0.04	0.39	-0.11	-0.21	-0.01	
4	<i>m</i> -Xylene	0.08	0.49***	0.89***	1.0***	0.91***	0.81***	0.76***	0.72***	0.29	0.57***	0.53***	0.41***	0.51***	0.07	0.29	0.01	-0.07	0.19	
5	<i>p</i> - Xylene																			
6	<i>o</i> -Xylene	0.15	0.61***	0.95***	0.91***	1.0***	0.76***	0.69***	0.48***	0.19	0.35**	0.53***	0.57***	0.39***	-0.0	0.4	0.01	-0.12	0.1	
7	1,2,4-Trimethylbenzene	0.43***	0.64***	0.7***	0.81***	0.76***	1.0***	0.76***	0.64***	0.41***	0.54***	0.23	0.64***	0.76***	0.12	0.36	0.13	0.13	0.38	
8	1,3,5-Trimethylbenzene	0.16	0.51***	0.68***	0.76***	0.69***	0.76***	1.0***	0.63***	0.26	0.54***	0.4***	0.29	0.51***	0.04	0.2	0.02	0.01	0.19	
9	Propylbenzene	0.08	0.43**	0.4**	0.72***	0.48***	0.64***	0.63***	1.0***	0.08	0.95***	0.24	-0.06	0.46***	-0.1	0.1	-0.04	-0.02	0.13	
10	Phenol	0.46***	-0.02	0.11	0.29	0.19	0.41***	0.26	0.08	1.0***	0.06	-0.1	0.31	0.75***	0.64***	0.0	0.41***	0.53***	0.67***	
11	Chlorobenzene	0.05	0.44***	0.34*	0.57***	0.35**	0.54***	0.54***	0.95***	0.06	1.0***	0.31	-0.08	0.38**	-0.16	0.07	-0.07	-0.03	0.09	
12	Benzaldehyde	-0.44***	0.12	0.67***	0.53***	0.53***	0.23	0.4***	0.24	-0.1	0.31	1.0***	0.19	-0.13	-0.17	0.13	-0.34*	-0.43***	-0.32	
13	3-Picoline	0.28	0.5***	0.58***	0.41***	0.57***	0.64***	0.29	-0.06	0.31	-0.08	0.19	1.0***	0.44***	0.28	0.54**	0.12	-0.35*	0.11	
14	Naphthalene	0.65***	0.25	0.27	0.51***	0.39***	0.76***	0.51***	0.46***	0.75***	0.38**	-0.13	0.44***	1.0***	0.61***	0.17	0.47***	0.56***	0.71***	
15	Fluorene	0.43**	-0.26	-0.04	0.07	-0.0	0.12	0.04	-0.1	0.64***	-0.16	-0.17	0.28	0.61***	1.0***	-0.09	0.58***	0.58***	0.42	
16	1,2-Dichloroethane	0.43*	0.51***	0.39	0.29	0.4	0.36	0.2	0.1	0.0	0.07	0.13	0.54**	0.17	-0.09	1.0***	-0.12	-0.18	-0.02	
17	Methylene chloride	0.64***	0.07	-0.11	0.01	0.01	0.13	0.02	-0.04	0.41***	-0.07	-0.34*	0.12	0.47***	0.58***	-0.12	1.0***	0.66***	0.48**	
18	<i>n</i> -Decane	0.61***	-0.01	-0.21	-0.07	-0.12	0.13	0.01	-0.02	0.53***	-0.03	-0.43***	-0.35*	0.56***	0.58***	-0.18	0.66***	1.0***	0.7***	
19	<i>n</i> -Heptane	0.69***	0.05	-0.01	0.19	0.1	0.38	0.19	0.13	0.67***	0.09	-0.32	0.11	0.71***	0.42	-0.02	0.48**	0.7***	1.0***	
20	CO	0.38	0.35	0.35	0.39	0.47*	0.75***	0.29	-0.09	0.48**	-0.07	-0.08	0.62***	0.6***	0.52	-0.35	0.22	0.18	0.3	
21	SO <sub>2</sub>	0.55***	-0.08	0.04	0.11	0.08	0.38	0.07	-0.32	0.54***	-0.21	-0.26	0.08	0.61***	0.54	-0.25	0.61***	0.61***	0.56	
22	NO <sub>2</sub>	0.24	0.15	0.06	0.08	0.2	0.15	0.0	-0.18	0.08	-0.03	-0.13	0.19	0.14	-0.01	0.09	0.28	0.21	-0.09	
23	PM <sub>2.5</sub>	0.62***	0.02	-0.01	0.09	0.08	0.31	0.15	-0.05	0.57***	-0.07	-0.41*	0.68***	0.64***	0.73***	0.08	0.59***	0.8***	0.65***	
24	Temperature, °C	-0.55***	0.08	0.27	0.11	0.17	-0.27	0.04	0.04	-	0.08	0.59***	-0.36*	-	-0.55***	0.01	-0.51***	-0.57***	-0.56***	
25	Humidity, %	0.01	-0.31*	-0.28	-0.08	-0.21	0.02	-0.06	0.11	0.27	0.07	-0.32*	-0.2	0.28	0.19	-0.1	0.05	0.2	0.35	
26	Wind speed, m/s	-0.24	-0.2	0.12	0.23	0.18	-0.19	-0.03	0.04	0.03	-0.08	0.18	-0.28	-0.15	0.08	-0.08	0.06	-0.08	0.02	
27	Precipitation, mm	-0.44***	-0.21	-0.09	-0.1	-0.14	-0.22	-0.13	-0.03	-0.24	0.01	0.1	-0.15	-0.32*	-0.23	-0.09	-0.37**	-0.36**	-0.24	
28	Pressure, mm Hg	0.5***	0.02	-0.19	-0.05	-0.09	0.31*	-0.03	-0.03	0.51***	-0.08	-0.55***	0.41***	0.57***	0.34	0.11	0.33	0.38**	0.54***	

Statistically significant:  
 \*\*\*p<0.01  
 \*\*p<0.05  
 \*p<0.1

The seasonal variations of toluene, 1,2-dichloroethane, ethylbenzene, *m*-,*p*-,*o*-xylenes, propylbenzene, chlorobenzene, 1,3,5-trimethylbenzene, 1,2,4-trimethylbenzene, and phenol were insignificant and varied from 0.070 to 61  $\mu\text{g}/\text{m}^3$  (Figure 9).

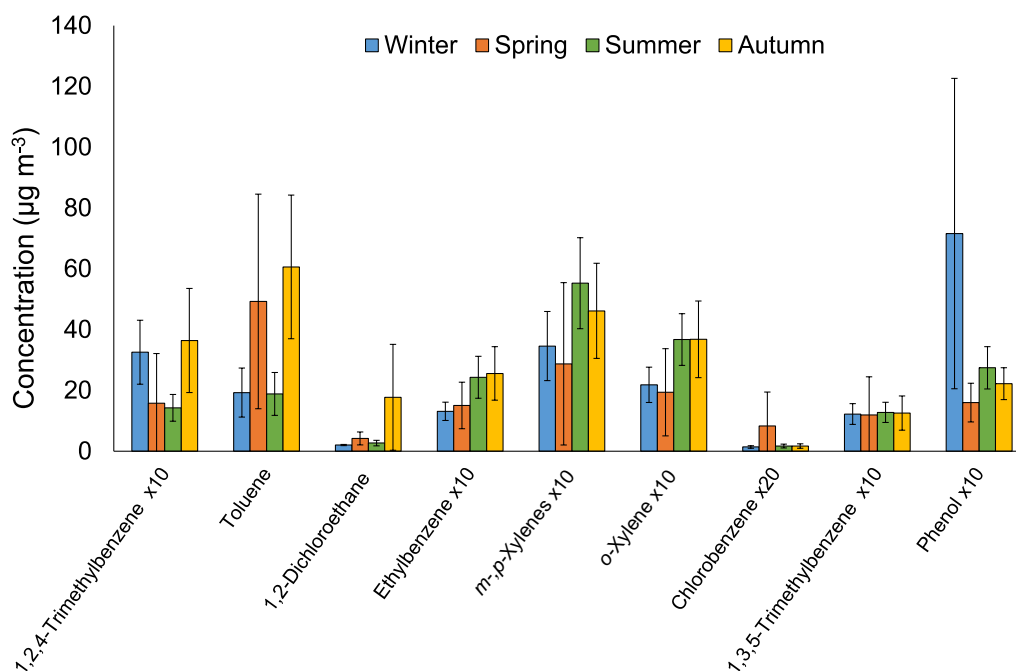


Figure 9 – Seasonal variations of the mean VOCs concentrations (mean of the sampling days in each season  $\pm$  SD)

The mean spring sampling period concentrations of VOCs were calculated as mean concentrations of sampling days in heating (3,5, 7 April) and non-heating (28, 30 April and 3 May) periods. Above-mentioned periods were chosen for sampling in spring for evaluation effect of the heating season, which ended a week before sampling on 28 April. Moreover, the sampling period in 3-7 April coincided with the COVID-19 lockdown in Kazakhstan (19 March – 13 April) with the absence of traffic activity [137]. Kerimray et al. [129, p.5] assessed the effect of the lockdown restrictions on benzene, toluene, ethylbenzene, and *o*-xylene emissions by comparing their concentrations in April 2020 with the same period in the previous years from 2015 to 2019. Authors proposed that an increase of benzene and toluene concentrations by 2-3 times in 2020 can be related to 2-fold higher temperature and no-precipitation conditions during sampling and indicated the non-traffic sources. In addition, the COVID-19 lockdown period can be associated with higher coal combustion by private houses and bathhouses (saunas).

The significant reduction of *n*-heptane, methylene chloride, benzene, *n*-decane, toluene, 1,2-dichloroethane, and naphthalene by 27-90% (t-test,  $p < 0.05$ ) was observed in the non-heating period compared to the heating period in spring (Figure 10).

Temperatures (14.0 vs. 17.6  $^{\circ}\text{C}$ ) and pressure (763 vs. 760 mm Hg) were comparable in both spring sampling periods. Therefore, such reduction may indicate that coal combustion during heating season primarily affected the emissions of the

above-mentioned VOCs. The obtained results of benzene and toluene emissions are in agreement with Kerimray et al. [129, p.7].

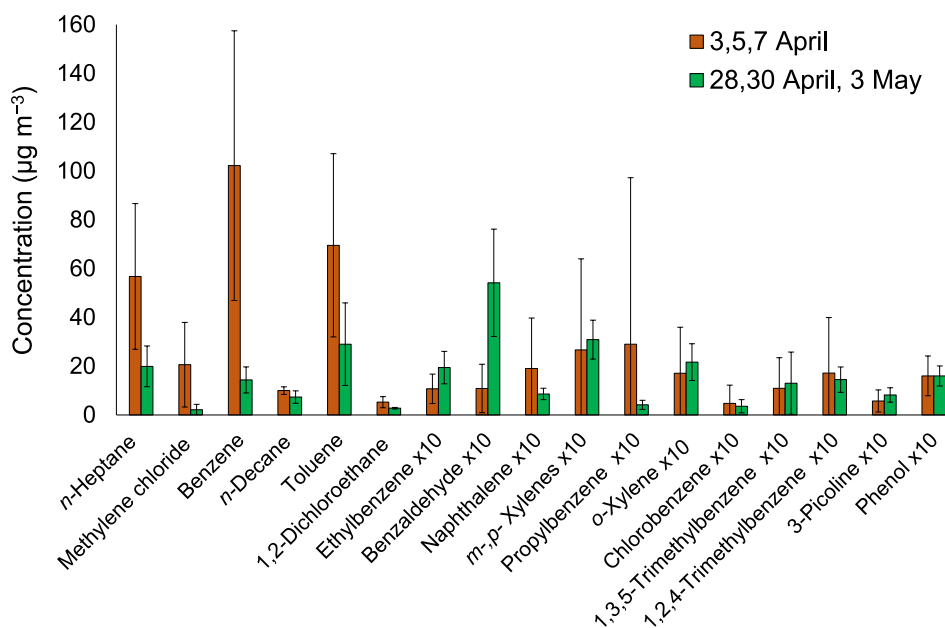


Figure 10 – Variations of the VOCs concentrations (mean of the three sampling days  $\pm$  SD) in spring sampling periods during heating and non-heating season

A significant increase by 2-5-fold of ethylbenzene and benzaldehyde concentrations was observed from the heating period to the non-heating period in spring, which can be explained by a substantial reduction of traffic in the heating period due to the lockdown and resuming traffic in the non-heating period [137]. A similar effect of traffic-free conditions was observed by Kerimray et al. [129, p.5], when concentrations of ethylbenzene and o-xylene decreased by 4 and 2.7 times in April 2020 (lockdown) compared to the same period in 2015-2019. The variations of mean concentrations of the rest of the analytes were insignificant and varied from 0.36 to 3.1  $\mu\text{g}/\text{m}^3$  (Figure 10).

### 3.3.2 Spatial differences of volatile organic compounds

The total VOCs concentrations (the sum of the mean concentrations of individual VOCs during the sampling period) varied across sampling sites during all seasons in 2020. The total VOCs variations were from 233 to 420, from 231 to 437, from 48 to 151, from 46 to 133, and from 72 to 393  $\mu\text{g}/\text{m}^3$  in sampling days in January, April, April-May, July, and October, respectively. TVOCs concentrations decreased on 28,30 April and 3 May by an average of 74 and 67% compared to 15, 17, 19 January and 3, 5, 7 April, respectively.

The spatial distribution of TVOCs (Figure 11) varied from the south to the north. All sampling seasons had a similar spatial profile, with lower TVOCs concentrations in the south and higher in the north of Almaty, where CHPs are located.

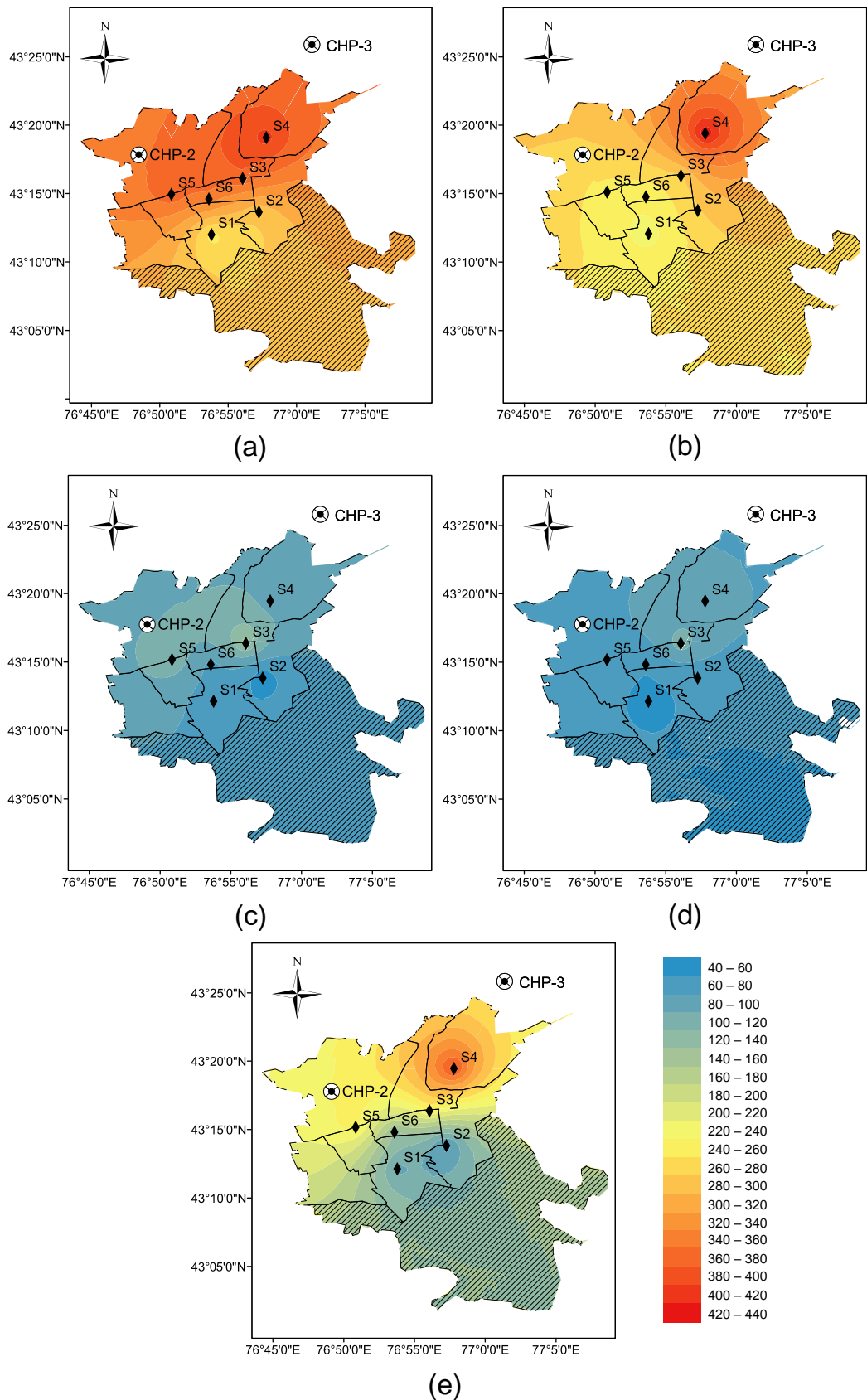


Figure 11 – Spatial distribution of total VOCs concentrations during sampling periods in 15, 17, 19 January (a), 3, 5, 7 April (b), 28, 30 April, 3 May (c), 22, 24, 26 July (d), and 21, 23, 25 October (e)

15, 17, 19 January and 21, 23, 25 October were characterized by a strong negative correlation between TVOCs level and elevation of sampling sites with  $r = -1.0$  and  $r = -0.89$ , while a moderate negative correlation was observed in sampling days in April, April-May, and July (Figure 12). These correlations indicate the possible effect of heating season on TVOCs spatial distribution due to increased coal consumption [120] at low ambient temperature.

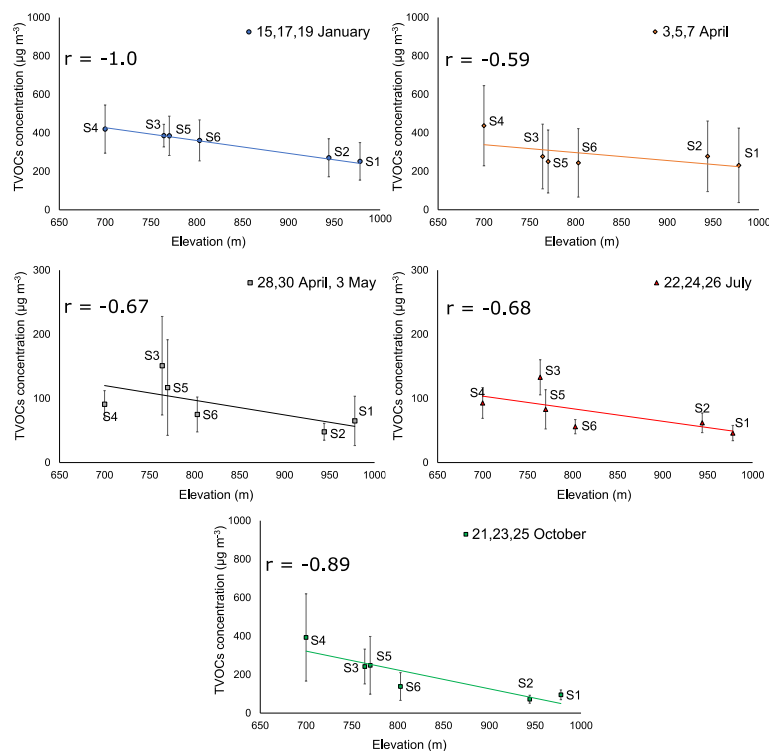


Figure 12 – TVOCs concentrations and sampling site’s (S1-S6) elevation above the sea level during sampling periods

For the studied periods, the most polluted sampling site in Almaty was site S4 (Papanin str. – Suyunbay ave.). The sampling site S4 is at 12 km from CHP-3 and 14 km from CHP-2 and the lowest elevation above the sea level (700 m). There is a number of private houses close to S4 sampling sites that use solid fuel for heating (coal) and avenues with heavy traffic, which could contribute to air pollution around the S4 sampling site. The lower TVOCs concentrations were obtained in sampling sites S1 and S2 during all sampling periods. These sampling sites are located at a higher level (978 and 944 m) close to mountains and far from CHP-3 (22-26 km) and CHP-2 (13-15 km).

### 3.3.3 BTEX source apportionment

Several studies have reported that the ratio of toluene to benzene can be used to find pollutants sources [37,138]. The T/B ratio can be applied to determine the emission sources of BTEX in ambient air.  $T/B < 1$  indicates the non-traffic-related sources (biomass/biofuel/coal burning), while  $T/B > 1$  shows the dominant

contribution of traffic-related sources (vehicle emissions) [33, p.187-188]. Figure 13 shows that sources of air pollution in Almaty have a complex nature. During the sampling in January, April, and July, the prevailing sources of BTEX were the combustion of biomass/biofuel/coal. While, in May and October sampling days, BTEX were mainly originated from vehicle emissions. In July sampling period, the lower contribution of vehicle-related sources can be explained by partial lockdown measures (5 July – 16 August) due to the second wave of COVID-19 in Kazakhstan [137]. However, CHPs had been operating for a whole year in Almaty explaining the contribution of coal-burning sources to air pollution.

The *m*-,*p*-xylenes to ethylbenzene ratio indicates the photochemical age of pollution. *m*- and *p*-Xylenes are more reactive than ethylbenzene and quickly react with •OH radicals [34, p.16]. The X/E ratio higher than 3 indicates the fresh and local emissions, while the ratio lower than 3 shows aged air masses and consequently emissions from remote sources [139]. The majority of X/E ratios were lower than 3 in all sampling periods, assuming the presence of aged air masses from remote sources (Figure 13). Several X/E ratios (6% of total) were higher or close to 3, which indicate the local, fresh emissions and a mixture of aged air masses (Figure 13). The strong correlation of ethylbenzene, *m*-,*p*-xylenes, and *o*-xylene ( $r \geq 0.9$ ,  $p \leq 0.01$ ) suggests the constant and familiar sources of these VOCs (Table 18). Based on these results, it can be concluded that the contribution of the remote sources is dominant in Almaty at all sites and periods.

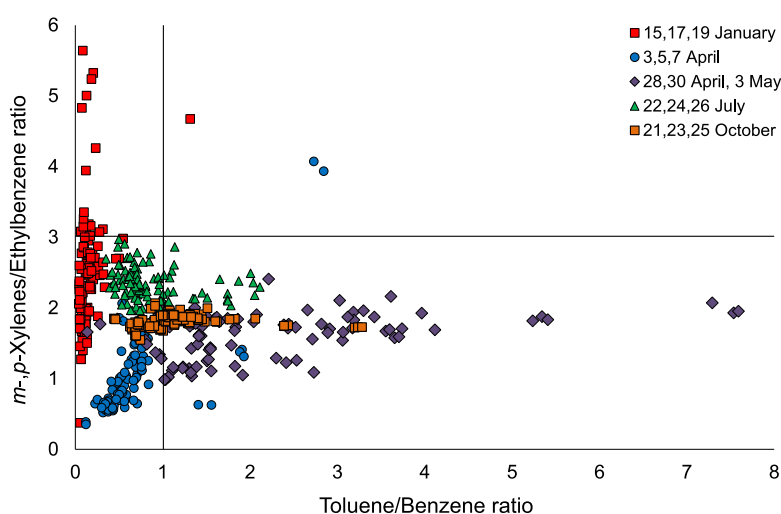


Figure 13 – The ratios of BTEX at different sampling periods

The benzene, toluene, and ethylbenzene (B:T:E) ratio is applied to evaluate aromatic sources in ambient air [26, p.16444, 37, p.6679, 139]. Biomass/biofuel/coal burning is characterized by the mean relative proportions of B:T:E – 0.69:0.27:0.04, traffic emissions – 0.31:0.59:0.10, industrial emissions – 0.06:0.59:0.35 [37, p.6679]. B:T:E ratio of each air sample was calculated and plotted in ternary diagrams to understand the emissions sources better. The obtained B:T:E ratio showed that in Almaty, there were two main sources of BTEX during the studied period: traffic

emissions and biomass/biofuel/coal burning (Figure 14). For all sampling sites, biomass/biofuel/coal burning was a prevalent source of VOCs on 15, 17, 19 January, with an average B:T:E ratio of 0.87:0.12:0.01. During the heating season, the use of coal increases by more than two times [120, p.9], which leads to dramatically increase in SO<sub>2</sub> emissions from CHP-2 [140] and PM<sub>2.5</sub> concentrations [120, p.9]. The moderate correlation of benzene with concentrations of a coal combustion marker SO<sub>2</sub> [141] and PM<sub>2.5</sub> ( $r \geq 0.5$ ,  $p \leq 0.01$ ) can also indicate that the burning of solid fuel is one of the primary sources of pollution during the heating season in Almaty (Table 18). Similar findings were obtained in the Dushanzi district, Northwest China [142], and in a rural area of North China [33, p.186, 36, p.9], where coal combustion was the main source of VOCs emissions during cold seasons.

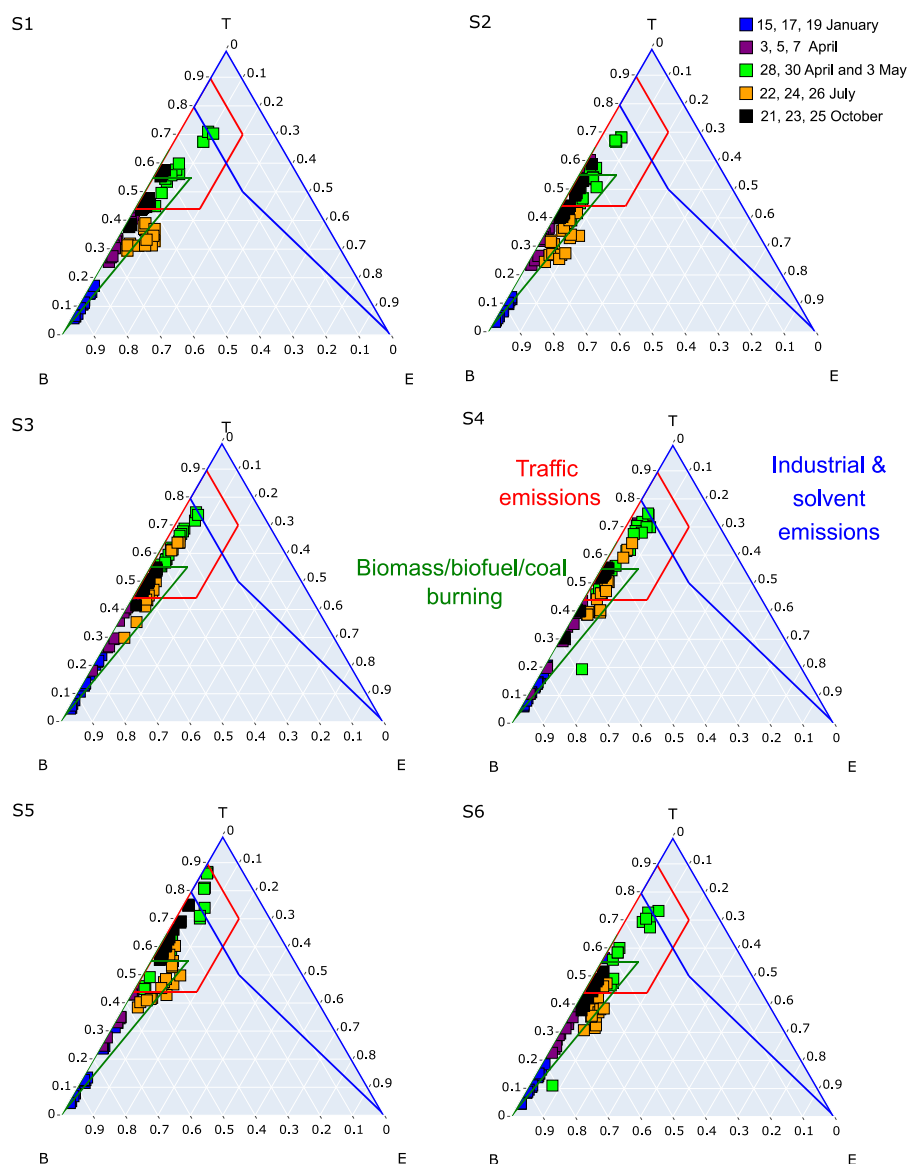


Figure 14 – B:T:E ratios in Almaty

On 3, 5, 7 April, sampling was carried out during the first lockdown (19 March – 13 April) under non-traffic conditions, and the B:T:E ratio was 0.61:0.39:0 indicating



the coal combustion as the main source of BTEX.

On 28, 30 April, 3 May and 21, 23, 25 October, B:T:E ratios were 0.32:0.64:0.04 and 0.48:0.50:0.02, respectively, which indicated the traffic and non-traffic-related BTEX sources. In July sampling days, three out of six sampling sites (S1, S2 and S6) depicted the distribution of B:T:E ratios in the coal combustion area. While the distribution of B:T:E ratios of the rest of the sampling sites (S3, S4, S5) was in both (traffic and coal combustion) areas. The B:T:E ratios at sampling sites S3, S4, and S5 differed from S1, S2, S6 due to their closest location to the main roads.

The correlation analysis of VOCs concentrations and BTEX source apportionment in Almaty showed the complex nature of air pollution and variation of the primary source depending on the season and sampling site.

### **3.4 Section conclusion**

Assessment of the air pollution in Almaty, Kazakhstan, in 2020 was conducted by measurements of VOCs concentrations using the previously developed method. The seasonal variations for 9 out of 19 VOCs were significant, with maximum concentration in sampling days in winter. The high concentrations of VOCs in the winter sampling period can be related to the higher emissions from coal combustion, meteorological parameters, and the geographic location of Almaty. In addition, in winter, the low planetary boundary layer heights and low-level inversion layers can affect VOCs dispersion. Insignificant seasonal variations of the rest of the analytes may indicate that their sources have a constant contribution to air pollution during all sampling periods.

Comparison of the two sampling periods (3, 5, 7 April and 28, 30 April, 3 May) in spring were used for evaluating the effect of the heating season and COVID-19 lockdown restrictions in Almaty on VOCs emissions. The obtained results and analysis of typical ratios of BTEX demonstrate that the primary sources in Almaty are associated with the burning of biomass/biofuel/coal and vehicle emissions with the dominant effect of solid fuel combustion in heating seasons. Additionally, the observed  $X/E$  ratios (lower than 3) indicate that sampling sites in Almaty are affected mainly by aged air masses from remote sources. It was found that the spatial distribution of the TVOCs concentrations depends on the sampling site's elevation and distance from CHPs. The spatial difference of TVOCs has a similar trend in all sampling periods, with the most polluted site in the north part of the city.

The limitation of this study is that the obtained results represent only short sampling periods and boundary layer height as well as temperature inversions were not investigated due to data gaps. However, it is the first attempt to study VOCs' seasonal and spatial air pollution in Almaty, one of the most polluted cities in Kazakhstan. The obtained data could serve as a basis for action plans for improving the air quality based on air monitoring data and could be an impulse for further comprehensive investigations. Moreover, observed complex air pollution in Almaty, Kazakhstan, requires further detailed source-apportionment studies of the VOCs and their diurnal, temporal, and seasonal variations.

## **4 ASSESSING AIR QUALITY CHANGES IN LARGE CITIES DURING COVID-19 LOCKDOWNS: THE IMPACTS OF TRAFFIC-FREE URBAN CONDITIONS IN ALMATY, KAZAKHSTAN**

### **Preamble**

The part of materials and results described in this section have been published in research articles “Aiyngul Kerimray, Nassiba Baimatova, Olga P. Ibragimova, Bauyrzhan Bukenov, Bulat Kenessov, Pavel Plotitsyn, Ferhat Karaca. Assessing air quality changes in large cities during COVID-19 lockdowns: The impacts of traffic-free urban conditions in Almaty, Kazakhstan // *Science of the Total Environment*. – 2020. – Vol.730. – 139179” [129, p.1-8] and reprinted with the journal permissions (Annex A). The copyright to these materials belongs to the Elsevier, and any request for further use of this information should be requested from them.

### **4.1 Introduction**

The first case of SARS-CoV-2 infection was registered in Kazakhstan on March 13, 2020. Learning from the experience of other countries, the reaction of authorities was fast. On March 16, 2020, an emergency situation was declared, and beginning on March 19, 2020, a city-scale quarantine or “lockdown” was introduced for the whole city of Almaty. Limits on entry and exit in the city were applied (with the exception of cargo trucks for vital purposes). Since March 28, more restrictive measures were introduced, and residents of Almaty could leave their homes only for grocery shopping and work (only with special permission). Since March 30, 2020, all organizations and enterprises were temporarily suspended, with a gradual staged opening of some selected industries expected in late April and in May. Such measures resulted in nearly absent of road traffic, while at the same time, coal-fired combined heat and power plants were continuously operating. Air quality changes due to the COVID-19 lockdowns quickly became a new topic of recent research studies. Decreases in nitrogen dioxide levels (NO<sub>2</sub>) over China during February 10-25 (during quarantine) compared to January 1-20, 2020 (before quarantine) were identified using satellite data from NASA and the European Space Agency (ESA) [143]. [144] also depicted substantial air quality improvements after two weeks of lockdown in Barcelona (Spain). The results support the idea that air pollution could be substantially improved in cities where transport was a major source. However, the air quality improvements during COVID-19 lockdowns may not clearly favor improving the air quality in areas with a more complex mix of sources, where transport emissions have minor impacts compared to emissions from other sources (e.g., coal combustion for power and heating).

In this Section, changes in the air quality before and during the period of COVID-19 lockdown in Almaty were quantified. The possible effects of traffic emissions were discussed. BTEX concentrations were measured during three days in the middle of the lockdown and compared with the concentrations observed during the same periods of previous years (2015-2019). This Section aims to assess the impacts of COVID-19 lockdown conditions (traffic-free) on the air quality of Almaty, which is one of the

most polluted large cities in the world.

## 4.2 Methodology

### 4.2.1 Methodology of sampling

Monitoring of benzene, toluene, ethylbenzene, and *o*-xylene was conducted every spring at 8 AM and 8 PM at six different locations (Figure 7) during the period from the end of March to the beginning of April from 2015 to 2020. The sampling and analysis methods developed by Baimatova et al. [56, p.49] and in Section 2.1 were followed. The lockdown BTEX sampling was conducted on three days in the middle of the lockdown.

The wind speed, wind direction, temperature, relative humidity, precipitation were obtained from the <http://rp5.kz> website [133], which collects data from the National Oceanic and Atmospheric Administration (USA) from the station located at 43.15°N, 76.57°E at an elevation of 848 m above sea level.

The cokriging method utilized in the ArcGIS® Geostatistical Analyst tool was used to map benzene distributions across Almaty in 2018-2019 and 2020, respectively. The digital elevation model of Almaty from the Shuttle Radar Topography Mission (SRTM) data was used as a secondary dataset. Ordinary cokriging was used to build the map with the first order of trend removal for the primary dataset and local polynomial interpolation, as in all cases, the data had a trend in distribution.

### 4.2.2 Meteorological conditions

Significant temperature variations in the region characterize the transitional period from February to April. Detailed information on the meteorological factors during the selected periods are summarized in Table 19. The period between February 21 to April 14, 2020 was characterized by a substantial difference (23.3 °C) between the minimum daily temperature (-6 °C) and the maximum daily temperature (17.3 °C). The average temperature before lockdown was 5.5 °C, while it was 8.7 °C during lockdown. Additionally, there were less frequent rains before lockdown period (9 days out of 27) compared to the lockdown period (16 days out of 27). These results show that the meteorological conditions were in favor of air pollution reductions during the lockdown period compared to the preceding days.

On the other hand, the meteorological conditions during the lockdown were almost similar to those of the same periods in the previous years of 2018 and 2019 (Table 19; Figure 15). The numbers of rainy days were 15, 16, and 16 days, and the average temperatures were 11.2, 11.6, and 8.7 °C in 2018, 2019, and 2020, respectively. The lockdown period was slightly colder compared to previous years, as there were six days during the lockdown period when the daily average temperature was below 5 °C, while such temperature falls were observed only on one day in 2018 and two days in 2019. These results show that the lockdown period had slightly unfavorable meteorological conditions for air pollution compared to the earlier years.

Table 19 – Meteorological conditions for the preceding days (February 21 – March 18), and the lockdown days (March 19 – April 14)

	Temperature (°C)		Relative humidity (%)		Wind speed (m/s)		Precipitation (mm)	
	Average	SD	Average	SD	Average	SD	Average	SD
February 21 – March 18								
2018	4.7	3.8	73.9	15.2	0.3	0.1	5.5	3.3
2019	4.6	4.5	66.5	16.5	0.3	0.2	3.5	2.3
2020	5.5	5.4	62.4	17.4	0.4	0.3	3.3	3.5
March 19 – April 14								
2018	11.2	4.2	60.3	14.9	0.4	0.2	5.5	4.2
2019	11.6	3.2	63.5	13.3	0.4	0.2	4.5	4.9
2020	8.7	4.7	66.1	16.4	0.4	0.2	5.2	4.9

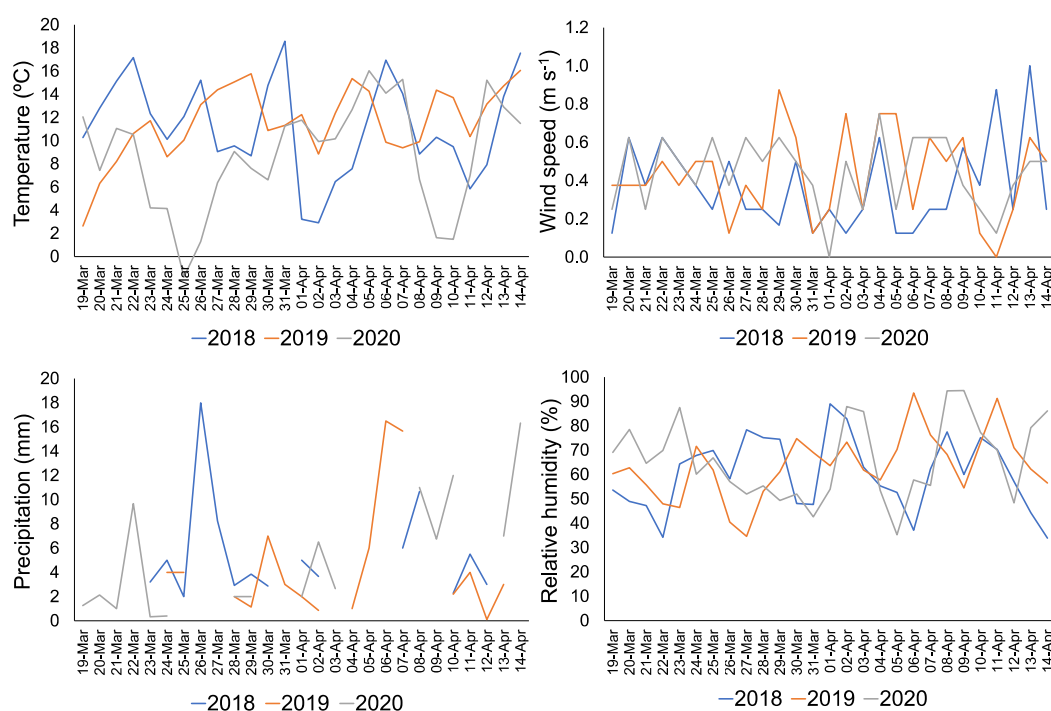


Figure 15 – Meteorological conditions in the period between March 19 and April 14, 2020

### 4.3 Results and discussion

#### 4.3.1 BTEX concentration analysis

The average concentrations of BTEX analytes from 2015 to 2020 are illustrated in Figure 16. The averages for benzene (101  $\mu\text{g}/\text{m}^3$ ) and toluene (67  $\mu\text{g}/\text{m}^3$ ) were 3 and 2 times higher, while those for ethylbenzene (1.0  $\mu\text{g}/\text{m}^3$ ) and *o*-xylene (1.6  $\mu\text{g}/\text{m}^3$ ) were 4 and 2.7 times lower in 2020 than during the same sampling period in 2015-2019 (Table 20). In addition, the average concentration of benzene was 15% higher in January 2020 compared to the lockdown period.

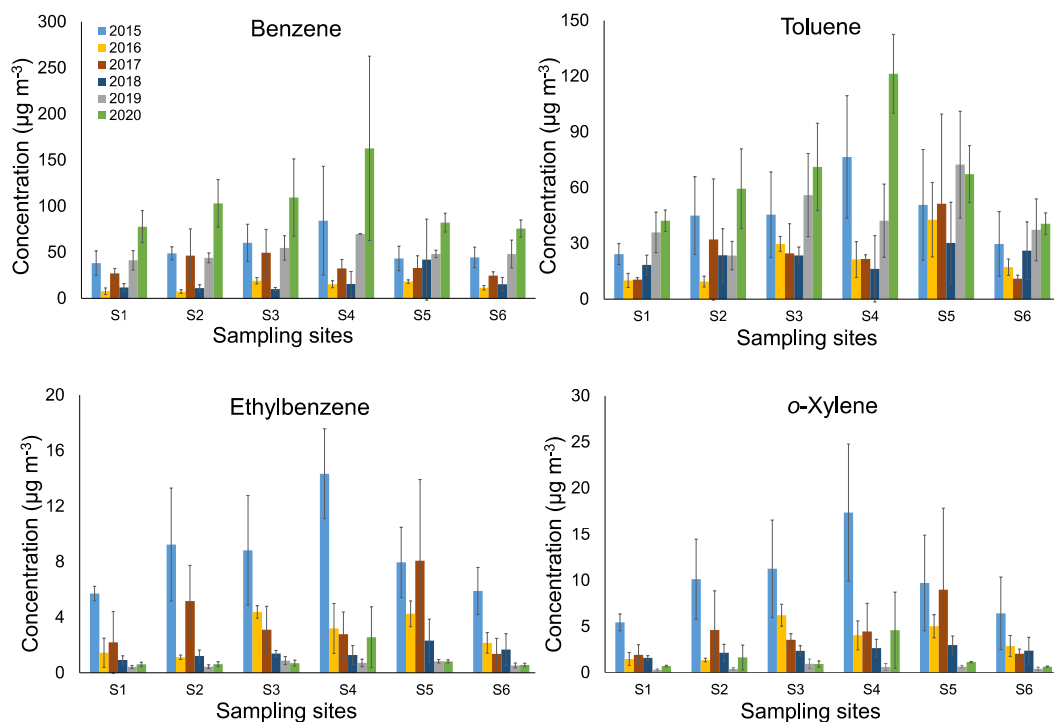


Figure 16 – Average ambient concentrations of BTEX from 2015 to 2020 (single measurements during three days in March and April) in Almaty

Table 20 – Percent change of BTEX concentrations during three days of spring 2020 lockdown compared to the average concentrations detected in the same periods of 2015-2019

Analyte	S1	S2	S3	S4	S5	S6	Average
Benzene	209%	227%	183%	274%	123%	164%	199%
Toluene	113%	123%	99%	241%	36%	67%	110%
Ethylbenzene	-72%	-82%	-81%	-43%	-83%	-76%	-72%
o-Xylene	-67%	-56%	-81%	-21%	-79%	-77%	-61%

#### 4.3.2 Differences in meteorology

The sampling period during the lockdown in April 2020 was characterized by warmer temperatures ranging from 10.2 to 16.2 °C, while the temperature ranged from -6.2 to 14.5 °C on the sampling days in 2015-2019 (Table 21, Figure 15). The average temperature was 14.0 °C in 2020 and 7.1 °C in 2015-2019. Wind speeds during the sampling period in 2015-2020 were similar and ranged from 0 to 1 m/s.

One of the reasons for the increased concentrations of benzene and toluene during the sampling days in 2020 could be attributed to the no-precipitation conditions. Since there was no traffic activity during the lockdown, the higher levels of benzene and toluene may indicate that their origins are predominantly nontraffic sources, and the declining levels of ethylbenzene and o-xylene by up to 3-fold could be linked to the traffic-free conditions.

Table 21 – Meteorological conditions on BTEX sampling days in 2015-2020

Sampling date	Temperature (°C)		Relative humidity, %		Wind speed, m/s		Precipitation, mm	
	Average	SD	Average	SD	Average	SD	Average	SD
2015								
31.03	-6.2	1.8	75.5	4.9	1.0	0.0	0.9	-
02.04	-0.5	3.1	82.5	12.0	0.0	0.0	1.5	0.7
04.04	7.4	3.7	50.0	8.5	0.5	0.7	n/d	-
2016								
31.03	13.1	1.8	85.5	12.0	0.5	0.7	0.4	-
02.04	7.8	1.4	96.5	0.7	0.0	0.0	6.0	4.2
05.04	11.6	1.9	69.5	6.4	0.0	0.0	n/d	-
2017								
01.04	11.2	6.2	65.0	29.7	0.5	0.7	19.0	-
04.04	2.4	1.3	88.0	8.5	0.5	0.7	2.0	-
06.04	2.1	0.2	77.0	4.2	0.0	0.0	8.0	7.1
2018								
03.04	6.1	2.4	50.5	17.7	0.0	0.0	n/d	-
05.04	9.8	7.3	61.5	17.7	0.0	0.0	n/d	-
07.04	12.4	4.3	75.0	28.3	0.0	0.0	6.0	-
2019								
30.03	8.8	1.2	85.5	9.2	1.0	0.0	6.0	4.2
02.04	7.1	1.4	79.0	5.7	0.0	0.0	0.3	-
04.04	14.5	1.3	69.5	17.7	1.0	0.0	1.0	-
2020								
03.04	10.2	1.2	85.5	6.4	0.5	0.7	1.0	-
05.04	16.2	1.1	33.0	4.2	0.5	0.7	n/d	-
07.04	15.6	2.6	51.0	5.7	0.0	0.0	n/d	-

#### 4.3.3 Spatial differences

BTEX concentrations were inversely proportional to the elevation (above the sea level) of the sampling sites (Figure 17) which was similar to the case for PM<sub>2.5</sub> concentrations. At the higher elevations (closer to the mountains), the concentrations of BTEX were lower than those at the lower elevations (Figure 17), and this could be explained by the location of the coal-fired power plants and households burning coal at the lower elevations.

The BTEX concentrations in 2020 were inversely correlated with the distance to CHP-3, with  $R^2=0.87$  for benzene and  $R^2=0.82$  for toluene. The distance–concentration correlations for CHP-2 were weak ( $R^2<0.1$ ), which could be due to the large distances of sampling sites from CHP-2 (Figure 18). The correlation of the benzene and toluene concentrations with the distance from CHP-3 was stronger than the correlation with the elevation (Figure 17), and this may indicate the dominant contribution of CHP-3 to BTEX pollution in the city. According to the environmental reports of CHP-3 in 2015, coal consumption at CHP-3 was expected to increase in the future due to the rising demand for electricity [145].

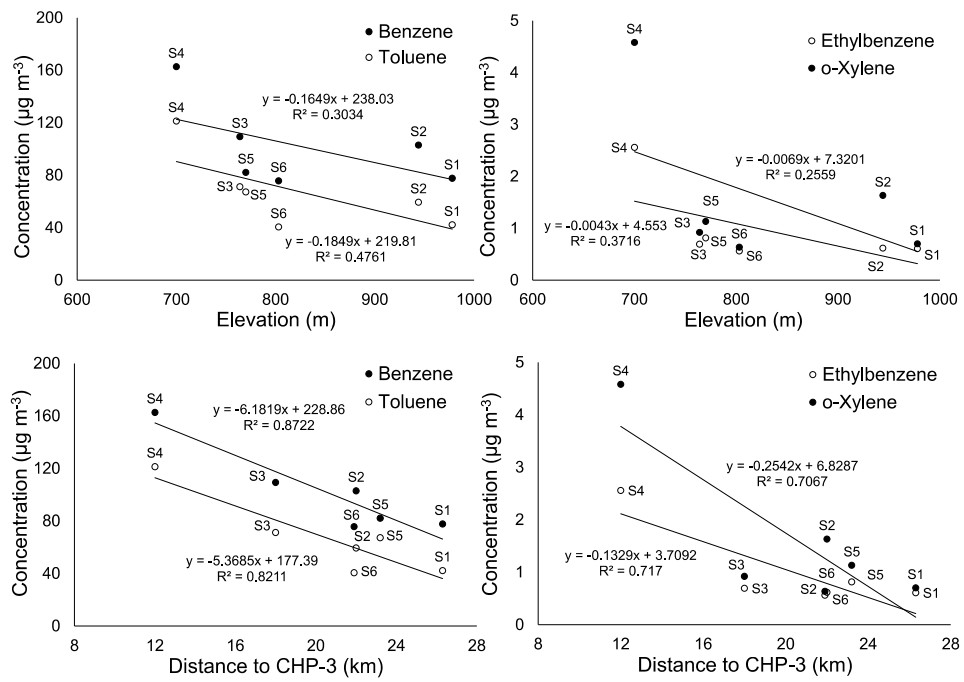


Figure 17 – Measured BTEX concentrations and elevation above sea level; and distance to CHP-3

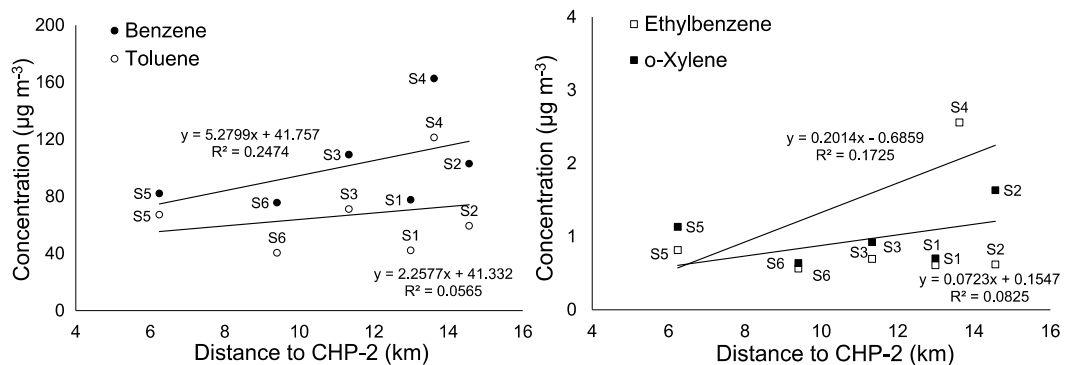


Figure 18 – Measured BTEX concentrations and distance to CHP-2

There were substantial increases in benzene and toluene during the lockdown period compared to the average during the 2015-2019 years, while some reductions were observed in ethylbenzene and *o*-xylene concentrations. The variations were significant and ranged between 123% and 227% for benzene and between 36% and 241% for toluene. The highest increases in the concentrations were observed at Station S4, which were 274% (by  $119 \mu\text{g/m}^3$ ) for benzene and 241% (by  $86 \mu\text{g/m}^3$ ) for toluene (Table 21). Station S4 is located at a low elevation (700 m), close to coal-burning housing developments and at the distances of 12 km from CHP-2 (Figure 18) and 14 km from CHP-3 (Figure 17). There is also an Almaty bus fleet park located 2.6 km away, and the public bus service was still in operation during the lockdown. The burning of coal at residential houses could have been higher, as people remained in their homes all the time during the 2020 lockdown, and there are plenty of nearby

public bathhouses (saunas) that are often heated by burning their garbage or coal. On one of the sampling days, a bonfire was also observed.

Relatively lower concentrations of benzene ( $76\text{--}78\ \mu\text{g}/\text{m}^3$ ) and toluene ( $41\text{--}42\ \mu\text{g}/\text{m}^3$ ) during the 2020 lockdown were observed at sites S1 (978 m) and S6 (803 m). Sampling site S1 is located in the upper part of Almaty (closer to the mountains), while site S6 is located in a public park at 803 m above sea level. Sampling sites S3 (764 m) and S5 (770 m) are located near significant roads; however, the high levels of BTEX at sites S3 and S5 during the 2020 lockdown indicate the significant contribution from coal combustion (Figure 19).

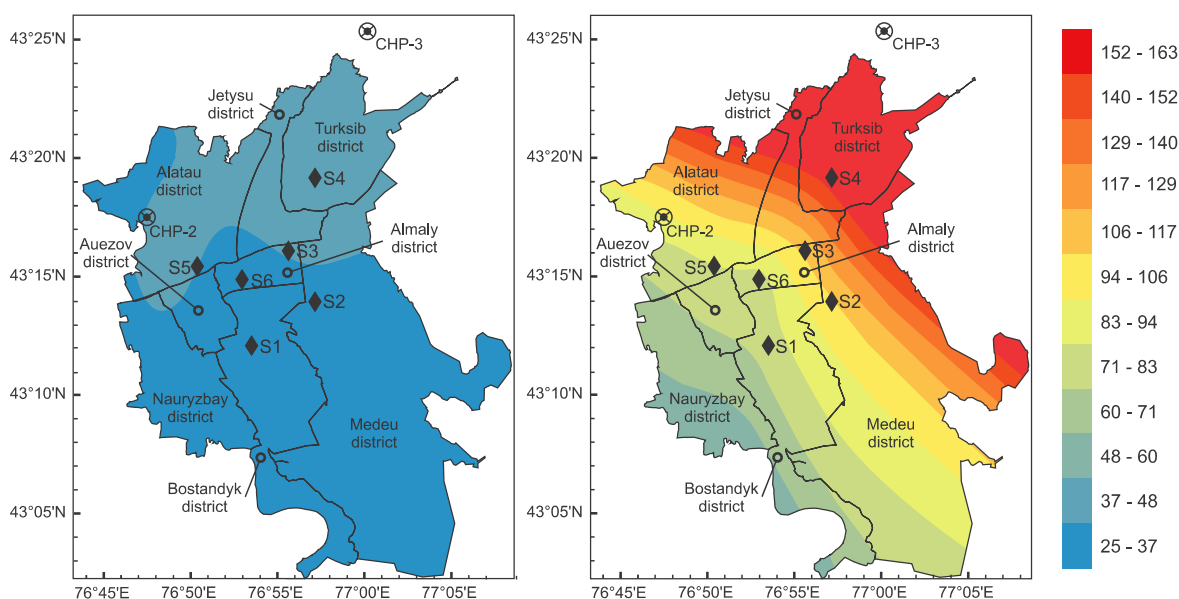


Figure 19 – Estimated average concentration of benzene in three days of spring in 2015–2019 (left) and 2020 (right),  $\mu\text{g}/\text{m}^3$

#### 4.3.4 Identification of BTEX emission sources

The varying T/B observed during 2015–2019 indicated the complex nature of BTEX in the ambient air of Almaty (Figure 20). In 2015, the obtained T/B ratios were  $<1$  in 18 out of 36 measurements, indicating that sources of BTEX were both vehicle exhaust and coal combustion [56, p.50]. The T/B found in most of the analyzed samples in 2016 (30 from 36 measurements) and 2018 (31 from 35 measurements) were  $\geq 1$ , suggesting that BTEX mainly originated from transport-related sources. The T/B of the vast majority of collected samples in 2017 (33 from 36 measurements) and 2019 (23 from 35 measurements) were  $<1$ , which indicated that BTEX mainly originated from coal burning [57, p.13].

Though there were higher concentrations of toluene and benzene, the T/B ratios were below 1 in most (32 of 36) measurements, indicating the minor effect of traffic emissions during the 2020 lockdown. Three measurements at sampling sites S2, S4, and S5 resulted in T/B values of more than 1, and one measurement at sampling site S4 showed  $\text{T/B} > 2$ . The results indicate that BTEX mostly originated from coal combustion (e.g., power plants and private houses) during the lockdown.



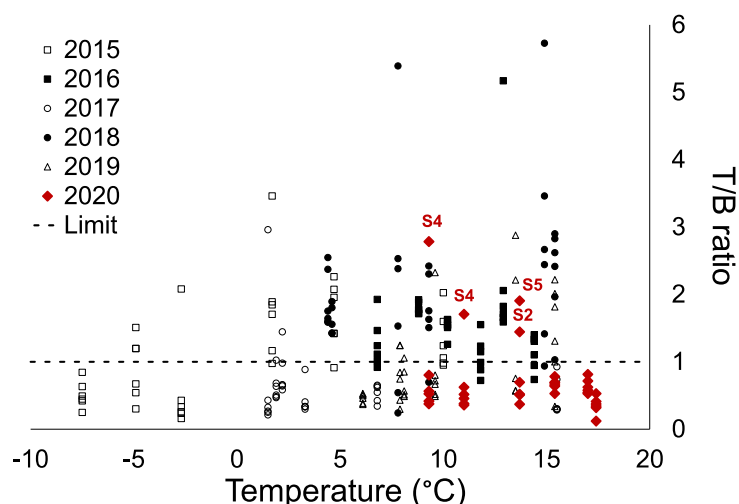


Figure 20 – Toluene-to-benzene ratios in ambient air during sampling periods in March–April of 2015–2020 (single measurements) in Almaty

#### 4.4 Section conclusion

Every year, the air quality in Almaty improves gradually from February to April due to seasonal changes in the temperature and precipitation, as well as due to a subsequent reduction of coal use at the combined heat and power plants and in individual houses. Therefore, it was not reliable to perform a temporal analysis and attribute the temporal reductions to the traffic-free conditions. As an alternative method to eliminate the weather impact, the same period was compared with that during the previous years.

Highly elevated concentrations of benzene and toluene on three sampling days during the lockdown (101 and 67  $\mu\text{g}/\text{m}^3$ ) and the toluene-to-benzene ratios suggest that these compounds originated from coal-related sources such as power plants and households and to possible episodic cases of garbage burning, bathhouses, and bus fleet stations.

This research demonstrates the complicated nature of air pollution in Almaty, which urgently needs further investigation through spatial inventories and source-apportionment studies. The SARS-CoV-2 lockdown period was a unique opportunity to test how any possible reductions in urban transport parameters may improve the air quality in the city. The results suggest that even traffic-free conditions could not cause substantial reductions in pollution levels since several primary emission sources dominate the pollution profile over the city.

## 5 OPTIMIZATION OF TIME-WEIGHTED AVERAGE AIR SAMPLING BY SOLID-PHASE MICROEXTRACTION FIBERS USING FINITE ELEMENT ANALYSIS SOFTWARE

### Preamble

The part of materials and results described in this section have been published in research articles “Kenessov B., Koziel J.A., Baimatova N., Demyanenko O.P., Derbissalin M. Optimization of time-weighted average air sampling by solid-phase microextraction fibers using finite element analysis software // *Molecules*. - 2018. – Vol.23. - Article 2736” [83, p.1-14] and reprinted with the journal permissions (Annex A). The copyright to these materials belongs to the MDPI, and any request for further use of this information should be requested from them. The materials are licensed under the Creative Commons Attribution 4.0 International License. To view a copy of this license, visit <http://creativecommons.org/licenses/by/4.0/> or send a letter to Creative Commons, PO Box 1866, Mountain View, CA 94042, USA.

### 5.1 Introduction

Calibration for determination of TWA concentrations is relatively simple compared with “classic” exposed SPME fiber that is subject to variable thickness of the boundary layer that affects the rate of extraction [146,147]. TWA sampling by retracted SPME fibers is described by the simplified version of the Fick’s law of diffusion [54, p.1514-1515] (Equation 1). Equation (1) can also be interpreted by extraction process, i.e., the amount of analyte extracted is proportional to TWA concentration outside of the SPME needle opening, needle opening area, sampling time, and the gas-phase molecular diffusion coefficient, and inversely proportional to retraction depth.

Several important assumptions are made with the application of Equation (1) to TWA-SPME, i.e., (1) fiber coating acts as a “zero sink” and does not affect the rate of sampling, (2) SPME fiber coating is consistent and reliably responding to changing concentrations in the bulk gas-phase outside of the needle opening, and (3) gas-phase concentration in the bulk are the same as at the face of the fiber needle opening.

To date, all published research on TWA-SPME used Equation (1) as the basis of quantification [53, p.457, 54,p.1515, 61, p.4, 62, p.554, 64, p.2008, 79, p.1482, 148–150]. of VOCs in laboratory air, pyrolysis reactor air, engine exhaust and process air. Equation (1) predicted measured gas concentrations with reasonable accuracy and precision. However, more evidence suggests that the discrepancies between the model and experimental data exist. Woolcock et al. [149, p.2] reported significant departure from the zero-sink assumption and from Equation (1) suggesting ‘apparent’ diffusion coefficient ( $D$ ) dependent on both sampling time ( $t$ ) and retraction depth ( $Z$ ). Baimatova et al. [61, p.7] reported significant differences in extracted mass of naphthalene gas for different SPME coatings, i.e., that Equation (1) does not incorporate. Recent research by Tursumbayeva [151] shows that the discrepancy between Equation (1) and experimental data are amplified when a wide-bore glass liner is used for passive sampling with SPME fiber retracted inside it. Work by Tursumbayeva suggests that not only the tip of the fiber coating (at the physical retraction depth  $Z$ ) is involved in extraction, but the whole fiber coating surface with

an ‘apparent’  $Z$  that is ~55% longer. Apparent saturation sorption kinetics might also be involved as predicted by Semenov et al. [152]. Thus, research is warranted to address apparent problems with the use of Equation (1).

Experimental optimization of the gas sampling process is very time-consuming, particularly at longer extraction times (>24 h). Such experimental setups are quite complex, difficult to build and properly maintain in steady-state conditions (e.g., without leaks and with minimal impact of sorption onto the system itself). During experiments, the sensitivity of the analytical instrument can change leading to additional uncertainties. Uncertainties during experimental method optimization do not allow studying effects of parameters having potentially minor impacts on accuracy and precision.

The numerical simulation could provide useful data at various sampling parameters in much faster and more accurate way. It could also allow modeling the sensitivity of Equation (1) to ranges of practical (user controlled) parameters for air sampling with retracted SPME. COMSOL Multiphysics allowed efficient numerical modeling of SPME process using finite element analysis-based model [153–157] for liquid-phase extraction and absorption by SPME coating. Using this approach, it was possible to predict sampling profiles of analytes, which were consistent with experimental data.

The goal of this Section was to develop a model for TWA-SPME and optimize time-weighted average SPME sampling of ambient air with both absorptive and adsorptive retracted fibers using finite element analysis-based model (COMSOL Multiphysics).

## 5.2 Materials and Methods

### 5.2.1 General parameters of modeling

Simulations were completed using COMSOL Multiphysics 5.2a on a desktop computer equipped with quad-core Core i7 processor, 8 Gb of random access memory and 1 Tb hard drive. For modeling, “Chemical Species Transport” module (“Transport of diluted species” physics) was used in “Time-Dependent” mode in two dimensions (axisymmetric). Fick’s second law of diffusion was used by the module:

$$\frac{\partial c_i}{\partial t} = \nabla \cdot (D_i \nabla c_i) \quad (4)$$

Benzene, a ubiquitous air pollutant, was used as a model analyte for most initial calculations. Diffusion coefficients of benzene in the air and PDMS coating were set to  $8.8 \cdot 10^{-6}$  and  $10^{-10}$  m<sup>2</sup>/s, respectively [158]. Distribution constant ( $K_d$ ) for benzene and common SPME coatings was set to 150,000 (85  $\mu$ m CAR/PDMS) [97, p.27], 8,300 (65  $\mu$ m PDMS/DVB) [97, p.27], and 301 (PDMS) [72, p.258]. For dichloromethane, acetone and toluene, distribution constants between 85  $\mu$ m Car/PDMS coating and air were set to 72,000, 71,000 and 288,000, respectively [97, p.27].

The geometry of a fiber assembly was built in as inputs based on the data provided by Pawliszyn [72, p.100]. Simulations were conducted for Stableflex (Supelco, Bellefonte, PA, USA) fibers with a core diameter of 130  $\mu$ m. For 85  $\mu$ m Car/PDMS

and 65  $\mu\text{m}$  PDMS/DVB, total fiber diameters were set to 290 and 270  $\mu\text{m}$ , respectively. Calculations were conducted for 24- and 23 ga coatings having internal diameter of 310 and 340  $\mu\text{m}$ , respectively.

The extra fine free triangular mesh was used for the modeling. To provide better meshing at the coating-air interface, the resolution of narrow regions was increased to “2”. The computation was completed in the range between 0 and 100,000 s at the step of 1000 s. The concentration of an analyte at the tip of the protecting needle was set to 0.641  $\mu\text{mol}/\text{m}^3$ , which corresponds to 50  $\mu\text{g}/\text{m}^3$  of benzene.

### 5.2.2 Sampling using absorptive coatings

Inward (and outward) fluxes from (or backward to) air into an absorptive coating ( $Flux_1$  and  $Flux_2$ , respectively) at the boundaries (marked by a red lines in Figure 21) were simulated using the equation, previously proposed by Mackay and Leinonen [159] for the water-air interface:

$$Flux_1 = k \times \left( C_a - C_f / K_d \right); Flux_2 = k \times \left( C_f / K_d - C_a \right) \quad (5)$$

where:

$k$  – flux coefficient, m/s;

$C_a$  and  $C_f$  – concentrations of an analyte in air and coating at the boundary layer, respectively,  $\text{mol}/\text{m}^3$ ;

$K_d$  – distribution constant for a VOC between SPME coating and air.

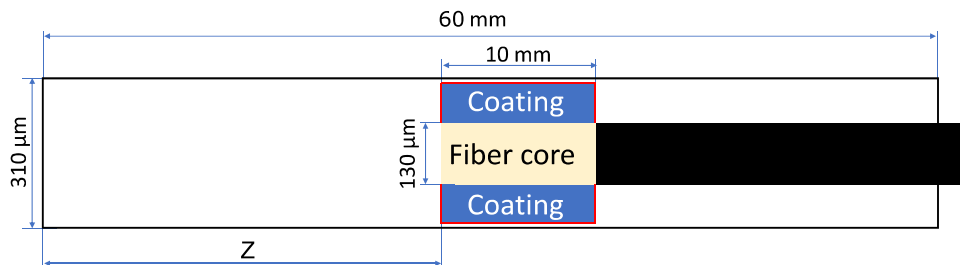


Figure 21 – The geometry of SPME device (retracted inside a protective needle for TWA sampling) used for modeling. Note: red lines indicate the boundaries between air and coating

The true value of flux coefficients was unknown, but in this research, it was assumed to be sufficiently high for not affecting flux, as was recently proposed by Alam et al. [154]. Thus, flux coefficient was set to 1000 m/s. A further increase of the flux coefficient did not affect the results of the modeling.

### 5.2.3 Sampling using adsorptive coatings

For adsorptive coatings, the “Adsorption” mechanism was activated in the model. The isotropic diffusion coefficient (in the air inside pores) was the same as for air (set

to 8.8, 8.7, 12.4 and 10.1 mm<sup>2</sup>/s for benzene, toluene, acetone and dichloromethane, respectively). The approach proposed by Mocho and Desauziers [160] involving Knudsen diffusion in micro-pores was also tested. However, it was later rejected for model simplification because the diffusion of analytes inside coating is mainly driven by molecular diffusion inside macro-pores. The presence of PDMS binder was not considered in the model because: 1) it has much weaker affinity to analytes than Carboxen; and 2) the layer of PDMS in the coating is very thin and should not affect the diffusion of analytes [72, p.50-51]; 3) there is not enough published information about exact structure of the coating.

Adsorption was set to “User defined” with a distribution constant ( $K_p$ , m<sup>3</sup>/kg) calculated as a dimensionless distribution constant divided by a coating density ( $K_d/\rho$ ). Coating porosities ( $\varepsilon = 0.685$  for Car/PDMS, and 0.775 for PDMS/DVB) were calculated using intra-particle porosities (0.37 for Car, and 0.55 for DVB [161]) and inter-particle porosity. The exact value of the latter is proprietary and not available in the open literature. Taking into account, the spherical shape of particles and available scanning electron microscope (SEM) photos, the inter-particle porosity of both coatings was set to the maximum possible value (0.50). A particle porosity ( $\varepsilon$ ) was calculated as the total volume of pores (0.78 mL for Car, and 1.54 mL for DVB) divided by the total volume of one gram of material (2.13 mL for Car, and 2.78 mL for DVB). Densities of the coatings were calculated using free fall densities of the particles (470 kg/m<sup>3</sup> for Car, and 360 kg/m<sup>3</sup> for DVB) [161] and inter-particle porosity. Effective diffusion coefficients were calculated during the calculations by the COMSOL software using the Tortuosity model proposed by Mocho and Desauziers:

$$D_e = \frac{\varepsilon D_p}{\tau} \quad (6)$$

where:

$\varepsilon$  – porosity;

$\tau$  – tortuosity factor calculated from the porosity [160]:

$$\tau = \varepsilon + 1.5(1 - \varepsilon) \quad (7)$$

For Car/PDMS and PDMS/DVB coatings, tortuosity was set to 1.16 and 1.1125, respectively.

## 5.3 Results and Discussion

### 5.3.1 Time-weighted average sampling profiles of benzene from air using different coatings

A sampling of VOCs from the air via retracted SPME has been described using a simplified form of the Fick’s first law of diffusion (Equation 1). However, this equation works only when a SPME fiber acts as a “zero sink” sorbent. Modeling using COMSOL software allowed obtaining sampling profiles for benzene (Figure 22).

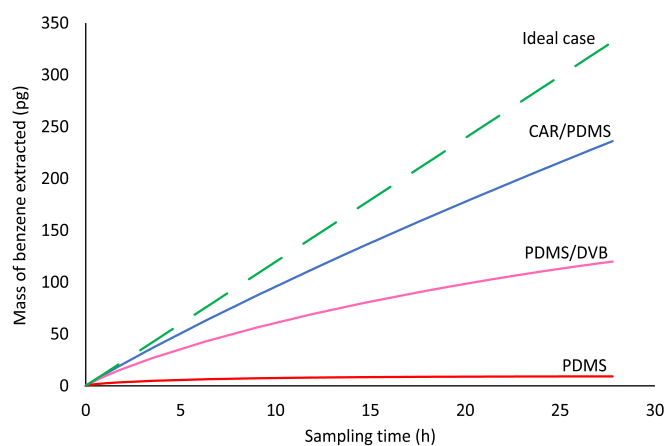


Figure 22 – Benzene sampling profiles from ambient air ( $T = 298 \text{ K}$ ,  $Z = 10 \text{ mm}$ ,  $24 \text{ ga}$  needle,  $p = 1 \text{ atm}$ ,  $C_{benzene} = 0.641 \text{ } \mu\text{mol/m}^3$ ) obtained using different fiber coatings. The ideal case pertains to Equation (1)

Closer inspection of Figure 22 illustrates that none of the studied coatings behave as “zero sink” sorbent adhering to Equation (1), an effect amplified by extended sampling time. After 100,000 s of sampling, Car/PDMS, PDMS/DVB and PDMS extracted 77, 38 and 2.7%, respectively, of the theoretically required for a passive sampling technique. Even if sampling time is decreased to 10,000 s, recoveries for these three SPME fiber coatings were 91, 69 and 12.6%, respectively. At sampling time 1000 s, recoveries were 97, 88 and 32% for Car/PDMS, PDMS/DVB and PDMS, respectively.

One possible explanation for the departure from Equation (1) is that it can be caused by the increase of the analyte concentration in the air near the fiber tip (Figure 23a), which is directly proportional to the analyte concentration in the fiber tip continuously increasing during the sampling. The increase of analyte concentration in the air near the fiber tip results in the decrease of the analyte flux (i.e., the number of moles of analyte entering protecting needle per cross-sectional area and time) from the sampled air with time. This affects the sampling rate (i.e., number of moles of an analyte extracted by a coating per unit of time), which was previously assumed to be constant [53, p.457, 54, p.1515, 61, p.4, 62, p.554, 64, p.2008, 79, p.1482, 148, p.801, 149, p.554, 150, p.3]. SPME fiber coating can affect the apparent rate of sampling. This was previously assumed to be negligible. According to the Figure 23, Car/PDMS is the most efficient coating for TWA sampling of benzene because it provides highest benzene extraction effectiveness indicated by the highest distribution constant. However, sampling by this coating is limited by the slow diffusion of an analyte via pores of the adsorbent. At sampling time 100,000 s, the closest 1 mm of the Car/PDMS coating to the needle opening contains 41% of the total extracted analyte. Benzene concentration in the fiber tip is about 500 times higher than in its other end (furthest from the needle opening). For PDMS/DVB coating, the concentration in the tip is about 24% higher. Slower diffusion of benzene via pores of Car/PDMS fiber is caused by the higher affinity of benzene to the surface of the solid phase (higher distribution

constant), and lower porosity. Such non-uniform distribution of analytes in the Car/PDMS may be the reason of their slow desorption after TWA sampling and highly tailing peaks, particularly for most volatile analytes, which cannot be cold-trapped and refocused in a column front without cryogenics. This problem also decreases the accuracy of the method.

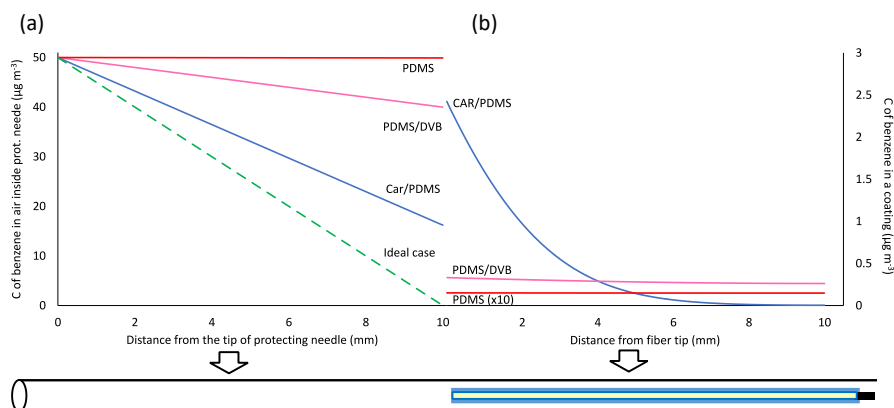


Figure 23 – Concentrations of benzene in diffusion path air (a) and coating (b) of the retracted SPME device after 100,000 s of TWA air sampling at  $Z = 10$  mm

The accuracy of the model was validated by increasing the pore diffusion coefficient of benzene inside Car/PDMS coating by three orders of magnitude. In this case, the benzene sampling profile was the same as predicted by Equation (1). This also confirms that an analyte diffusion coefficient inside a coating affects sampling profile and the accuracy of its quantification using TWA SPME. The model has also been validated in the 3D mode of COMSOL software, which is much slower compared to 2D. The difference between the results of 2D and 3D modeling were below 2%, which confirms the accuracy of the 2D model.

### 5.3.2 Effect of diffusion coefficient and distribution constant on sampling of analytes by 85- $\mu\text{m}$ Car/PDMS coating

The Car/PDMS coating was used for simulating extraction of other common VOCs associated with a wide range of diffusion coefficients and distribution constants. During 100,000 s, 3.3, 3.9, 3.5 and 3.3 pmol of dichloromethane, acetone, toluene, and benzene, respectively, were extracted, which corresponds to 68, 65, 82 and 77% of the theoretical values predicted by Equation (1) (Figure 24). The lowest value was observed for acetone having a distribution constant close to dichloromethane, and the highest diffusion coefficient among studied compounds. Highest recovery was observed for toluene having the lowest diffusion coefficient and the highest distribution constant. Thus, both diffusion coefficient and distribution constant affect the recovery of sampled analytes. Highest recovery can be achieved at the lowest diffusion coefficient and highest distribution constant. At sampling times 1000 and 10,000 s, recoveries are greater (95-98 and 85-93%, respectively) and less affected by the analyte's properties.

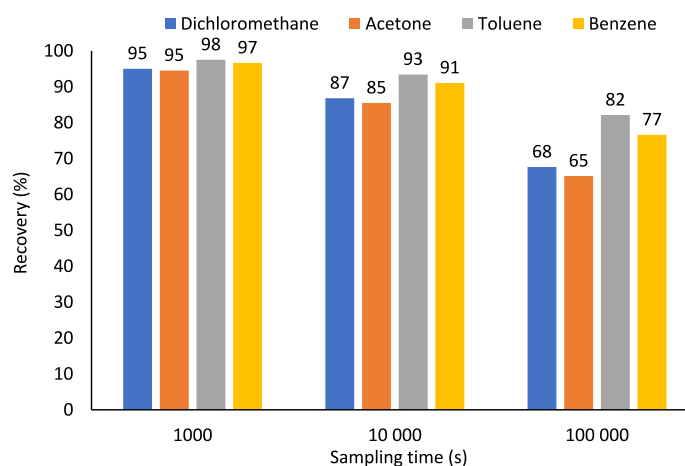


Figure 24 – Effect of sampling time of TWA recoveries of analytes having different diffusion coefficients and distribution constants using 85- $\mu\text{m}$  Car/PDMS fiber ( $T = 298\text{ K}$ ,  $Z = 10\text{ mm}$ , 24 gauge needle,  $p = 1\text{ atm}$ ,  $C = 0.641\ \mu\text{mol/m}^3$ )

### 5.3.3 Effect of a protecting needle gauge size

Commercial SPME fiber assemblies are available with two different sizes of a protecting needle 24 and 23 ga having an internal diameter (i.d.) 310 and 340  $\mu\text{m}$ , respectively. A cross-section area of the 23 ga needle is 20.3% greater than that of 24 ga needle, which (according to Equation 1) should result in the proportionally greater amount of an analyte extracted by a 23 ga SPME assembly. However, as shown above, faster extraction rates result in a faster saturation of the coating and lower recovery at longer sampling times. According to the results of COMSOL simulations, despite ~19% greater amounts of extracted analytes compared to a 24 ga assembly, sampling with a 23 ga assembly provided similar recoveries of analytes.

Such results can be explained by considering the effect of a greater space between the coating and the internal wall of the protecting needle allowing faster diffusion of analytes to the side and rear sides of a coating (Figure 25).

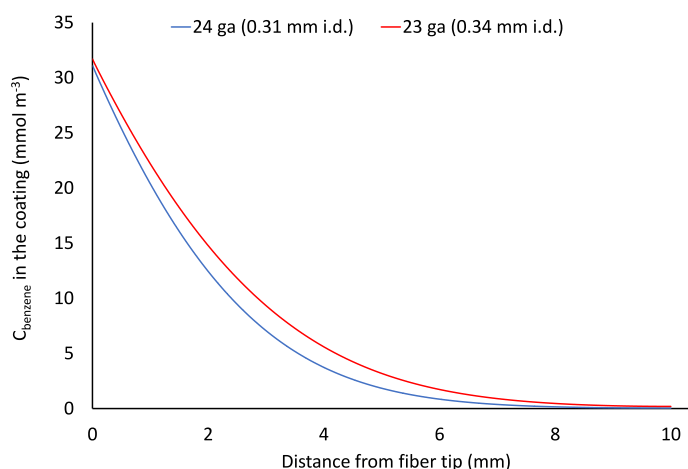


Figure 25 – Effect of protecting needle gauge size concentration profile of benzene in the Car/PDMS coating after 100,000 s sampling



This is consistent with recent experimental observations where straight glass GC liners were used (actual measured I.D. is ~0.84 mm compared with the nominal 0.75 mm I.D.) instead of SPME needle for sampling with retracted fiber [151, p.9]. Thus, TWA sampling using 23 ga SPME assembly is recommended over 24 ga for achieving lower detection limits without negative impact on the accuracy. All further modeling was conducted using a 23 ga SPME device.

#### 5.3.4 Effect of diffusion path (Z) at constant analyte concentration in sampled air

Diffusion path length is one of the two parameters that can easily be adjusted by users for achieving the optimal sampling conditions (the other one being sampling time). The increase of Z decreases the rate of sampling. It slows down the saturation of the fiber tip and increases recoveries of analytes (Figure 26) at longer sampling times. For all studied analytes, at  $t = 100,000$  s and  $Z = 40$  mm, recovery was 86-93 % compared to 66-82% at  $Z = 10$  mm (Figure 26).

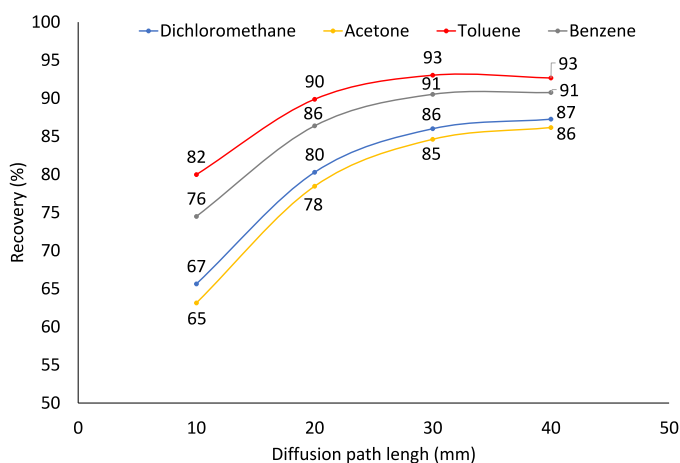


Figure 26 – Effect of diffusion path length on recoveries of four analytes ( $C = 0.641 \mu\text{mol}/\text{m}^3$ ) after sampling for 100,000 s using 23 ga Car/PDMS fiber assembly

The only major drawback of the increase of Z is the decrease of an analyte amount extracted by a coating and a lower analytical signal, which result in the increased detection limits. At  $Z = 40$  mm,  $C = 50 \mu\text{g}/\text{m}^3$  ( $C = 0.641 \mu\text{mol}/\text{m}^3$ ) and  $t = 100,000$  s, 23 ga Car/PDMS assembly extracts ~100 pg of benzene. For GC-MS, the detection limit of benzene is less than 2 pg [56, p.49] meaning that the detection limit will be ~1  $\mu\text{g}/\text{m}^3$ , which is five times lower than the maximum permissible annual average concentration of benzene in ambient air in the European Union (5  $\mu\text{g}/\text{m}^3$ ). In other countries, permissible concentrations are even higher.

#### 5.3.5 Effect of diffusion path (Z) at variable analyte concentration in sampled air (worst-case scenario)

Time-weighted average sampling is conducted during long time periods (e.g., 24 h), during which concentrations of analytes in the sampled air can vary significantly. The apparent worst-case scenario can be when in the first half of sampling,

concentration is much higher than during the second half. When the concentration of an analyte in the sampled air becomes close to or lower than the concentration near the fiber tip, the flux of analytes inside protecting needle can go to a reverse direction resulting in desorption of analytes from a coating. However, this violates the main principle of TWA sampling: the rate of sampling should depend only on the concentration of an analyte in a sampled air. It means that if an analyte concentration in sampled air is zero, a rate of extraction should also be equal to zero. Thus, the aim of this part of the work was to model such a case and estimate the highest possible uncertainty of the TWA SPME sampling approach.

As was assumed, desorption of dichloromethane, acetone, and benzene from a fiber started after concentrations of analytes dropped from  $1.176$  to  $0.1176 \mu\text{mol}/\text{m}^3$  in the middle of extraction process (Figure 27).

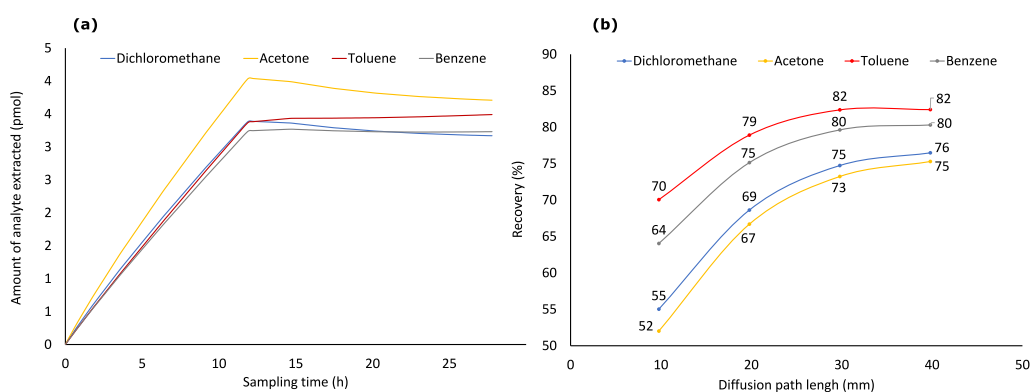


Figure 27 – Sampling ( $Z = 10$  mm) profiles (a) of four analytes from air having their varying concentrations ( $C_{0-49,000s} = 1.176 \mu\text{mol}/\text{m}^3$ ,  $C_{49,000-51,000s} = 1.176 - 0.1176 \mu\text{mol}/\text{m}^3$ ,  $C_{49,000-100,000s} = 0.1176 \mu\text{mol}/\text{m}^3$ ) and recoveries of analytes (b) at  $t = 100,000$  s and different  $Z$

Desorption of toluene was not observed because it has the highest distribution constant among all studied analytes. However, the toluene sampling rate after the drop of its concentration in sampled air was lower than theoretical. Recoveries of analytes at  $Z = 10$  mm dropped from 65-82 to 52-70%, at  $Z = 20$  mm from 78-90 to 67-79%, at  $Z = 30$  mm from 85-93 to 73-82, at  $Z = 40$  mm from 86-93 to 75-82 % (Figure 27). Only at  $Z = 40$  mm, it was possible to keep recovery of all analytes above 75%. Thus, if possible, for greater accuracy, sampling must be arranged so that no significant drop in concentration takes place. Such a drop can be observed, e.g., if the end of sampling is planned for the night when VOCs concentrations in ambient air are typically lower due to much lower road traffic and other human activities. Also, using shorter sampling times can minimize the risk of the reverse diffusion when ambient concentrations are predicted to drop significantly.

### 5.3.6 Alternative geometries for time-weighted average solid-phase microextraction sampling

As was shown above, recoveries of analytes can be increased by increasing the

internal diameter of a protecting needle because analytes can faster diffuse around and to the side of the fiber coating than inside it. It decreases the controlling role of the fiber coating and should lead to a more accurate and reproducible results.

Tursumbayeva [151, p.12] proposed using SPME liner for TWA SPME to avoid sorption of analytes onto metallic walls of a protecting needle. The same approach can be used to avoid equilibration of analytes between the fiber tip and surrounding space after sampling over longer time periods. At variable concentrations of analytes (as simulated in the previous section), calculated recoveries for VOCs using  $Z = 67$  mm (Figure 28a) are 73-84%, which is close to the values obtained using retracted fiber at  $Z = 40$  mm.

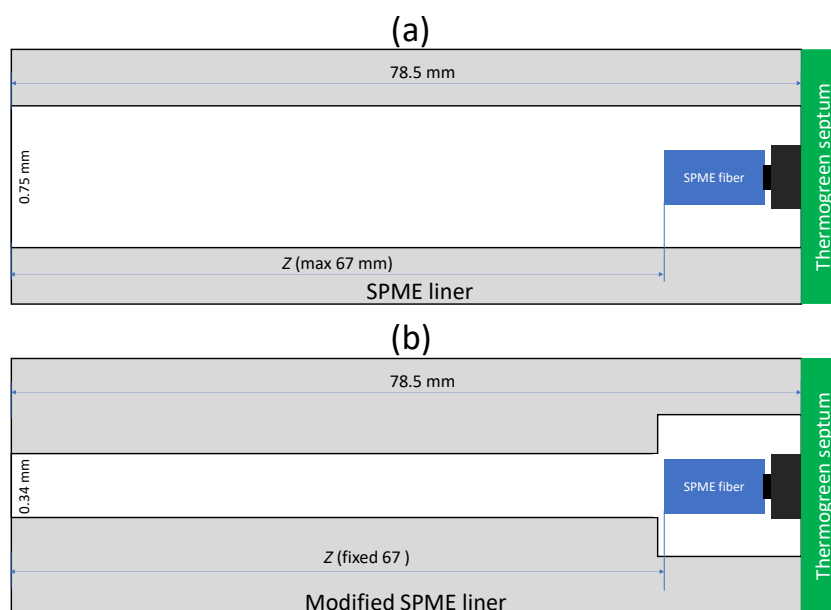


Figure 28 – Alternative geometries for TWA SPME sampling: (a) used by Tursumbayeva [151], and (b) proposed in this research to minimize sources of deviation from Fick’s law of diffusion calibration

No improvement was observed because 0.75 mm i.d. SPME liner has 4.9 times greater cross-sectional area than 23 ga protecting needle, which results in a 2.9 times greater theoretical flux of analytes from sampled air to the coating under the set  $Z$  (67 and 40 mm, respectively). To decrease flux of analytes, the liner can be modified to a lower i.d. (e.g., 0.34 mm as for 23 ga needle) from the sampling side almost to the expected location of the fiber as shown in Figure 28b. Under these conditions, recoveries increased to 88-91% (Figure 29).

The use of these alternative geometries (Figure 30) resulted in a more uniform distribution of the analytes in a coating; for 0.75 mm i.d. SPME liner concentrations of analytes near the fiber tip were only 1.1-2.7 times greater than at another side of the coating. This should result in a faster desorption of analytes, less pronounced peak tailing and greater accuracy of the method. A similar effect is achieved when using Radiello<sup>®</sup> passive air sampler [41, p.899], which provide a greater surface area of an

adsorbent available for the diffusive air sampling.

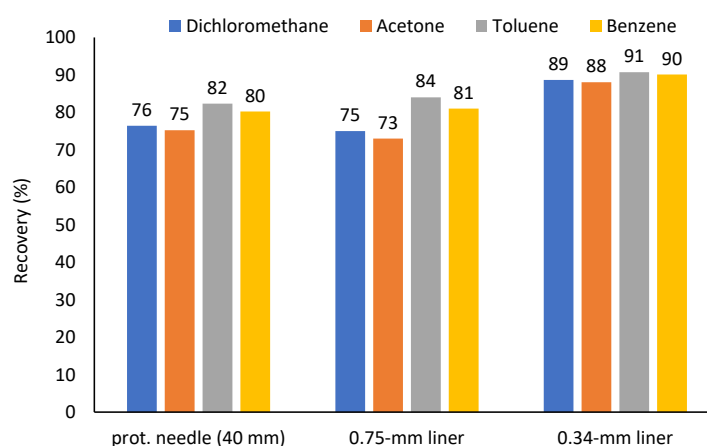


Figure 29 – Effect of TWA SPME sampling geometry on recoveries ( $t = 100,000$  s,  $C_{0-49,000s} = 1.176 \mu\text{mol}/\text{m}^3$ ,  $C_{49,000-51,000s} = 1.176 - 0.1176 \mu\text{mol}/\text{m}^3$ ,  $C_{49,000-100,000s} = 0.1176 \mu\text{mol}/\text{m}^3$ )

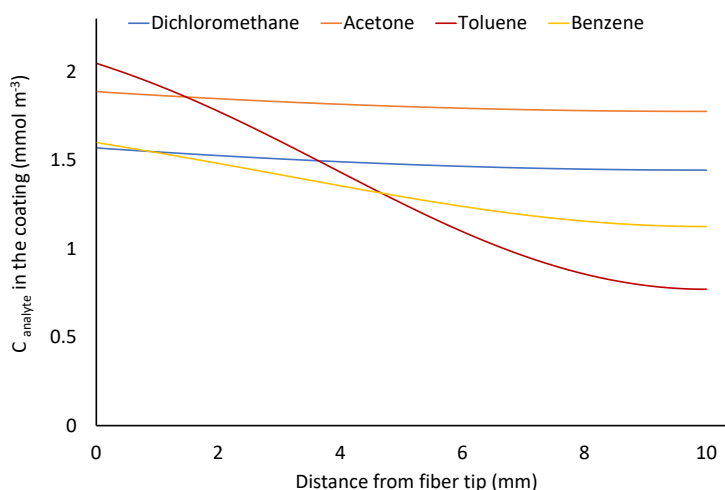


Figure 30 – Profiles of analyte concentration in the Car/PDMS coating after sampling ambient air ( $C_{0-49,000s} = 1.176 \mu\text{mol}/\text{m}^3$ ,  $C_{49,000-51,000s} = 1.176 - 0.1176 \mu\text{mol}/\text{m}^3$ ,  $C_{49,000-100,000s} = 0.1176 \mu\text{mol}/\text{m}^3$ ) for 100,000 s using the geometry presented in Figure 28a

### 5.4 Section conclusion

A finite element analysis-based model (based on COMSOL Multiphysics software) allowed efficient simulation of TWA air sampling of VOCs using retracted SPME fibers. It was possible to model the effects of sampling time, coating type (including adsorptive coatings for the first time) and composition, diffusion coefficient, the distribution constant, the internal diameter of a protecting needle and diffusion path on the recovery of analytes, their concentration profiles in the air inside protecting needle, and the coating. The advantages of such a simulation compared to an experiment are: (1) time and cost savings; (2) lower uncertainty and the possibility to

discover minor impacts of sampling parameters on its performance; and (3) the possibility to understand and optimize a sampling process in greater detail. The results of this research allowed disclosing potential sources of the apparent departure from Fick's law of a diffusion-based model used for quantification of VOCs with retracted SPME.

It was established that sampling by porous coatings with high affinity to the analyte (Car/PDMS) is affected by the saturation of the fiber tip and slow diffusion of analytes in the coating. Highest recoveries are achieved for analytes having lowest diffusion coefficients and highest affinities to a coating. The increase of an internal diameter of a protecting needle from 24 to 23 ga allows proportionally greater responses to be obtained at similar recoveries.

The most important parameter of a sampling process that users can control is a retraction depth. The increase of  $Z$  allows slowing down the sampling and achieving higher recoveries of analytes. In this study, at  $Z = 40$  mm and constant analyte concentration in a sampled air, recoveries of studied analytes reached 86–93% compared to 65–82% at  $Z = 10$  mm. The developed model allowed simulation of the worst sampling case when analyte concentrations significantly drop in the middle of sampling. For the first time, it has been proven that at such sampling conditions and  $Z = 40$  mm, recoveries of analytes can drop by ~10%, while at  $Z = 10$  mm by ~15%.

According to the results of the simulation, it is optimal to conduct sampling of studied VOCs using a 23 ga Car/PDMS assembly at  $Z = 40$  mm. Expected detection limits at these parameters are about  $1 \mu\text{g}/\text{m}^3$ .

Alternative geometries of a protective TWA SPME sampling devices could be used to increase recoveries of analytes. Sampling using 0.75-mm I.D. SPME GC liner at  $Z = 67$  mm provides similar recoveries compared to sampling using a protecting needle at  $Z = 40$  mm, but it provides greater amounts of analytes extracted and lower detection limits. To achieve greater recovery, part of the liner should have narrower I.D. (e.g., 0.34 mm). The increase of the diameter of the extraction zone where the coating is located results in a more uniform distribution of analytes, which should lead to faster desorption, less pronounced peak tailing and greater accuracy. Specific sampler parameters should be selected for particular sampling time and environmental conditions (temperature and atmospheric pressure) using the developed model. The methodology used in this study could also be used for more accurate and simpler calibration of the method. It can be used to model the sampling of other environments (process gases, water) by retracted SPME fibers. Further modification of this model could allow simulation of soil and soil gas sampling.

## 6 DEVELOPMENT OF THE METHOD FOR THE DETERMINATION OF TIME-WEIGHTED AVERAGE CONCENTRATIONS OF VOLATILE ORGANIC POLLUTANTS IN THE AIR BASED ON A MODIFIED SAMPLER WITH AN ALTERNATIVE GEOMETRY AND SOLID-PHASE MICROEXTRACTION

In Section 5, an alternative geometry of a protective TWA SPME sampler was proposed. It was suggested that the narrow inner diameter (0.34 mm) of the glass liner during the diffusion path and the wider diameter (0.75 mm) in the extraction zone would provide higher recoveries of the TWA concentrations of VOCs. Experimental optimization is required to confirm the developed model based on numerical modeling using COMSOL Multiphysics. This Section aims to the development of a modified sampler with an alternative geometry and method for the determination of TWA concentrations of VOCs in ambient air using SPME.

### 6.1 Experimental part

#### 6.1.1 Reagents and materials

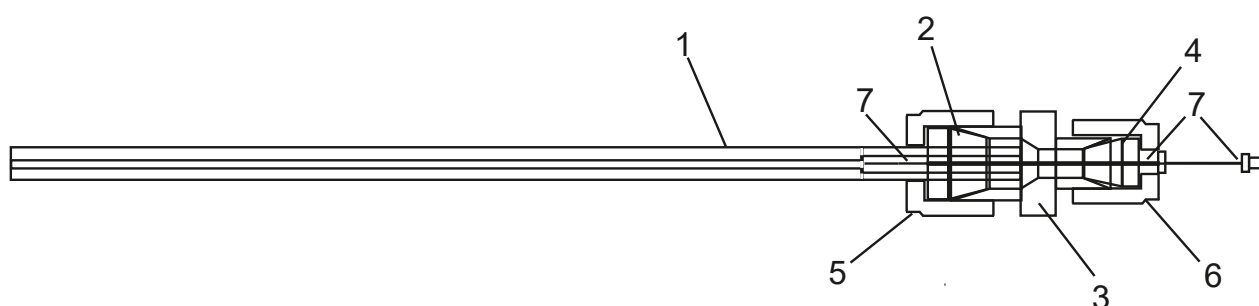
A wide range of VOCs was used in this study (Table 22). All standard solutions for experiments were prepared in methanol (purity  $\geq 99.9\%$ ) that was obtained from Sigma-Aldrich (St. Louis, MO, USA). Helium (purity  $> 99.995\%$ ) for GC-MS analysis was obtained from “Orenburg-Tehgas” (Orenburg, Russia). Nitrogen (99.5%) was obtained from Ihsan Technogaz (Almaty, Kazakhstan) for the gas generation system.

Table 22 – The list of VOCs and their physical properties

Compound	Purity (%)	Origin	CAS No.	Molar mass (g/mol)	Boiling Point (°C)
<i>n</i> -Dodecane	$\geq 99.0$	Sigma-Aldrich (St. Louis, MO, USA)	112-40-3	170.3	216.3
Tetrachloroethane			79-34-5	167.8	146
Ethylbenzene			100-41-4	106.2	136
<i>m</i> -Xylene			108-38-3	106.2	139
<i>p</i> -Xylene			106-42-3	106.2	138
<i>o</i> -Xylene			95-47-6	106.2	144
Naphthalene			91-20-3	128.2	218
Benzene	$\geq 99.8$	EKOS-1 LLP (Moscow, Russia)	71-43-2	78.11	80
Toluene			108-88-3	92.14	111
<i>n</i> -Undecane	$\geq 99.0$	LLO Ekroschem (St. Petersburg, Russia)	1120-21-4	156.3	196
1,3,5-Trimethylbenzene			108-67-8	120.2	165
1,2-Dichloroethane	$\geq 99.0$	Component-reactive LLO (Moscow, Russia)	107-06-2	98.96	83
Methyl tert-butyl ether	$\geq 99.9$		1634-04-4	88.15	55.2
1,2,4-Trimethylbenzene	$\geq 98.0$	Topan LLP (Uralsk, Kazakhstan)	95-63-6	120.2	169

### 6.1.2 The modified sampler with an alternative geometry for time-weighted average sampling of volatile organic compounds

The main concept of sampler modification was proposed by Kenessov et al. [83] and by the results obtained in Section 5. The use of glass liner with alternative geometry was proposed: an increased inner diameter in the extraction zone (0.80 mm) and a reduced inner diameter during the diffusion path (0.34 mm) (Figure 31). Before sampling with the developed sampler, a glass capillary (1) was installed on the adapter (3) from the 1/4" side and screwed with a PTFE ferrule (2) and metal nut (5). Subsequently, the inner part of the modified sampler was purged with pure nitrogen to avoid contamination by VOCs. SPME fiber (7) was inserted from the 1/8" side to the adapter and fixed with a PTFE ferrule (4) and metal nut (6). For determination time-weighted average concentrations of VOCs, the SPME fiber was exposed inside the glass capillary at the extraction zone.



1 – glass capillary, 2,4 – PTFE ferrules, 3 – 1/8 to 1/4 adapter, 5,6 – metal nuts, 7 – SPME fiber

Figure 31 – The modified TWA sampler with alternative geometries

### 6.1.3 Gas chromatography-mass spectrometry conditions

All analyses were conducted on a 7890A/5975C (Agilent, USA) GC-MS system equipped with split/spitless inlet and the MPS (Gerstel, Germany) autosampler. Separations were performed using 30 m × 0.25 mm HP-INNOWax column (Agilent, USA) with a 0.25 μm film thickness at a constant helium flow of 1.0 mL/min. Thermal desorption of analytes from SPME fiber in the GC injector was performed in spitless mode at 240 °C using 0.75 mm i.d. liner (Supelco, USA). The oven temperature was programmed from 40 °C (held for 5 min) to 205 °C with a heating rate of 10 °C/min, then to 240 °C (held for 3 min) with a heating rate of 50 °C/min. The total GC run time was 25.2 min. Temperatures of MS ion source, quadrupole and interface were 230, 150 and 250 °C, respectively. MS detection was performed using the electron impact ionization at 70 eV in selected ion monitoring mode. For better separation and peaks shape, ions were divided into 4 groups (Table 23).

### 6.1.4 Variability of solid-phase microextraction fibers

The study of SPME fibers variability was carried out in static mode and was based on a comparison of analyte responses obtained by six 85 μm Car/PDMS fibers. During extraction, the SPME fibers were exposed inside a glass capillary at Z=20 mm. The glass capillary was similar to the GC glass liner for SPME, but the internal diameter

was equal to 0.80 mm. Extraction was conducted for 1 and 8 hours in a 1 L jar with modified caps, which consisted of seven holes (6 for glass capillary and 1 for solution injection) (Figure 32). Gas with known concentrations of VOCs was prepared by adding 5  $\mu\text{L}$  of a standard solution of analytes with a concentration of 100  $\text{ng}/\mu\text{L}$  through Thermogreen septa in a 1 L jar. The concentration of analytes added to jar was  $500 \mu\text{g}/\text{m}^3$ .

Table 23 – MS detection program of analytes in SIM mode

№	Retention time, min	Group №	Compounds	Quantification Ion $m/z$ , amu (dwell)	Group Start Time (min)
1	3.50	1	Benzene	78 (50)	3.10
2	5.77		Toluene	91 (50)	
3	6.66		1,2-Dichloroethane	62 (50)	
4	7.25	2	<i>n</i> -Undecane	57 (50)	7.10
5	7.91		Ethylbenzene	106 (50)	
6	8.07		<i>m</i> -Xylene	106 (50)	
7	8.22		<i>p</i> -Xylene	106 (50)	
8	9.14	3	<i>o</i> -Xylene	106 (50)	9.00
9	9.42		<i>n</i> -Dodecane	57 (50)	
10	10.29		1,3,5-Trimethylbenzene	105 (50)	
11	10.95		1,2,4-Trimethylbenzene	105 (50)	
12	14.41	4	Tetrachloroethane	83 (50)	14.00
13	17.33		Naphthalene	128 (50)	



Figure 32 – The 1 L jar with modified caps and six glass capillaries

#### 6.1.5 The development of system for generation of gas with known concentrations of volatile organic compounds

The developed system for gas generation with known VOC concentrations is shown in Figure 33. The gas line of the developed system consisted of a nitrogen gas



cylinder with valve (1), which was connected to gas reduction valves including switch (2) (Brass 1/4 in. Swagelok, USA), and needle valves (3) (Stainless Steel Low-Flow Metering Valve, 1/4 in., Swagelok, USA). The gas line was connected to two 20 mL vials filled with activated carbon (4) to purify nitrogen to achieve “zero” air that required for the accurate determination of TWA concentrations. Before each series of experiments, the blank of nitrogen flow was checked to avoid possible inaccuracy due to contamination. After purification, the gas line was connected to the thermostated station, consisting of mixing port (5), motorized syringe pump (6) (KD Scientific, Inc., Holliston, MA, USA), and a 250  $\mu$ L gas tight syringe (7) (Hamilton, Reno, NV, USA). A mixing port was required for the injection of a standard solution of VOCs into the system. To equilibrate the VOCs concentration in the system, 5 m PTFE tubing (8) was used.

The equilibration zone was connected to the extraction zone, which consisted of a custom-made gas sampling bulb (9) with four sampling ports. The developed samplers with alternative geometry (10) were installed in the sampling ports. The heating and temperature control in the developed system was performed using a custom-made heating system and thermocouple thermometer, respectively. For stability assessment a 20 mL vial (11) was connected to the developed system. The vial was placed on a GC autosampler tray (12), which was installed on GC-MS. The gas line of the system was connected to SKC check-mate Flowmeter (13) (SKC Inc., Dorset, UK) to control airflow during extraction and for the accurate preparation of gas with known concentrations. All the connections were made of PTFE to avoid the adsorption of VOCs.

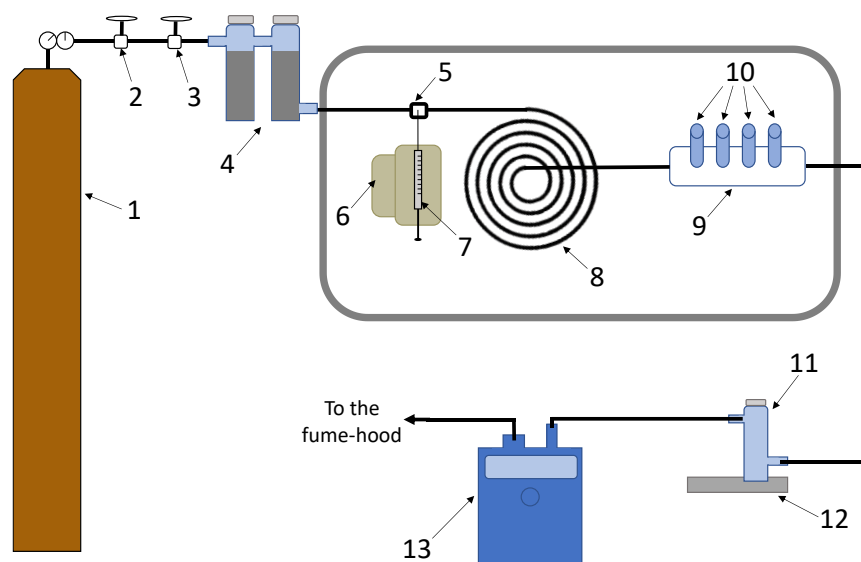


Figure 33 – The scheme of the developed system for determination of TWA concentrations

Extraction of VOCs was carried out in a 20 mL vial by exposed 85  $\mu$ m Car/PDMS for 1 min every 3 h. The total duration of stability assessment was 48 h. The concentration of the VOCs in the system was 333  $\mu$ g/m<sup>3</sup>, which was prepared by

injection a standard solution with an analytes concentration 2000 ng/ $\mu$ L using a syringe pump at speed of 3  $\mu$ L/h. The nitrogen flow rate was set at 300 mL/min. Stabilization of VOCs concentrations in the developed system was carried out for 24 h.

#### 6.1.6 Methodology of optimization of solid-phase microextraction fiber coating

Five commercially available fibers (50/30  $\mu$ m DVB/Car/PDMS with 1 and 2 cm coatings, 100  $\mu$ m PDMS, 85  $\mu$ m Car/PDMS and 65  $\mu$ m PDMS/DVB) and one synthesized in our laboratory SPME fiber with a metal-organic framework (MOF)-199 coating were chosen for optimization. Extraction was carried out in the developed system using modified TWA sampler at Z=67 mm for 24 h at 30 °C. The concentrations of VOCs in the system were 345  $\mu$ g/m<sup>3</sup> for MOF-199, DVB/Car/PDMS with 1 and 2 cm coatings and PDMS, and 408  $\mu$ g/m<sup>3</sup> for Car/PDMS and PDMS/DVB.

The selection of the optimal SPME fiber coating was based on the recovery of the analyte adsorption/absorption masses:

$$R = \frac{m_{meas}}{m_{theory}} \times 100\% \quad (8)$$

where:  $m_{meas}$  and  $m_{theory}$  – measured and theoretical masses of the analytes on the SPME fiber extracted during TWA sampling, respectively.

The measured masses of the analytes were calculated using calibration plots obtained by liquid injection of the standard solution in the GC-MS. The theoretical masses were calculated using Fick's law:

$$m = \frac{C_{TWA}tDA}{Z} \quad (9)$$

where:  $C_{TWA}$  – time-weighted average concentration of an analyte in system,  $\mu$ g/m<sup>3</sup>;

$t$  – extraction time, s;

$D$  – diffusion coefficient of analytes, sm<sup>2</sup>/s;

$A$  – cross sectional area of modified sampler, m<sup>2</sup>;

$Z$  – diffusion path length, m.

#### 6.1.7 Comparison of GC liner and modified sampler for determination of time-weighted average concentrations

The experiment was conducted using the developed system with VOC concentrations of 376  $\mu$ g/m<sup>3</sup>. Extraction was carried out by exposed 85  $\mu$ m Car/PDMS and MOF-199 at Z=67 mm for 24 h at 30 °C in developed modified sampler and common GC liner for SPME. The use of a GC liner for TWA extraction was proposed by Tursumbayeva et al. [89]. Before each extraction, blanks of the nitrogen flow were obtained under the same conditions.

### 6.1.8 Effect of diffusion path length

The effects of the diffusion path length on the analyte recoveries were studied at VOCs concentrations of  $350 \mu\text{g}/\text{m}^3$  in the developed system. Extraction was conducted at  $30 \text{ }^\circ\text{C}$  for 24 h by  $85 \mu\text{m}$  Car/PDMS at 27, 67, 97 and 127 mm. All diffusion path lengths were analyzed using two replicates.

### 6.1.9 Comparison of the developed method with sorbent tube-based method

The developed method was compared with the sorbent tube-based method, which was used as the “reference” method. For comparison, the sampling of real air samples was conducted simultaneously by  $85 \mu\text{m}$  Car/PDMS SPME fiber exposed in sampler with alternative geometry at  $Z=67$  mm and sorbent tubes packed with Carbo-pack® B+X. In addition, the developed system was applied for air sampling to assess the difference between the static and dynamic modes for the determination of analyte TWA concentrations. Extraction was conducted for 24 h.

The sampling was conducted simultaneously using a developed sampler installed in a box that protects SPME fibers from meteorological conditions (rain, snow, and strong wind) (Figure 34) and in the developed thermostated system. The sampling part of the sampler was exposed to the ambient air. SPME fiber analysis of was conducted immediately after sampling.

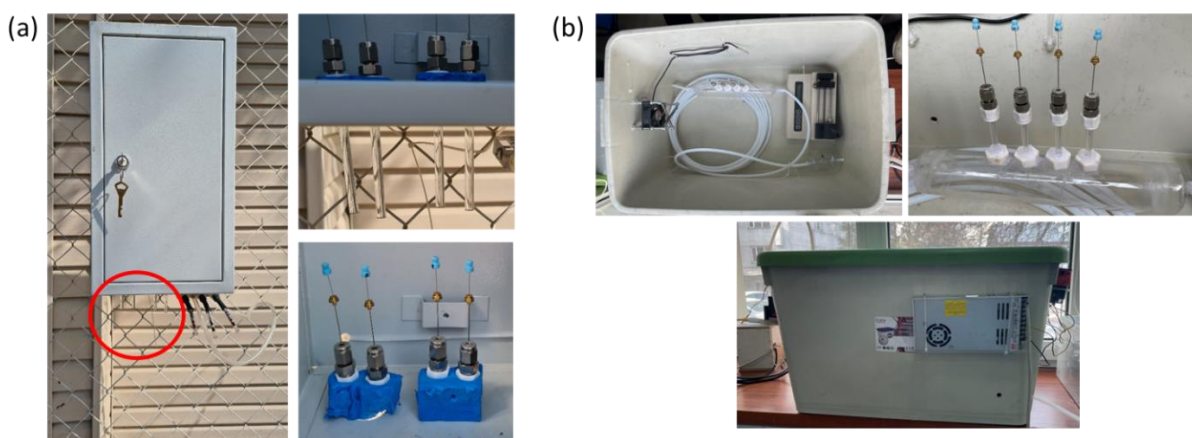


Figure 34 – The sampling of ambient air: (a) using developed sampler; (b) using developed sampler and system

Before sampling, the sorbent tubes were preconditioned at  $300 \text{ }^\circ\text{C}$  under helium flow for 25 min and sealed in special containers for storage and transportation using PTFE ferrules and Swagelok-type fitting. Sampling was carried out using the Pocket pump TOUCH (SKC Inc., Dorset, UK) at a flow rate of  $30 \text{ mL}/\text{min}$  for 24 hours. The total sample volume was 43.2 L. Analysis was conducted on a 7890A/5975C (Agilent, USA) GC-MS system equipped with a CIS4 programmable temperature vaporization (PTV) inlet, commanded by a C506 controller (Gerstel, Germany), and MPS2 (Gerstel, Germany) autosampler. Separations were performed using a  $60 \text{ m} \times 0.25 \text{ mm}$  DB-624 column (Agilent, USA) with a  $1.4 \mu\text{m}$  film thickness at a constant helium flow of  $1.0 \text{ mL}/\text{min}$ . Samples were injected via the TDU-PTV inlet at the solvent vent mode, and

50 mL/min helium flow was purged through the sorbent tube in the thermal desorption unit TDU2, then directed to the cooled injection system.

TDU was heated from 10 °C (held for 0.5 min) to 300 °C (held for 10 min) at a heating rate of 100 °C/min. In the PTV, analytes were trapped in a Carbotrap® B-packed liner at -80 °C. For cryofocusing liquid nitrogen was obtained from Laboratory of Cryophysics and Cryotechnologies (Almaty, Kazakhstan). The PTV injection temperature was programmed from -80 °C (held for 5 min) to 250 °C (held for 15 min) at a heating rate of 10 °C/min. The transfer temperature was set at 200 °C. The oven temperature was programmed from 35 °C (held for 5 min) to 240 °C (held for 10 min) at a heating rate of 10 °C/min. The total run time was 35.5 min.

## 6.2 Results and Discussion

### 6.2.1 Study of variability of solid-phase microextraction fibers

A study of SPME fibers variability is necessary to assess the possibility of simultaneous use of several fibers with the same coating. Simultaneous use reduces the time required for experiments and allows parallel measurement of TWA concentrations.

The experiment was carried out using a modified 1 L jar, which should provide an infinite volume for long-term extraction by six SPME fibers without substantial changes in the VOCs concentrations in the jar. COMSOL Multiphysics was used to prove the infinite volume for 1 L jar. The modified 1 L jar was built in COMSOL for extraction by one and six SPME fibers over 50 h. According to the simulation, the difference between analyte masses adsorbed by one and six fibers was insignificant ( $\leq 5\%$ ) during 50 h of extraction (Figure 35). The obtained results indicated the possibility of using a 1 L jar for simultaneous extraction by six SPME fibers for further experiments.

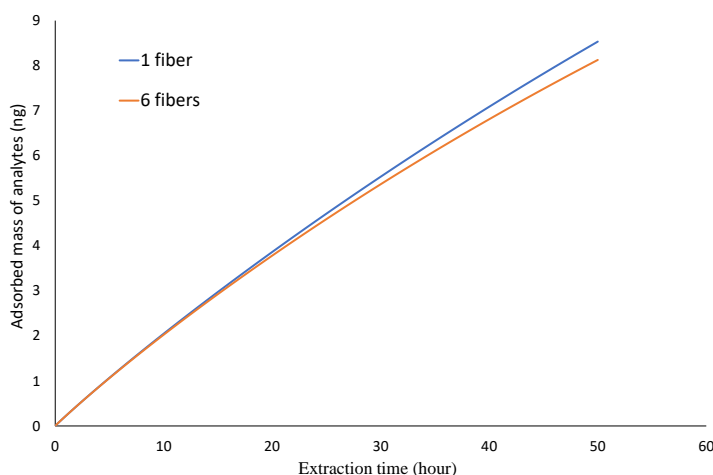


Figure 35 – Simulation of extraction in 1L jar with one and six SPME fibers

The responses of the analytes obtained by the six Car/PDMS fibers were statistically analyzed using the Grubbs test to study the variability (Minitab 19, trial version, USA). Two outliers were determined using Grubbs test for methyl tert-butyl

ether and *n*-dodecane after 8 h of extraction ( $p < 0.05$ ) (Table 24). All outliers were obtained by fiber №4. According to the Grubbs test, the differences between analytes extracted by different Car/PDMS fibers were statistically insignificant, except fiber №4. Therefore, in further experiments all fibers can be used for parallel measurements. Fiber №4 was not used in further experiments.

Table 24 – *p*-values obtained by Grubbs test

Compounds	<i>p</i> (1 h)	<i>p</i> (8 h)
MTBE	0.244	0.013*
1,2-Dichloroethane	0.528	0.909
Benzene	1.000	0.200
Toluene	0.925	0.622
Ethylbenzene	1.000	0.593
<i>m,p</i> -Xylene	0.814	0.453
<i>o</i> -Xylene	1.000	0.453
Tetrachloroethane	0.121	1.000
1,3,5-Trimethylbenzene	0.352	1.000
1,2,4-Trimethylbenzene	1.000	0.880
<i>n</i> -Undecane	0.294	0.239
<i>n</i> -Dodecane	0.134	0.013*
Naphtalene	0.293	0.473
Note: * - statistically significant		

The relative standard deviations of the responses obtained by studied six SPME fibers were calculated for determination of precision. Maximal RSDs were obtained for *n*-dodecane at extraction time of 1 h (39%) and 8 h (23%) and naphthalene at 1 h (33%). The RSDs of the remaining analytes varied from 2 to 15% (Table 25).

Table 25 – The RSDs of the analytes responses obtained at 1h and 8 h extraction

Compounds	RSD at 1 h (%)	RSD at 8 h (%)
MTBE	7	9
1,2-Dichloroethane	11	5
Benzene	11	3
Toluene	9	12
Ethylbenzene	11	5
<i>m,p</i> -Xylene	9	4
<i>o</i> -Xylene	11	4
Tetrachloroethane	15	5
1,3,5-Trimethylbenzene	15	5
1,2,4-Trimethylbenzene	13	4
<i>n</i> -Undecane	12	15
<i>n</i> -Dodecane	39	23
Naphtalene	33	7

However, RSDs for all analytes, except MTBE, toluene and *n*-undecane, were 1.7-4.5 times higher at 1 h extraction than at 8 h. To achieve less variability between fibers, it is recommended to carry out simultaneous extraction by six SPME fibers for 8 h or longer.

### 6.2.2 Study of the stability of the developed system for generation of gas with known concentrations of volatile organic compounds

The stability of the VOCs concentrations generated by the system was assessed by extraction using exposed Car/PDMS fiber every 3 h. Each extraction was conducted in one replicate due to the time-consuming analysis (~30 min) and automatization of the system, which does not allow for extraction in replicates.

The 48 h operating of the developed system resulted in variations in analyte responses from 85 to 111% of the initial values (Figure 36). The responses of VOCs ranged between 81 and 147% during all operating times of the system, which proved the stability of the gas generation. During the stability study, after 12 h of system operation, only one outlier was determined, which was 44% for *o*-xylene. The results indicate that the developed system can be used to produce stable analyte responses over 48 h. This stable system provides reproducible results for further experiments. In addition, each set of experiments will be followed by the extraction of analytes using the exposed Car/PDMS fiber to control the concentrations of analytes generated by the developed system.

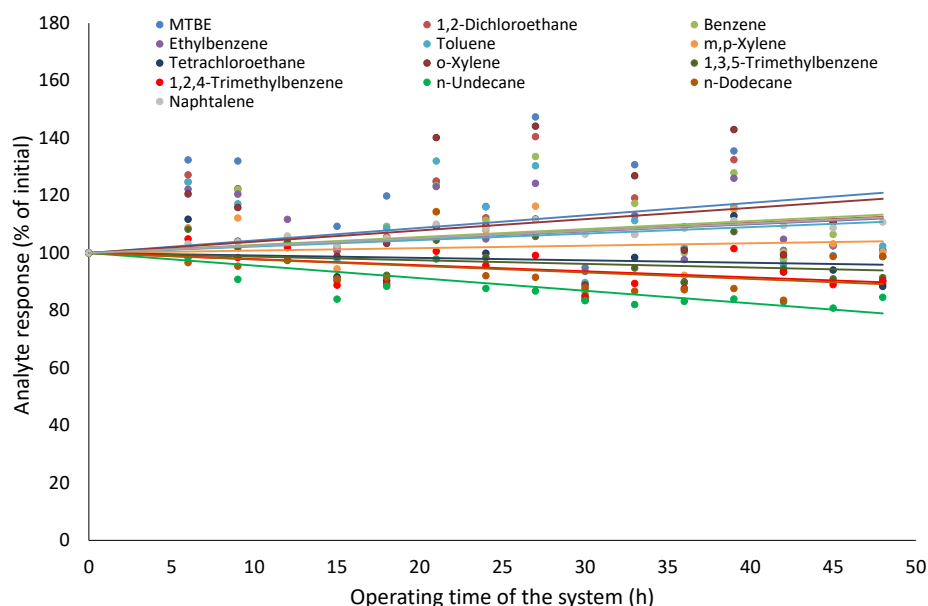


Figure 36 – Changes in responses of VOCs during the stability study of developed system for 48 hours

### 6.2.3 Study of effect of solid-phase microextraction fiber coatings on analytes recoveries

The selection of the optimal SPME fiber coating was based on the recovery of the VOCs masses adsorbed/absorbed by the fiber during TWA extraction in the developed

system. The blanks of the system and the extraction of gas with known VOCs concentrations were carried out for each fiber.

The obtained results indicated two most appropriate fibers, Car/PDMS and DVB/Car/PDMS with a 2-cm coating, which showed recoveries for 9 out of 13 VOCs ranged from 99 to 120% and from 93 to 118%, respectively (Figure 37). However, the RSDs obtained by the 2-cm DVB/Car/PDMS were 16-41% for 9 VOCs, which will effect the accuracy of VOCs determination. PDMS provided the lowest recoveries for most analytes, with the exception of *o*-xylene, 1,3,5-trimethylbenzene, 1,2,4-trimethylbenzene and naphthalene, for which lowest recoveries were obtained with 1-cm DVB/Car/PDMS. Recoveries higher than 120% were achieved for 9 VOCs using the PDMS/DVB fiber that is not appropriate for accurate determination of TWA concentrations in ambient air. The synthesized fiber with MOF-199 coating provided 75-115% recoveries for 8 out of 13 VOCs, and RSDs 3-21%, except for tetrachloroethane, 1,3,5-trimethylbenzene and *n*-dodecane (Figure 37). Overall, the Car/PDMS and 2-cm DVB/Car/PDMS fibers provided the greatest recoveries for most of studied VOCs. At the same time, the Car/PDMS provided the lowest RSDs, which varied from 2 to 22% for all analytes. Thus, based on the obtained results the Car/PDMS SPME fiber was chosen as optimal for determination of the TWA concentrations of VOCs, which is in accordance with results in Section 5. In addition, MOF-199 fiber coating was chosen for further experiments for comparison with commercially available SPME fiber.

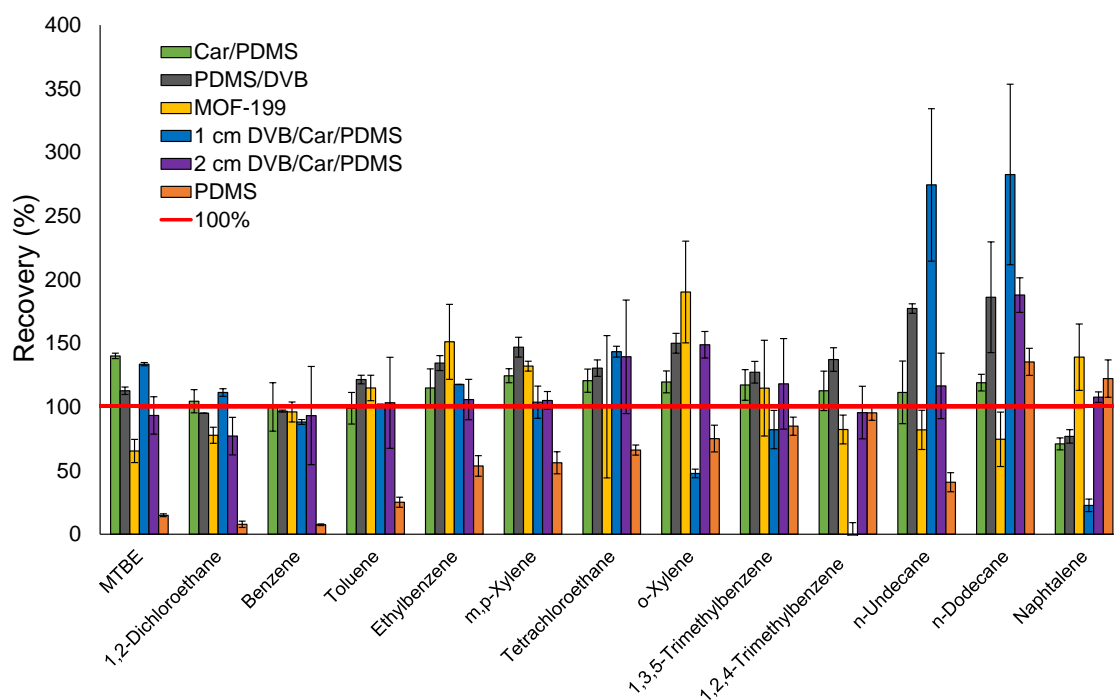


Figure 37 – Recovery of determination of VOCs TWA concentrations by different SPME fiber coatings

#### 6.2.4 Comparison of the accuracy of determination of time-weighted average concentrations by GC liner and modified sampler using solid-phase microextraction fiber

The modified sampler was compared with the sampler proposed by Tursumbayeva et al. [89, p.11] using a GC liner with an exposed SPME fiber inside it. The comparison was conducted based on the recovery of VOCs obtained by the Car/PDMS and MOF-199 fibers using modified sampler and GC liner.

The modified sampler with Car/PDMS showed better recovery than the GC liner for 9 out of 13 VOCs, which varied from 91 to 137%, except for MTBE (Figure 38).

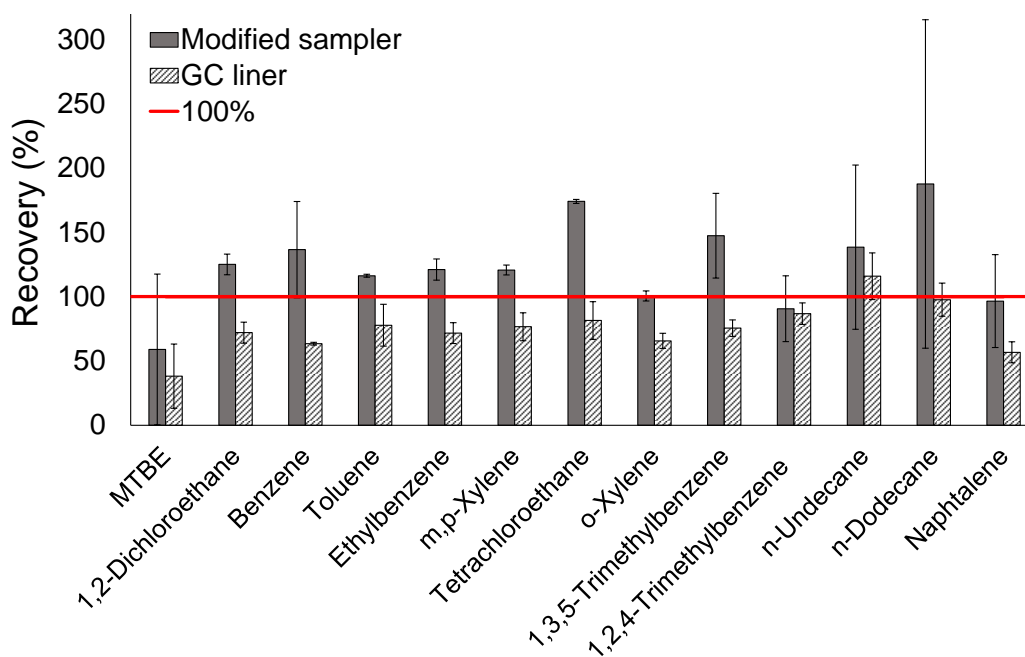


Figure 38 – Recovery of determination of VOCs TWA concentrations by Car/PDMS fiber using modified sampler and GC liner

The minimum recoveries achieved for MTBE using a modified sampler and GC liner were 59% and 38%, respectively. The GC liner with Car/PDMS resulted in better recoveries of tetrachloroethane, 1,3,5-trimethylbenzene, *n*-undecane and *n*-dodecane, which were 82, 76, 116% and 98%, respectively.

The use of MOF-199 with a modified sampler provided better recovery for all the studied analytes than the GC liner. The minimum recovery was obtained for *n*-dodecane using a modified sampler (44%) and GC liner (34%) (Figure 39). For the rest of the VOCs recovery ranged from 52 to 90% for the modified sampler and from 37 to 64% for the GC liner. The obtained results are in accordance with previous theoretical simulations in COMSOL Multiphysics (Section 5 and [83, p.1-14]) and prove that the modified sampler achieves better analytes recovery compared to GC liner.



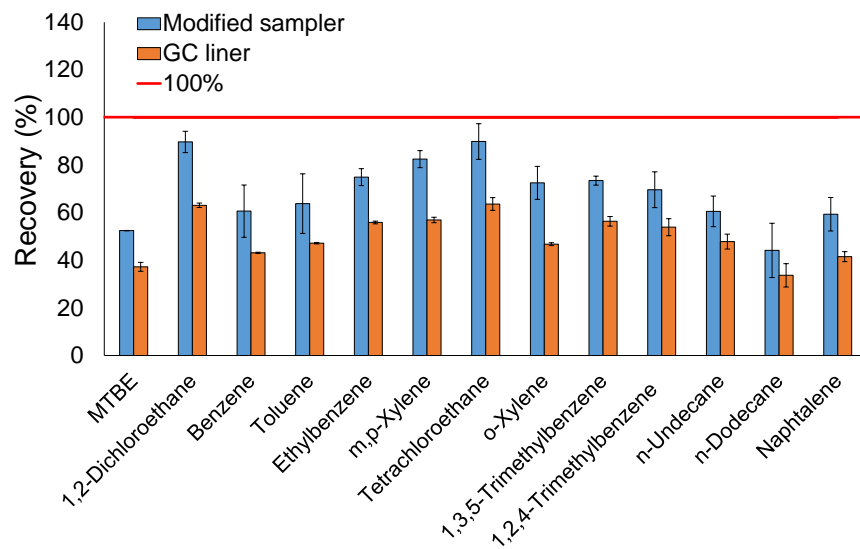


Figure 39 – Recovery of determination of VOCs TWA concentrations by MOF-199 fiber using modified sampler and GC liner

### 6.2.5 Effect of diffusion path length on the recovery obtained using a modified sampler

As mentioned previously, an increase in the diffusion path length leads to a decrease in the sampling rate, and consequently, to a decrease in the saturation of the fiber. The saturation of the fiber tip decreases analyte recovery [83, p.6]. The modified sampler avoids saturation of the fiber tip, which leads to an increase in analyte recovery. The extraction process was simulated in COMSOL Multiphysics to assess the effect of diffusion path length. The model described in Section 2.5 was used in the simulation.

In the modified sampler, the entire surface of the fiber works, which makes it possible to achieve recovery of >80% at constant analyte concentrations, even at short diffusion path lengths (17 mm) (Figure 40).

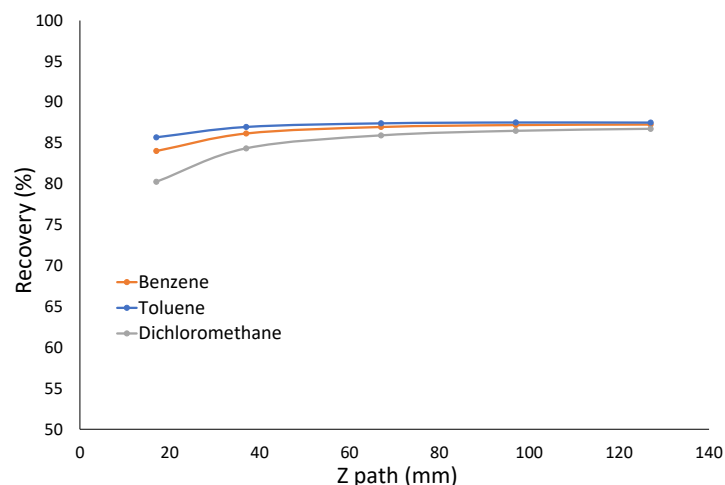


Figure 40 – Effect of diffusion path length on analytes recovery obtained using a modified sampler from air with constant concentrations ( $100 \mu\text{g}/\text{m}^3$ ) at  $t = 100,000 \text{ s}$

The effect of diffusion path length was assessed at 100,000 s (~27.8 h) with an analyte concentration of 100  $\mu\text{g}/\text{m}^3$ . According to the obtained results, the recoveries of benzene, toluene, and dichloromethane were 84-87%, 86-88% and 80-87%, respectively (Figure 40). During the sampling of real ambient air samples, the analyte concentrations are not constant and can vary substantially. The extraction process was simulated when the analyte concentrations substantially decreased in the middle of the extraction.

The decrease was simulated from 100 to 10  $\mu\text{g}/\text{m}^3$  during 2000 s (from 49,000 (~13.6 h) to 51,000 s (~14.2 h) of extraction). Increasing the diffusion path length from 17 to 67 mm increased the analyte recovery at varying analyte concentrations and an extraction time of 100,000 s (Figure 41). A further increase in the diffusion path length led to a decrease in the recovery of benzene, toluene, and dichloromethane from 83-85% to 78-79%.

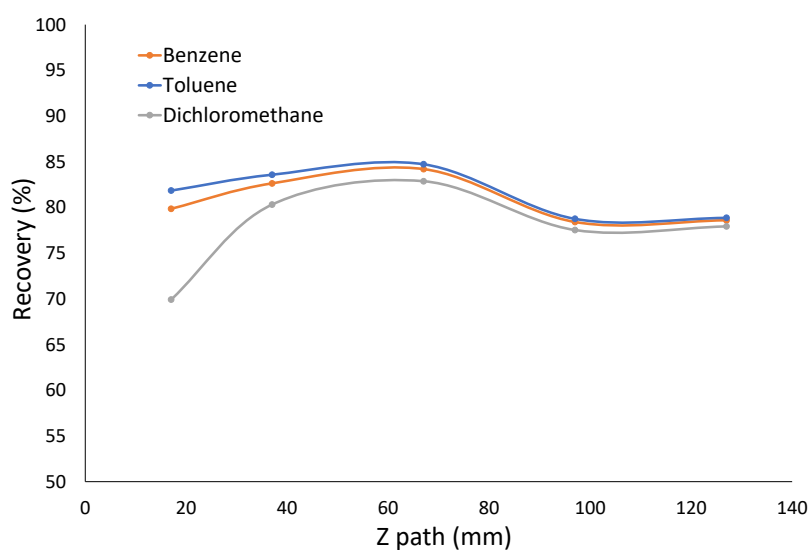


Figure 41 – Effect of diffusion path length on analytes recovery obtained using a modified sampler from air with varying concentrations ( $C_{0-49,000\text{s}} = 100 \mu\text{g}/\text{m}^3$ ,  $C_{49,000-51,000\text{s}} = 100 - 10 \mu\text{g}/\text{m}^3$ ,  $C_{51,000-100,000\text{s}} = 10 \mu\text{g}/\text{m}^3$ ) at  $t = 100,000$  s

For a short diffusion path (17 mm), changes in the concentration reduced the recovery compared to a constant concentration from 84 to 80%, 86 to 82%, and 80 to 70% for benzene, toluene, and dichloromethane, respectively. A minimal effect (reduction of approximately 3%) of varying concentrations on analyte recovery was achieved at 67 mm. According to the simulation of the extraction process in COMSOL Multiphysics, the 67 mm diffusion path length provided better recovery at constant and varying concentrations of analytes in the sampled air.

To confirm the computational model results, the effect of the diffusion path length on analyte recovery as experimentally studied using a modified sampler w. Four diffusion path lengths ( $Z=27, 67, 97, \text{ and } 127$  mm) were used to study the effect of retraction depth on analyte recovery (Figure 42).

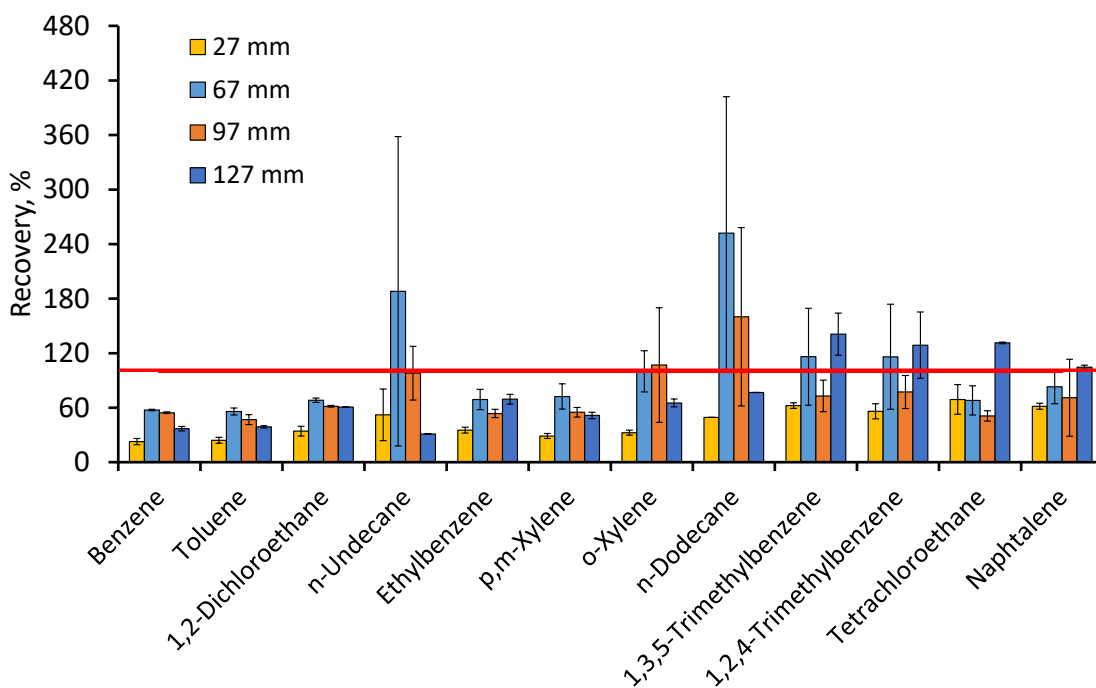


Figure 42 – Effect of diffusion path length on analytes recovery

The 17 mm diffusion path was not studied due to the impossibility of installing a modified sampler with  $Z=17$  mm into the developed system for the determination of TWA concentrations. The lowest recoveries of the studied VOCs were obtained at  $Z=27$  mm, and were in the range of 23 - 69% (Figure 42).

The 67 mm diffusion path length showed the highest recoveries (56-116%) for the greatest number of analytes (9 out of 12), except for *n*-undecane, *n*-dodecane, and naphthalene. The subsequent increase in the diffusion path length led to a decrease in analyte recovery. The recoveries of 11 out of 12 VOCs were 47-107% at  $Z=97$  mm, whereas  $Z=127$  mm showed 31-105% recoveries for 9 out of 12 analytes. The recoveries of *n*-dodecane (160%) at  $Z=97$  mm, and 1,3,5-trimethylbenzene (141%), 1,2,4-trimethylbenzene (129%), and tetrachloroethane (131%) at  $Z=127$  mm were extremely high. Based on the obtained results,  $Z=67$  mm was chosen as the optimal value for the accurate determination of the TWA concentrations of VOCs. The obtained results are in accordance with COMSOL simulations, which showed that  $Z=67$  mm is optimal for TWA determination of VOCs.

#### 6.2.6 Determination of the developed method accuracy by comparison with sorbent tube-based method

Fick's law was used to calculate the TWA concentrations of VOCs determined using SPME. However, real air samples are sampled at different temperatures and pressures, which affect the diffusion coefficients of the analytes. The calculation of diffusion coefficients at different pressures and temperatures is required to consider the effect of environmental conditions on diffusion and to increase the accuracy of determination of TWA concentrations. The calculations were performed using the

following equation:

$$D = D_0 \times \left(\frac{T_n}{T_0}\right)^{3/2} \times \frac{p_0}{p_n} \quad (10)$$

where:  $D$  – diffusion coefficient at sampling pressure and temperature,  $\text{cm}^2/\text{s}$ ;

$D_0$  – diffusion coefficient at  $T_0$  and  $p_0$ ,  $\text{cm}^2/\text{s}$ ;

$T_n$  – sampling temperature, K;

$T_0$  – zero temperature, 273 K;

$p_0$  – zero pressure, 760 mmHg;

$p_n$  – sampling pressure, mmHg.

The sampling of real air samples was conducted in Almaty on December 8, 2022 at  $-3\text{ }^\circ\text{C}$  and  $p=690\text{ mmHg}$  using developed samplers with SPME fiber, which were installed in the sampling box (static mode), developed system (dynamic mode) and sorbent tubes.

The TWA concentrations of VOCs determined by SPME and developed sampler in static and dynamic modes were similar and varied from  $0.7$  to  $14.5\text{ }\mu\text{g}/\text{m}^3$  and from  $1.1$  to  $15.3\text{ }\mu\text{g}/\text{m}^3$ , respectively (Table 25). The dynamic mode differed from the static mode by 0.5-2.1 times for all analytes, except 1,3,5-trimethylbenzene and 1,2,4-trimethylbenzene, which differed by 3.0 and 3.6 times, respectively. The standard method, based on the sorbent tube, showed lower TWA concentrations of the studied VOCs, ranging from  $0.07$  to  $7.5\text{ }\mu\text{g}/\text{m}^3$ . Concentrations of *n*-dodecane and tetrachloroethane were not detected by the sorbent tube; therefore, it was not possible to compare their concentrations. A comparison of the SPME method (static and dynamic modes) and sorbent tube-based methods showed that the TWA concentrations of the VOCs obtained by SPME were higher. The static mode showed concentrations higher by 1.5-4.4 times than sorbent tube-based method, except for 1,2-dichloroethane and 1,2,4-trimethylbenzene, which concentrations were 16.1-fold higher and 1.4-fold lower, respectively. VOCs concentrations obtained by the dynamic mode were by 1.1-4.6 times higher than those obtained by sorbent tubes, except for 1,2-dichloroethane, naphthalene and *m,p*-xylene, which were 15.0, 9.2 times higher and 1.8 times lower, respectively.

The differences between static and dynamic modes using SPME and sorbent tube methods were statistically significant (ANOVA, Tukey test,  $p<0.05$ ), except for toluene, and varied depending on the analytes (Table 25). Such differences can be caused by the type of sampling used: passive sampling for SPME methods and active sampling for sorbent tubes. However, the comparison of concentrations obtained by SPME dynamic mode and sorbent tube showed statistically insignificant differences for toluene, ethylbenzene, *m,p*- and *o*-xylenes (ANOVA, Tukey test,  $p>0.05$ ). The limits of detection and quantification of the developed method were calculated by multiplying analyte concentrations by 3:1 and 10:1, respectively, and dividing by the signal-to-noise ratio. LOD and LOQ varied from  $0.2$  to  $4.0\text{ }\mu\text{g}/\text{m}^3$  and from  $0.7$  to  $13.2\text{ }\mu\text{g}/\text{m}^3$ , respectively.

Table 25 – TWA concentrations of VOCs determined by SPME in static and dynamic mode and by sorbent tube

Compound	Mean concentration ( $\mu\text{g}/\text{m}^3$ )			Differences			<i>p</i> -Value
	Dynamic mode (D)	Static mode (S)	Sorbent tube (T)	D/S	D/T	S/T	
Benzene	15.3	14.5	3.4	1.1	4.5	4.2	0
Toluene	14.4	12.8	7.5	1.1	1.9	1.7	0.164
1,2-Dichloroethane	1.1	1.2	0.1	0.9	15.0	16.1	0.001
Ethylbenzene	1.4	2.0	1.3	0.7	1.1	1.6	0.001
<i>m,p</i> -xylene	1.9	4.0	2.4	0.5	0.8	1.7	0.001
<i>o</i> -xylene	2.2	3.0	1.9	0.7	1.1	1.6	0.004
<i>n</i> -Dodecane	2.7	1.3	n/d	2.1	n/a	n/a	n/a
1,3,5-Trimethylbenzene	1.9	0.7	0.4	3.0	4.6	1.5	0
1,2,4-Trimethylbenzene	3.6	1.0	1.4	3.6	2.5	0.7	0.001
Tetrachloroethane	4.9	3.5	n/d	1.4	n/a	n/a	n/a
Naphtalene	7.9	3.8	0.9	2.1	9.2	4.4	0.001

Note: n/d – not detected; n/a – not available.

Based on the obtained results, the developed SPME method in dynamic mode in combination with the developed system can be recommended for the determination of daily average concentrations of the studied VOCs with appropriate accuracy and reproducibility. In the case of 1,2-dichloroethane and naphthalene, additional experiments are required to increase accuracy of TWA concentration determination.

### 6.3 Section conclusions

A method for determining the time-weighted average concentrations of VOCs using solid-phase microextraction and a modified sampler with an alternative geometry was developed. The results obtained in Section 3.4 were confirmed in this section. It was proven that 85  $\mu\text{m}$  Car/PDMS provided better recoveries and RSDs for the determination of TWA concentrations of the studied VOCs in comparison with 50/30  $\mu\text{m}$  DVB/Car/PDMS with 1 and 2 cm coatings, 100  $\mu\text{m}$  PDMS, 65  $\mu\text{m}$  PDMS/DVB and MOF-199 (synthesized fiber). However, MOF-199 showed great recoveries for 8 out of 13 VOCs, ranging from 75 to 115%, and was used for further method development. The developed modified sampler in combination with Car/PDMS provided better recovery for 9 out of 13 studied VOCs than the sampler based on GC liner for SPME proposed by Tursumbayeva et al. [89, p.11]. MOF-199 with modified sampler showed better recoveries for all analytes.

The diffusion path length (retraction depth), which is one of the most important parameters, affecting the recovery and rate of sampling, was optimized. The 67 mm diffusion path length provided the best recoveries (56-116%) for the greatest number of analytes. According to the obtained results, it is optimal to use 85  $\mu\text{m}$  Car/PDMS with the developed sampler at  $Z=67$  mm for accurate determination of daily average concentrations of studied VOCs.

The developed method was compared with the standard method, which is based on sorbent tubes, to demonstrate accuracy under field conditions. According to the obtained results TWA sampling with the modified sampler and SPME showed a reasonable match with the standard method, except 1,2-dichloroethane and naphthalene.

The developed method is simple, accurate, reusable, and does not require additional expensive devices for sampling and/or desorption of VOCs. The method can be applied for the determination of the daily average concentrations of the studied VOCs in ambient air. However, there are some limitations of the proposed method. The simultaneous use of multiple fibers requires the study of fiber variability before each new sampling. Also, additional experiments are needed to understand the effect of environmental conditions on method accuracy and reproducibility.

## CONCLUSION

In accordance with the results obtained in the framework of this thesis, the following conclusions were made:

– The 65  $\mu\text{m}$  PDMS/DVB fiber provides a better combination of LODs and RSDs of slopes for the simultaneous determination of single concentrations of 25 VOCs. The LODs for 25 VOCs varied from 0.010 to 7  $\mu\text{g}/\text{m}^3$ , and the RSDs were low 10% for 22 out of 25 VOCs. The RSDs for methyl ethyl ketone, 1,2-dichloroethane, and *p*-xylene were 25, 20 and 15%, respectively.

– The effects of the extraction, desorption and storage times were investigated. According to the obtained results, the extraction time of 10 min and desorption time of 1 min were chosen as optimal. To achieve the highest accuracy of the developed method, samples should be analyzed during the first 8 h after sampling.

– The developed method for the determination of single VOC concentrations provides spike recoveries of 90–105% for all analytes, except methyl ethyl ketone, methylene chloride, 3-picoline, and *n*-hexadecane. Ambient air in Almaty was monitored using the developed method. Mean concentrations of 23 out of 25 VOCs, except methyl ethyl ketone and 1,2-dichloroethane, were 0.2 – 83, 0.1 – 70 and 0.1 – 74  $\mu\text{g}/\text{m}^3$  on 30 March, 2 and 4 April 2019, respectively.

– The developed method of simultaneous determination of single concentrations of 25 VOCs was used for the first time to study the seasonal variation and spatial distribution of the total VOCs in the air of Almaty in 2020. Significant seasonal variations were observed for 9 out of 19 VOCs with maximum concentrations in the winter sampling days, which can be associated with higher emissions from coal combustion, environmental conditions, and geographic location of the city. The total VOCs were 233 – 420, 231 – 437, 48 – 151, 46 – 133, and 72 – 393  $\mu\text{g}/\text{m}^3$  on the sampling days in January, April, April-May, July, and October, respectively. The spatial distribution of TVOCs was similar in all studied seasons, with lower concentrations in the south and higher concentrations in the north of Almaty, where CHPs are located.

– The comparison of heating and non-heating periods and analysis of typical BTEX ratios showed that air pollution in Almaty has a complex nature with two main sources: burning of biomass/biofuel/coal and vehicle emissions. Solid fuel combustion had a dominant effect on air pollution during the heating season in Almaty, especially coal combustion by CHPs and private houses. In addition, it was found that the sampling sites were mostly affected by aged air masses from remote sources.

– The effect of COVID-19 lockdown measures (traffic-free conditions) in 2020 on improving air quality in Almaty was studied by comparing the BTEX concentrations during the lockdown period with the same periods in previous years (2015-2019) to exclude the influence of meteorological parameters. The average concentrations of benzene and toluene were 3- and 2-times higher during the lockdown period, respectively, which indicates that the sources of these compounds were active during the lockdown and could be associated with coal combustion by power plants and households. The average concentrations of ethylbenzene and *o*-xylene were 4 and 2.7

times lower, respectively, in 2020 than during the same sampling period in 2015-2019.

- The simulation of TWA air sampling by retracted SPME fiber using a finite element analysis-based model (using COMSOL Multiphysics software) decreases the time and cost of experiments for method optimization and/or development, decreases the uncertainty, and helps understand the extraction processes more deeply.

- The proposed sampler with an alternative geometry allows to increase the accuracy of the determination of TWA concentrations of VOCs in ambient air in comparison with the SPME GC liner. The developed method based on a sampler with an alternative geometry and 85  $\mu\text{m}$  Car/PDMS SPME fiber provides greater recoveries at  $Z=67$  mm for 9 out of the 12 studied VOCs. The developed method in dynamic mode showed substantial similarity to the sorbent tube-based method, except for 1,2-dichloroethane and naphthalene.

Based on these conclusions, the following recommendations were proposed:

- For simultaneous quantification of single concentrations of multiple VOCs in ambient air, it is recommended to conduct sampling in 20 mL vials with subsequent analysis by 65  $\mu\text{m}$  PDMS/DVB SPME fiber at 10 min extraction time and GC-MS.

- Ambient air monitoring in Almaty showed the complicated nature of air pollution and the lack of data, outdated methodologies, and non-transparent energy statistics needed to assess air quality. The obtained results can increase the awareness of decision-makers and the population to develop reliable measures to improve air quality in Almaty. According to the obtained data, it was proposed to use less toxic fossil fuel for heating and electricity, to improve the quality of low-grade coal or change the fossil fuel to alternative fuel (natural gas), and to apply strict standards for transport, industrial, power plants and household emissions.

- For a better understanding of sampling processes by SPME and for reducing the time of experiments, the simulation of optimization of time-weighted average air sampling using finite element analysis software is recommended. The simulation allows the investigation of the effects of parameters such as sampling time, SPME coating type, diffusion path length, and internal diameter of the fiber protecting needle or alternative samplers on analyte recovery.

- For a more accurate and simple determination of the daily average concentrations of VOCs in ambient air, it is recommended to use a developed sampler with an alternative geometry in combination with an 85  $\mu\text{m}$  Car/PDMS SPME fiber at  $Z=67$  mm and a developed system.

As a result of this study, two new methods and one sampler were developed:

- determination of single concentrations of multiple VOCs in ambient air based on exposed fiber of solid-phase microextraction combined with GC-MS;

- sampler with an alternative geometry for the determination of time-weighted average concentrations of VOCs by solid-phase microextraction;

- determination of time-weighted average concentrations of VOCs in ambient air based on retracted SPME fiber in sampler with alternative geometry with subsequent analysis by GC-MS.



## REFERENCES

- 1 Fuller R., Landrigan L. P., Balakrishnan K., Bathan G., Bose-O'Reilly S., Brauer M., Caravanos J., Chiles T. et al. Pollution and health: a progress update // *The Lancet Planetary Health*. - 2022. - Vol. 6, Is. 6. - P. e535–e547.
- 2 Health Effects Institute. *State of Global Air 2019*. – Boston: Health Effects Institute, 2019. – 24p.
- 3 World Health Organization. Health consequences of air pollution on populations. – 2019. – URL: <https://www.who.int/news/item/15-11-2019-what-are-health-consequences-of-air-pollution-on-populations#:~:text=Exposure to high levels of,people who are already ill> (20.01.2023).
- 4 Domingo J.L., Marquès M., Rovira J. Influence of airborne transmission of SARS-CoV-2 on COVID-19 pandemic. A review // *Environmental Research*. - 2020. - Vol. 188, Is. June. - P. 17–20.
- 5 Conticini E., Frediani B., Caro D. Can atmospheric pollution be considered a co-factor in extremely high level of SARS-CoV-2 lethality in Northern Italy? // *Environmental Pollution*. - 2020. - Vol. 261. – Article 114465.
- 6 Bashir M.F., MA B.J., Bilal, Komal B., Bashir M.A., Farooq T.H., Iqbal N., Bashir M. Correlation between environmental pollution indicators and COVID-19 pandemic: A brief study in Californian context // *Environmental Research*. - 2020. - Vol. 187, Is. May. - Article 109652.
- 7 Li H., Xu X.L., Dai D.W., Huang Z.Y., Ma Z., Guan Y.J. Air pollution and temperature are associated with increased COVID-19 incidence: A time series study // *International Journal of Infectious Diseases*. - 2020. - Vol. 97. - P. 278–282.
- 8 Zhu Y., Xie J., Huang F., Cao L. Association between short-term exposure to air pollution and COVID-19 infection: Evidence from China // *Science of the Total Environment*. - 2020. - Vol. 727, Is. December 2019. - Article 138704.
- 9 World Bank Group. *The Global Health Cost of PM 2.5 Air Pollution: A Case for Action Beyond 2021*. – Washington: World Bank Group, 2022. – 89p.
- 10 Our world data. Outdoor Air Pollution. – 2019. – URL: <https://ourworldindata.org/outdoor-air-pollution#concentrations-of-air-pollution> (20.01.2023).
- 11 European Environment Agency. Air pollution sources. – 2022. – URL: <https://www.eea.europa.eu/themes/air/air-pollution-sources-1> (21.01.2023).
- 12 World Health Organization. Ambient (outdoor) air pollution. – 2022. – URL: [https://www.who.int/news-room/fact-sheets/detail/ambient-\(outdoor\)-air-quality-and-health](https://www.who.int/news-room/fact-sheets/detail/ambient-(outdoor)-air-quality-and-health) (20.01.2023).
- 13 Ministry for the Environment. *Good practice guide for air quality monitoring and data management 2009*. – Wellington: Ministry of the Environment, 2009. – 97p.
- 14 Eastern Research Group, Inc. *2014 National Monitoring Programs Annual Report (UATMP, NATTS, CSATAM)*. – Morrisville: Eastern research Group, Inc., 2017. – 1128p.
- 15 RSE “KAZGYDROMET” Information bulletins on the state of the environment. URL: <https://kazhydromet.kz/ru/bulleten/okrsreda> (21.01.2023).

16 Shuai J., Kim S., Ryu H., Park J., Lee C.K., Kim G.-B., Ultra V.U., Yang W. Health risk assessment of volatile organic compounds exposure near Daegu dyeing industrial complex in South Korea // *BMC Public Health*. - 2018. - Vol. 18, Is. 528. - P. 1-13.

17 Hua X., Wu Y.J., Zhang X., Cheng S., Wang X., Chu J., Huang Q. Analysis on ambient volatile organic compounds and their human gene targets // *Aerosol and Air Quality Research*. - 2018. - Vol. 18, Is. 10. - P. 2654–2665.

18 Sarigiannis D.A., Karakitsios S.P., Gotti A., Liakos I.L., Katsoyiannis A. Exposure to major volatile organic compounds and carbonyls in European indoor environments and associated health risk // *Environment International*. - 2011. - Vol. 37, Is. 4. - P. 743–765.

19 Paterson C.A., Sharpe R.A., Taylor T., Morrissey K. Indoor PM2.5, VOCs and asthma outcomes: A systematic review in adults and their home environments // *Environmental Research*. - 2021. - Vol. 202. - Article 111631.

20 Alford K.L., Kumar N. Pulmonary Health Effects of Indoor Volatile Organic Compounds – A Meta-Analysis // *International Journal of Environmental Research and Public Health*. - 2021. - Vol. 18, Is. 4. - Article 1578.

21 Bolden A.L., Kwiatkowski C.F., Colborn T. New look at BTEX: Are ambient levels a problem? // *Environmental Science and Technology*. - 2015. - Vol. 49, Is. 9. - P. 5697–5703.

22 World Health Organization. IARC monographs on the evaluation of carcinogenic risks to humans – Benzene. - Lyon: International Agency for Research on Cancer, 2018. – Vol. 120. – 309p.

23 Agency for Toxic Substances and Disease Registry (ATSDR) Toxicological Profile for Toluene (Update) // U.S. Public Health Service, U.S. Department of Health and Human Services. - 200AD. - P. 357.

24 Agency for Toxic Substances and Disease Registry (ATSDR) Toxicological Profile for Xylenes (Update) // Public Health Service, U.S. Department of Health and Human Services. - 2007. - P. 385.

25 Wang P. Z.W. Assessment of ambient volatile organic compounds (VOCs) near major roads in urban Nanjing, China // *Atmospheric Research*. - 2008. - Vol. 89. - P. 289–297.

26 Ding Y., Lu J., Liu Z., Li W., Chen J. Volatile organic compounds in Shihezi, China, during the heating season: pollution characteristics, source apportionment, and health risk assessment // *Environmental Science and Pollution Research*. - 2020. - Vol. 27, Is. 14. - P. 16439–16450.

27 Juráň S., Grace J., Urban O. Temporal Changes in Ozone Concentrations and Their Impact on Vegetation // *Atmosphere*. - 2021. - Vol. 12, Is. 1. - P. 82.

28 Calfapietra C., Fares S., Manes F., Morani A., Sgrigna G., Loreto F. Role of Biogenic Volatile Organic Compounds (BVOC) emitted by urban trees on ozone concentration in cities: A review // *Environmental Pollution*. - 2013. - Vol. 183. - P. 71–80.

29 Duan C., Liao H., Wang K., Ren Y. The research hotspots and trends of volatile organic compound emissions from anthropogenic and natural sources: A

systematic quantitative review // *Environmental Research*. - 2023. - Vol. 216, Is. P1. - Article 114386.

30 Brusseau M.L., Matthias A.D., Comrie A.C., Musil S.A. Atmospheric Pollution // *Environmental and Pollution Science*. - 2019. - P. 293–309.

31 Zhang T., Yue X., Unger N., Feng Z., Zheng B., Li T., Lei Y., Zhou H., Dong X., Liu Y., Zhu J., Yang X. Modeling the joint impacts of ozone and aerosols on crop yields in China: An air pollution policy scenario analysis // *Atmospheric Environment*. - 2021. - Vol. 247. - Article 118216.

32 Sahu S.K., Liu S., Liu S., Ding D., Xing J. Ozone pollution in China: Background and transboundary contributions to ozone concentration & related health effects across the country // *Science of The Total Environment*. - 2021. - Vol. 761. - Article 144131.

33 Liu K., Zhang C., Cheng Y., Liu C., Zhang H., Zhang G., Sun X., Mu Y. Serious BTEX pollution in rural area of the North China Plain during winter season // *Journal of Environmental Sciences (China)*. - 2015. - Vol. 30. - P. 186–190.

34 Xiong Y., Bari M.A., Xing Z., Du K. Ambient volatile organic compounds (VOCs) in two coastal cities in western Canada: Spatiotemporal variation, source apportionment, and health risk assessment // *Science of the Total Environment*. - 2020. - Vol. 706. - Article 135970.

35 Wang M., Shao M., Lu S.H., Yang Y.D., Chen W.T. Evidence of coal combustion contribution to ambient VOCs during winter in Beijing // *Chinese Chemical Letters*. - 2013. - Vol. 24, Is. 9. - P. 829–832.

36 Zhang F., Shang X., Chen H., Xie G., Fu Y., Wu D., Sun W., Liu P., Zhang C., Mu Y., Zeng L., Wan M., Wang Y., Xiao H., Wang G., Chen J. Significant impact of coal combustion on VOCs emissions in winter in a North China rural site // *Science of the Total Environment*. - 2020. - Vol. 720. - Article 137617.

37 Zhang Z., Zhang Y., Wang X., Lü S., Huang Z., Huang X., Yang W., Wang Y., Zhang Q. Spatiotemporal patterns and source implications of aromatic hydrocarbons at six rural sites across china's developed coastal regions // *Journal of Geophysical Research*. - 2016. - Vol. 121, Is. 11. - P. 6669–6687.

38 Wang M., Li S., Zhu R., Zhang R., Zu L., Wang Y., Bao X. On-road tailpipe emission characteristics and ozone formation potentials of VOCs from gasoline, diesel and liquefied petroleum gas fueled vehicles // *Atmospheric Environment*. - 2020. - Vol. 223. - Article 117294.

39 U.S. Department of Health and Human Services, Public Health Service, Center for Disease Control N.I. for O.S. and H. The Industrial Environment-Its Evaluation and Control. -1983. - P. 37–42.

40 Palmes E. Personal monitoring device for gaseous contaminants // *American Industrial Hygiene Association journal*. - 1973. - Vol. 34. - P. 78–81.

41 Boaretto C., Sacco P. C. V. High Uptake Rate Radial Diffusive Sampler Suitable for Both Solvent and Thermal Desorption // *Industrial Hygiene Association*. - 1996. - Vol. 57. - P. 897–904.

42 Esteve-Turrillas F.A., Pastor A., de la Guardia M. Passive sampling of atmospheric organic contaminants // *Comprehensive Sampling and Sample Preparation*. - 2012. - Vol. 1, Is. 11. - P. 201–222.

43 Huckins J., Petty J. B.K. Monitors of Organic Chemicals in the Environment. Semipermeable Membrane Devices // Springer: New York. - 2006. - P. 86.

44 Compendium of Methods for the Determination of Toxic Organic Compounds in Ambient Air // U.S. Environmental Protection Agency (EPA). - 1999. - P. 1–90.

45 Compendium Method TO-15 Determination of Volatile Organic Compounds (VOCs) In Air Collected In Specially Prepared Canisters and Analyzed By Gas Chromatography/Mass Spectrometry (GC/MS) // U.S. Environmental Protection Agency (EPA). - 1999. - P. 12.

46 Batterman S., Zhang G. B.M. Analysis and stability of aldehydes and terpenes in electropolished canisters // *Atmospheric Environment*. - 1998. - Is. 32. - P. 1647–1655.

47 Compendium Method TO-17 Determination of Volatile Organic Compounds in Ambient Air Using Active Sampling Onto Sorbent Tubes // U.S. Environmental Protection Agency (EPA). - 1999. - 1–53 p.

48 16017-2-2007 G.O.S.T. Atmospheric air, the working area and enclosed spaces. Sampling of volatile organic compounds using a sorption tubes with subsequent thermal desorption and gas chromatographic analysis on capillary columns // Moscow, Russia. - 2007. - P. 40.

49 Sanchez JM S.R. Performance characteristics of a new prototype for a portable GC using ambient air as carrier gas for on-site analysis. // *Journal of separation science*. - 2007. - Vol. 30, Is. 7. - P. 1052–1060.

50 Feng C., Mitra S. Breakthrough and desorption characteristics of a microtrap // *Journal of Microcolumn Separations*. - 2000. - Vol. 12, Is. 4. - P. 267–275.

51 Helmig D. Development and Application of Needle Trap Device // *Journal of Chromatography A*. - 2005. - Is. 732. - P. 414–417.

52 Elke K., Jermann E. Determination of benzene, toluene, ethylbenzene and xylenes in indoor air at environmental levels using diffusive samplers in combination with headspace solid-phase microextraction and high-resolution gas chromatography-flame ionization detection // *Journal of Chromatography*. - 1998. - Vol. 826, Is. 2. - P. 191–200.

53 Khaled A., Pawliszyn J. Time-weighted average sampling of volatile and semi-volatile airborne organic compounds by the solid-phase microextraction device // *Journal of Chromatography A*. - 2000. - Vol. 892, Is. 1–2. - P. 455–467.

54 Martos P.A., Pawliszyn J. Time-weighted average sampling with solid-phase microextraction device: Implications for enhanced personal exposure monitoring to airborne pollutants // *Analytical Chemistry*. - 1999. - Vol. 71, Is. 8. - P. 1513–1520.

55 Koziel J.A., Pawliszyn J. Air Sampling and Analysis of Volatile Organic Compounds with Solid Phase Microextraction // Air and waste management association. - 2001. - P. 173–184.

56 Baimatova N., Kenessov B., Koziel J.A., Carlsen L., Bektassov M., Demyanenko O.P. Simple and accurate quantification of BTEX in ambient air by SPME and GC-MS // *Talanta*. - 2016. - Vol. 154. - P. 46–52.

57 Ibragimova O.P., Baimatova N., Kenessov B. Low-cost quantitation of multiple volatile organic compounds in air using solid-phase microextraction // *Separations*. - 2019. - Vol. 6. - P. 1-17.

58 Hippelein M. Analysing selected VVOCs in indoor air with solid phase microextraction (SPME): A case study // *Chemosphere*. - 2006. - Vol. 65. - P. 271–277.

59 Koziel J., Jia M., Khaled A., Noah J., Pawliszyn J. Field air analysis with SPME device // *Analytica Chimica Acta*. - 1999. - Vol. 400. - P. 153–162.

60 A. Ulanowska, T. Kowalkowski, K. Hryniewicz, M. Jackowski B.B. Determination of volatile organic compounds in human breath for *Helicobacter pylori* detection by SPME-GC/MS // *Biomed Chromatography* - 2011. - Vol. 25, Is. 3. - P. 391–397.

61 Baimatova N., Koziel J., Kenessov B. Passive Sampling and Analysis of Naphthalene in Internal Combustion Engine Exhaust with Retracted SPME Device and GC-MS // *Atmosphere*. - 2017. - Vol. 8, Is. 7. - P. 130.

62 Woolcock P.J., Koziel J.A., Johnston P.A., Brown R.C., Broer K.M. Analysis of trace contaminants in hot gas streams using time-weighted average solid-phase microextraction: Pilot-scale validation // *Fuel*. - 2015. - Vol. 153. - P. 552–558.

63 Martos P.A., Pawliszyn J. Calibration of solid phase microextraction for air analyses based on physical chemical properties of the coating // *Analytical Chemistry*. - 1997. - Vol. 69, Is. 2. - P. 206–215.

64 Chen Y., Pawliszyn J. Time-weighted average passive sampling with a Solid-Phase Microextraction device // *Analytical Chemistry*. - 2003. - Vol. 75, Is. 9. - P. 2004–2010.

65 Gómez-Ríos G.A., Reyes-Garcés N., Pawliszyn J. Development of a new in-vial standard gas system for calibrating solid-phase microextraction in high-throughput and on-site applications // *Journal of Separation Science*. - 2013. - Vol. 36, Is. 17. - P. 2939–2945.

66 Grandy J.J., Gómez-Ríos G.A., Pawliszyn J. Development of a standard gas generating vial comprised of a silicon oil-polystyrene/divinylbenzene composite sorbent // *Journal of Chromatography A*. - 2015. - Vol. 1410. - P. 1–8.

67 Grandy J.J., Murtada K., Raul J., Alejandra P., Suárez O., Pawliszyn J. Development and validation of an improved , thin film solid phase microextraction based , standard gas generating vial for the repeatable generation of gaseous standards // *Journal of Chromatography A*. - 2020. - Vol. 1632. - Article 461541.

68 Tumbiolo S., Gal J.-F.J.-F., Maria P.-C., Zerbinati O. Determination of benzene , toluene , ethylbenzene and xylenes in air by solid phase micro-extraction / gas chromatography / mass spectrometry. // *Anal Bioanal Chem*. - 2004. - Vol. 380. - P. 824–830.

69 Lee J.H., Hwang S.M., Lee D.W., Heo G.S. Determination of volatile organic compounds (VOCs) using tedlar bag/solid-phase microextraction/gas

chromatography/mass spectrometry (SPME/GC/MS) in ambient and workplace air // Bulletin of the Korean Chemical Society. - 2002. - Vol. 23, Is. 3. - P. 488–496.

70 Ouyang G., Pawliszyn J. A critical review in calibration methods for solid-phase microextraction // Analytica Chimica Acta. - 2008. - Vol. 627, Is. 2. - P. 184–197.

71 Tena M.T., Carrillo J.D. Multiple solid-phase microextraction: Theory and applications // TrAC - Trends in Analytical Chemistry. - 2007. - Vol. 26, Is. 3. - P. 206–214.

72 Pawliszyn J. Handbook of Solid Phase Microextraction – Amsterdam: Elsevier, 2012. – 290p.

73 Carter R.A.A., West N., Heitz A., Joll C.A. An analytical method for the analysis of trihalomethanes in ambient air using solid-phase microextraction gas chromatography-mass spectrometry: An application to indoor swimming pool complexes // Indoor Air. - 2019. - Vol. 29, Is. 3. - P. 499–509.

74 Ouyang G., Chen Y., Setkova L., Pawliszyn J. Calibration of solid-phase microextraction for quantitative analysis by gas chromatography // Journal of Chromatography A. - 2005. - Vol. 1097, Is. 1–2. - P. 9–16.

75 Llompart M., Celeiro M., García-Jares C., Dagnac T. Environmental applications of solid-phase microextraction // TrAC - Trends in Analytical Chemistry. - Elsevier B.V., 2019. - Vol. 112. - P. 1–12.

76 Chai M., Pawliszyn J., Air E. Analysis of Environmental Air Samples by Solid-Phase Microextraction and Gas Chromatography / Ion Trap Mass Spectrometry // Environmental Science & Technology. - 1995. - Vol. 29, Is. 3. - P. 693–701.

77 Wang J., Tuduri L., Mercury M., Millet M., Briand O., Montury M. Sampling atmospheric pesticides with SPME: Laboratory developments and field study // Environmental Pollution. - 2009. - Vol. 157, Is. 2. - P. 365–370.

78 Parshintsev J., Niina K., Hartonen K., Miguel L., Jussila M., Kajos M., Kulmala M., Riekkola M. Field measurements of biogenic volatile organic compounds in the atmosphere by dynamic solid-phase microextraction and portable gas chromatography-mass spectrometry // Atmospheric Environment. - 2015. - Vol. 115. - P. 214–222.

79 Koziel J.A., Noah J. P.J. Field sampling and determination of formaldehyde in indoor air with solid phase microextraction and on-fiber derivatization // Environmental Science and Technology. - 2001. - Vol. 35. - P. 1481–1486.

80 Lan H., Hartonen K., Riekkola M.L. Miniaturised air sampling techniques for analysis of volatile organic compounds in air // TrAC - Trends in Analytical Chemistry. - 2020. - Vol. 126. - Article 115873.

81 Sayed Mohamed Zain S.M., Shaharudin R., Kamaluddin M.A., Daud S.F. Determination of hydrogen cyanide in residential ambient air using SPME coupled with GC–MS // Atmospheric Pollution Research. - 2017. - Vol. 8, Is. 4. - P. 678–685.

82 Chen Y., Pawliszyn J. Solid-phase microextraction field sampler. // Analytical chemistry. - 2004. - Vol. 76, Is. 22. - P. 6823–6828.

83 Kenessov B., Koziel J.A., Baimatova N., Demyanenko O.P., Derbissalin M. Optimization of time-weighted average air sampling by solid-phase microextraction

fibers using finite element analysis software // *Molecules*. - 2018. - Vol. 23, Is. 11. - P. 1–14.

84 Raepfel C., Fabritius M., Nief M., Appenzeller B.M.R., Millet M. Coupling ASE, syllation and SPME-GC/MS for the analysis of current-used pesticides in atmosphere // *Talanta*. - 2014. - Vol. 121. - P. 24–29.

85 Levy M., Al-Alam J., Delhomme O., Millet M. An integrated extraction method coupling pressurized solvent extraction, solid phase extraction and solid-phase micro extraction for the quantification of selected organic pollutants in air by gas and liquid chromatography coupled to tandem mass spectrometry // *Microchemical Journal*. - 2020. - Vol. 157, Is. April. - P. 104889.

86 Schummer C., Tuduri L., Briand O., Appenzeller B.M., Millet M. Application of XAD-2 resin-based passive samplers and SPME-GC-MS/MS analysis for the monitoring of spatial and temporal variations of atmospheric pesticides in Luxembourg // *Environmental Pollution*. - 2012. - Vol. 170. - P. 88–94.

87 Mokbel H., Al Dine E.J., Elmoll A., Liaud C., Millet M. Simultaneous analysis of organochlorine pesticides and polychlorinated biphenyls in air samples by using accelerated solvent extraction (ASE) and solid-phase micro-extraction (SPME) coupled to gas chromatography dual electron capture detection // *Environmental Science and Pollution Research*. - 2016. - Vol. 23, Is. 8. - P. 8053–8063.

88 Tuduri L., Desauziers V., Fanlo J.L. Dynamic versus static sampling for the quantitative analysis of volatile organic compounds in air with polydimethylsiloxane-Carboxen solid-phase microextraction fibers // *Journal of Chromatography A*. - 2002. - Vol. 963, Is. 1–2. - P. 49–56.

89 Tursumbayeva M., Koziel J.A., Maurer D.L., Kenessov B., Rice S. Development of Time-Weighted Average Sampling of Odorous Volatile Organic Compounds in Air with Solid-Phase Microextraction Fiber Housed inside a GC Glass Liner: Proof of concept // *Molecules*. - 2019. - Vol. 24, Is. 3. - P. 1–18.

90 Krol S., Zabiegala B. N.J., Król S., Zabiegała B., Namieśnik J. Monitoring VOCs in atmospheric air II. Sample collection and preparation // *TrAC - Trends in Analytical Chemistry*. - 2010. - Vol. 29, Is. 9. - P. 1101–1112.

91 Miller L., Xu X. Multi-season, multi-year concentrations and correlations amongst the BTEX group of VOCs in an urbanized industrial city // *Atmospheric Environment*. - 2012. - Vol. 61. - P. 305–315.

92 Goodman N.B., Steinemann A., Wheeler A.J., Paevere P.J., Cheng M., Brown S.K. Volatile organic compounds within indoor environments in Australia // *Building and Environment*. - 2017. - Vol. 122. - P. 116–125.

93 Woolfenden E. Monitoring VOCs in air using sorbent tubes followed by thermal desorption-capillary GC analysis: summary of data and practical guidelines // *Journal of the Air & Waste Management Association*. - 1997. - Vol. 47, Is. 1. - P. 20–36.

94 Pawliszyn J. *Applications of Solid Phase Microextraction*. – Cambridge: Royal Society of Chemistry, 1999. – 674p.

95 Haberhauer-Troyer C., Rosenberg E., Grasserbauer M. Evaluation of solid-phase microextraction for sampling of volatile organic sulfur compounds in air for

subsequent gas chromatographic analysis with atomic emission detection // *Journal of Chromatography A*. - 1999. - Vol. 848, Is. 1–2. - P. 305–315.

96 Ouyang G. SPME and Environmental Analysis // *Handbook of Solid Phase Microextraction*. - 2012. - P. 251–290.

97 Prikryl P., Sevcik J.G.K. Characterization of sorption mechanisms of solid-phase microextraction with volatile organic compounds in air samples using a linear solvation energy relationship approach // *Journal of Chromatography A*. - 2008. - Vol. 1179. - P. 24–32.

98 Yassaa N., Meklati B.Y., Cecinato A. Analysis of volatile organic compounds in the ambient air of Algiers by gas chromatography with a  $\beta$ -cyclodextrin capillary column 1999. - Vol. 846. - P. 287–293.

99 Tumbiolo S., Gal J.-F., Maria P., Zerbinati O. SPME sampling of BTEX before GC/MS analysis: examples of outdoor and indoor air quality measurements in public and private sites // *Annali di Chimica*. - 2005. - Vol. 95, Is. 11–12. - P. 757–766.

100 Curran K., Underhill M., Gibson L.T., Strlic M. The development of a SPME-GC / MS method for the analysis of VOC emissions from historic plastic and rubber materials // *Microchemical Journal*. - 2016. - Vol. 124. - P. 909–918.

101 Luca A., Kjær A., Edelenbos M. Volatile organic compounds as markers of quality changes during the storage of wild rocket // *Food Chemistry*. - 2017. - Vol. 232. - P. 579–586.

102 Jalili V., Barkhordari A., Ghiasvand A. A comprehensive look at solid-phase microextraction technique: A review of reviews // *Microchemical Journal*. - 2020. - Vol. 152. - Article 104319.

103 Jalili V., Barkhordari A., Ghiasvand A. Solid-phase microextraction technique for sampling and preconcentration of polycyclic aromatic hydrocarbons: A review // *Microchemical Journal*. - 2020. - Vol. 157. - Article 104967.

104 Mokbel H., Al Dine E.J., Elmoll A., Liaud C., Millet M. Simultaneous analysis of organochlorine pesticides and polychlorinated biphenyls in air samples by using accelerated solvent extraction (ASE) and solid-phase micro-extraction (SPME) coupled to gas chromatography dual electron capture detection // *Environmental Science and Pollution Research*. - 2016. - Vol. 23, Is. 8. - P. 8053–8063.

105 Carlsen L., Kenessov B.N., Baimatova N.K., Kenessova O.A. Assessment of the Air Quality of Almaty . Focussing on the Traffic Component // *International Journal of Biology and Chemistry*. - 2013. - Vol. 1 (5). - P. 49–69.

106 Naccarato A., Tassone A., Moretti S., Elliani R., Sprovieri F., Pirrone N., Tagarelli A. A green approach for organophosphate ester determination in airborne particulate matter: Microwave-assisted extraction using hydroalcoholic mixture coupled with solid-phase microextraction gas chromatography-tandem mass spectrometry // *Talanta*. - 2018. - Vol. 189, Is. July. - P. 657–665.

107 Hussam A., Alauddin M., Khan A.H., Chowdhury D., Bibi H., Bhattacharjee M., Sultana S., Island S. Solid phase microextraction: Measurement of volatile organic compounds (VOCs) in Dhaka city air pollution // *Journal of Environmental Science and Health - Part A Toxic/Hazardous Substances and Environmental Engineering*. - 2002. - Vol. 37, Is. 7. - P. 1223–1239.



- 108 Nicoara S., Tonidandel L., Traldi P., Watson J., Morgan G., Popa O. Determining the levels of volatile organic pollutants in urban air using a gas chromatography-mass spectrometry method // *Journal of Environmental and Public Health*. - 2009. - Vol. 2009. – Article 148527.
- 109 Lee S.C., Chiu M.Y., Ho K.F., Zou S.C., Wang X. Volatile organic compounds (VOCs) in urban atmosphere of Hong Kong // *Chemosphere*. - 2002. - Vol. 48, Is. 3. - P. 375–382.
- 110 Khan A., Szulejko J.E., Kim K.H., Brown R.J.C. Airborne volatile aromatic hydrocarbons at an urban monitoring station in Korea from 2013 to 2015 // *Journal of Environmental Management*. - 2018. - Vol. 209. - P. 525–538.
- 111 Li L., Li H., Zhang X., Wang L., Xu L., Wang X., Yu Y., Zhang Y., Cao G. Pollution characteristics and health risk assessment of benzene homologues in ambient air in the northeastern urban area of Beijing, China // *Journal of Environmental Sciences (China)*. - 2014. - Vol. 26, Is. 1. - P. 214–223.
- 112 Zhang Y., Mu Y., Liang P., Xu Z., Liu J., Zhang H., Wang X., Gao J., Wang S., Chai F., Mellouki A. Atmospheric BTEX and carbonyls during summer seasons of 2008-2010 in Beijing // *Atmospheric Environment*. - 2012. - Vol. 59. - P. 186–191.
- 113 Bigazzi A.Y., Figliozzi M.A., Luo W., Pankow J.F. Breath Biomarkers to Measure Uptake of Volatile Organic Compounds by Bicyclists // *Environmental Science and Technology*. - 2016. - Vol. 50, Is. 10. - P. 5357–5363.
- 114 Lee S.C., Chiu M.Y., Ho K.F., Zou S.C., Wang X. Volatile organic compounds (VOCs) in urban atmosphere of Hong Kong // *Chemosphere*. - 2002. - Vol. 48. - P. 375–382.
- 115 Kenessov B., Derbissalin M., Koziel J.A., Kosyakov D.S. Modeling solid-phase microextraction of volatile organic compounds by porous coatings using finite element analysis // *Analytica Chimica Acta*. - 2019. - Vol. 1076. - P. 73–81.
- 116 Lion L.W. Sorption and transport of polynuclear aromatic hydrocarbons in low-carbon aquifer materials. – New-York: Food and Agriculture Organization of the United States, 1989. – 59p.
- 117 Ibragimova O.P., Omarova A., Bukenov B., Zhakupbekova A., Baimatova N. Seasonal and Spatial Variation of Volatile Organic Compounds in Ambient Air of Almaty City, Kazakhstan // *Atmosphere*. - 2021. - Vol. 12. - Article 1592.
- 118 Serik L., Ibragimova O., Ussenova G., Baimatova N. Monitoring of volatile organic compounds in ambient air of Taldykorgan, Kazakhstan // *Chemical Bulletin of Kazakh National University*. - 2019. - Is. 4. - P. 4–12.
- 119 Agency for Strategic Planning and Reforms of the Republic of Kazakhstan Bureau of National Statistics Dynamic Tables of Demographic Statistics. Available online: <https://stat.gov.kz/official/industry/61/statistic/8> (accessed on 1 November 2021).
- 120 Assanov D., Zapasnyi V., Kerimray A. Air Quality and Industrial Emissions in the Cities of Kazakhstan // *Atmosphere*. - 2021. - Vol. 12. - Article 314.
- 121 Agency for Strategic Planning and Reforms of the Republic of Kazakhstan Bureau of National Statistics Main Indicators of Statistics of Transport. Available

online: <https://stat.gov.kz/official/industry/18/statistic/7> (accessed on 1 November 2021).

122 Kenessary D., Kenessary A., Adilgireiuly Z., Akzholova N., Erzhanova A., Dosmukhametov A., Syzdykov D., Masoud A.R., Saliev T. Air pollution in kazakhstan and its health risk assessment // *Annals of Global Health*. - 2019. - Vol. 85, Is. 1. - P. 1–9.

123 Vinnikov D., Tulekov Z., Raushanova A. Occupational exposure to particulate matter from air pollution in the outdoor workplaces in Almaty during the cold season // *PLOS ONE*. - 2020. - Vol. 15, Is. 1. - Article e0227447.

124 Vinnikov D., Raushanova A., Kyzayeva A., Romanova Z., Tulekov Z., Kenessary D., Auyezova A. Lifetime Occupational History, Respiratory Symptoms and Chronic Obstructive Pulmonary Disease: Results from a Population-Based Study // *International Journal of Chronic Obstructive Pulmonary Disease*. - 2019. - Vol. 14. - P. 3025–3034.

125 Kerimray A., Assanov D., Kenessov B., Karaca F. Trends and health impacts of major urban air pollutants in Kazakhstan // *Journal of the Air and Waste Management Association*. - 2020. - Vol. 70, Is. 11. - P. 1148-1164.

126 Russell A., Ghalaieny M., Gazdiyeva B., Zhumabayeva S., Kurmanbayeva A., Akhmetov K.K., Mukanov Y., McCann M., Ali M., Tucker A., Vitolo C., Althonayan A. A Spatial Survey of Environmental Indicators for Kazakhstan: An Examination of Current Conditions and Future Needs // *International Journal of Environmental Research*. - 2018. - Vol. 12, Is. 5. - P. 735–748.

127 Kerimray A., Azbanbayev E., Kenessov B., Plotitsyn P., Alimbayeva D., Karaca F. Spatiotemporal variations and contributing factors of air pollutants in Almaty, Kazakhstan // *Aerosol and Air Quality Research*. - 2020. - Vol. 20, Is. 6. - P. 1340–1352.

128 Aiman N., Gulnaz S., Alena M. The characteristics of pollution in the big industrial cities of Kazakhstan by the example of Almaty // *Journal of Environmental Health Science and Engineering*. - 2018. - Vol. 16, Is. 1. - P. 81–88.

129 Kerimray A., Baimatova N., Ibragimova O.P., Bukenov B., Kenessov B., Plotitsyn P., Karaca F. Assessing air quality changes in large cities during COVID-19 lockdowns: The impacts of traffic-free urban conditions in Almaty, Kazakhstan // *Science of the Total Environment*. - 2020. - Vol. 730. - Article 139179.

130 Carlsen L., Bruggemann R., Kenessov B. Use of partial order in environmental pollution studies demonstrated by urban BTEX air pollution in 20 major cities worldwide // *Science of the Total Environment*. - 2018. - Vol. 610–611. - P. 234–243.

131 Kazhydromet. Monthly newsletter on the state of the environment. – 2022. – URL: <https://kazhydromet.kz/en/ecology/ezhemesyachnyy-informacionnyy-byulleten-o-sostoyanii-okruzhayuschey-sredy> (28.12.2022).

132 Airkaz.org. Air pollution map. – 2022. – URL: <https://www.airkaz.org/> (26.12.2022).

133 rp5.co.za. Weather Schedule Weather in 243 countries. – 2022. – URL: [http://rp5.co.za/Weather\\_in\\_the\\_world](http://rp5.co.za/Weather_in_the_world) (28.12.2022).

134 Liu W., Zhang J., Kwon J., Weisel C., Turpin B., Zhang L., Korn L., Morandi M., Stock T., Colome S. Concentrations and source characteristics of airborne carbonyl compounds measured outside urban residences // *Journal of the Air and Waste Management Association*. - 2006. - Vol. 56, Is. 8. - P. 1196–1204.

135 Liang Y., Liu X., Wu F., Guo Y., Fan X., Xiao H. The year-round variations of VOC mixing ratios and their sources in Kuytun City (northwestern China), near oilfields // *Atmospheric Pollution Research*. - 2020. - Vol. 11, Is. 9. - P. 1513–1523.

136 Lyu X.P., Chen N., Guo H., Zhang W.H., Wang N., Wang Y., Liu M. Ambient volatile organic compounds and their effect on ozone production in Wuhan, central China // *Science of the Total Environment*. - 2016. - Vol. 541. - P. 200–209.

137 Zakon.kz. Which cities of Kazakhstan are in quarantine and what is the regime in them?. – 2020. – URL: [https://online.zakon.kz/Document/?doc\\_id=34591808&pos=6;-106#pos=6;-106](https://online.zakon.kz/Document/?doc_id=34591808&pos=6;-106#pos=6;-106) (28.12.2022).

138 Wu Y., Hu J., Wang H., Li H., Zhang H., Chai F., Wang S. The characteristics of ambient non-methane hydrocarbons (NMHCs) in Lanzhou, China // *Atmosphere*. - 2019. - Vol. 10, Is. 12. - P. 1–17.

139 Huang Y.S., Hsieh C.C. VOC characteristics and sources at nine photochemical assessment monitoring stations in western Taiwan // *Atmospheric Environment*. - 2020. - Vol. 240, Is. January. - P. 117741.

140 Ecoexpert LLP. Report on Monitoring of Environmental Quality Targets of Almaty 2020; Ecoexpert LLP: Almaty, Kazakhstan, 2020.

141 Zhao B., Wang P., Ma J.Z., Zhu S., Pozzer A., Li W. A high-resolution emission inventory of primary pollutants for the Huabei region, China // *Atmospheric Chemistry and Physics*. - 2012. - Vol. 12, Is. 1. - P. 481–501.

142 Zhang X., Ding X., Wang X., Talifu D., Wang G., Zhang Y., Abulizi A. Volatile organic compounds in a petrochemical region in arid of NW China: Chemical reactivity and source apportionment // *Atmosphere*. - 2019. - Vol. 10, Is. 11. - Article 641.

143 Earth Observatory. Airborne nitrogen dioxide plummets over China. – 2020. – URL: [https://earthobservatory.nasa.gov/images/146362/airborne-nitrogen-dioxide-plummets-over-china#:~:text=NASA%20and%20European%20Space%20Agency,\(NO2\)%20over%20China](https://earthobservatory.nasa.gov/images/146362/airborne-nitrogen-dioxide-plummets-over-china#:~:text=NASA%20and%20European%20Space%20Agency,(NO2)%20over%20China) (28.12.2022).

144 Tobias A., Carnerero C., Reche C., Massagué J., Via M., Minguillón M.C., Alastuey A., Querol X. Changes in air quality during the lockdown in Barcelona (Spain) one month into the SARS-CoV-2 epidemic // *Science of the Total Environment*. - 2020. - Vol. 726. - Article 138540.

145 Department of Ecology of Almaty region, 2015. State Environmental Review Report on “Adjustment of the Draft Standards for Maximum Permissible Emissions (MPE) of JSC ALES CHP-3 for 2015–2024” in the Almaty Region.

146 Koziel J., Jia M., Pawliszyn J. Air Sampling with porous Solid-Phase Microextraction fibers // *Analytical Chemistry*. - 2000. - Vol. 72, Is. 21. - P. 5178–5186.

147 Augusto F., Koziel J., Pawliszyn J. Design and validation of portable SPME-devices for rapid field air // *Analytical Chemistry*. - 2001. - Vol. 73, Is. 3. - P. 481–486.

148 Koziel J.A., Nguyen L.T., Glanville T.D., Ahn H., Frana T.S., (Hans) van Leeuwen J. Method for sampling and analysis of volatile biomarkers in process gas from aerobic digestion of poultry carcasses using time-weighted average SPME and GC–MS // *Food Chemistry*. - 2017. - Vol. 232. - P. 799–807.

149 Woolcock P.J., Koziel J.A., Cai L., Johnston P.A., Brown R.C. Analysis of trace contaminants in hot gas streams using time-weighted average solid-phase microextraction: Proof of concept // *Journal of Chromatography A*. - 2013. - Vol. 1281. - P. 1–8.

150 Baimatova N., Koziel J., Kenessov B. Quantification of benzene, toluene, ethylbenzene and o-xylene in internal combustion engine exhaust with time-weighted average solid phase microextraction and gas chromatography mass spectrometry // *Analytica Chimica Acta*. - 2015. - P. 1–13.

151 Tursumbayeva M. Simple and accurate quantification of odorous volatile organic compounds in air with solid phase microextraction and gas chromatography - mass spectrometry. M.S. thesis. Ames, Iowa, USA: Iowa State University, 2017. - 43 p.

152 Semenov S.N., Koziel J.A., Pawliszyn J. Kinetics of solid-phase extraction and solid-phase microextraction in thin adsorbent layer with saturation sorption isotherm // *Journal of Chromatography A*. - 2000. - Vol. 873, Is. 1. - P. 39–51.

153 Zhao W. Solid Phase Microextraction in Aqueous Sample Analysis: PhD Thesis. – Canada, 2008. – 181p.

154 Alam M.N., Ricardez-Sandoval L., Pawliszyn J. Numerical Modeling of Solid-Phase Microextraction: Binding Matrix Effect on Equilibrium Time // *Analytical Chemistry*. - 2015. - Vol. 87, Is. 19. - P. 9846–9854.

155 Alam M.N., Ricardez-Sandoval L., Pawliszyn J. Calibrant Free Sampling and Enrichment with Solid-Phase Microextraction: Computational Simulation and Experimental Verification // *Industrial & Engineering Chemistry Research*. - 2017. - Vol. 56, Is. 13. - P. 3679–3686.

156 Souza-Silva E.A., Gionfriddo E., Alam M.N., Pawliszyn J. Insights into the Effect of the PDMS-layer on the Kinetics and Thermodynamics of Analyte Sorption onto the Matrix-Compatible SPME Coating // *Analytical Chemistry*. - 2017. - Vol. 89, Is. 5. - P. 2978–2985.

157 Alam M.N., Pawliszyn J. Numerical simulation and experimental validation of calibrant-loaded extraction phase standardization approach // *Analytical Chemistry*. - 2016. - Vol. 88, Is. 17. - P. 8632–8639.

158 Chao K.-P., Wang V.-S., Yang H.-W., Wang C.-I. Estimation of effective diffusion coefficients for benzene and toluene in PDMS for direct solid phase microextraction // *Polymer Testing*. - 2011. - Vol. 30, Is. 5. - P. 501–508.


159 Mackay D., Leinonen P.J. Rate of evaporation of low-solubility contaminants from water bodies to atmosphere // *Environmental Science & Technology*. - 1975. - Vol. 9, Is. 13. - P. 1178–1180.

160 Mocho P., Desauziers V. Static SPME sampling of VOCs emitted from indoor building materials: Prediction of calibration curves of single compounds for two different emission cells // *Analytical and Bioanalytical Chemistry*. - 2011. - Vol. 400, Is. 3. - P. 859–870.

161 Tuduri L., Desauziers V., Fanlo J.L. Potential of Solid-Phase Microextraction Fibers for the Analysis of Volatile Organic Compounds in Air // *Journal of Chromatographic Science*. - 2001. - Vol. 39. - P. 521–529.

# ANNEX A

## Letters of copyright permission




### Attribution 4.0 International (CC BY 4.0)

This is a human-readable summary of (and not a substitute for) the [license](#). [Disclaimer](#).


#### You are free to:


- Share** — copy and redistribute the material in any medium or format
- Adapt** — remix, transform, and build upon the material for any purpose, even commercially.


The licensor cannot revoke these freedoms as long as you follow the license terms.



#### Under the following terms:

-  **Attribution** — You must give [appropriate credit](#), provide a link to the license, and [indicate if changes were made](#). You may do so in any reasonable manner, but not in any way that suggests the licensor endorses you or your use.

Home Help Email Support Sign in Create Account



**Assessing air quality changes in large cities during COVID-19 lockdowns: The impacts of traffic-free urban conditions in Almaty, Kazakhstan**  
Author: Aiyngul Kerimray, Nassiba Baimatova, Olga P. Ibragimova, Bauyrzhan Bukenov, Bulat Kenessov, Pavel Plotitsyn, Ferhat Karaca  
Publication: Science of The Total Environment  
Publisher: Elsevier  
Date: 15 August 2020  
© 2020 Elsevier B.V. All rights reserved.

#### Journal Author Rights

Please note that, as the author of this Elsevier article, you retain the right to include it in a thesis or dissertation, provided it is not published commercially. Permission is not required, but please ensure that you reference the journal as the original source. For more information on this and on your other retained rights, please visit: <https://www.elsevier.com/about/our-business/policies/copyright#Author-rights>

[BACK](#) [CLOSE WINDOW](#)

© 2022 Copyright - All Rights Reserved | [Copyright Clearance Center, Inc.](#) | [Privacy statement](#) | [Data Security and Privacy](#) | [For California Residents](#) | [Terms and Conditions](#)  
Comments? We would like to hear from you. E-mail us at [customercare@copyright.com](mailto:customercare@copyright.com)